THE ASTRONOMICAL JOURNAL

VOLUME 77 | 1972 August ~ No. 1401 | NUMBER 6

Flux Densities, Positions, and Structures for a Complete Sample of Intense Radio Sources at 1400 MHz

A. H. BRIDLE
Astronomy Group, Department of Physics, Queen's University at Kingston, Ontario, Canada

M. M. DAVIS AND E. B. FOMALONT
National Radio Astronomy Observatory, Green Bank, West Virginia*

AND

J. LEQUEUX
Département de Radioastronomie, Observatoire de Paris, Section d'Astrophysique, Meudon, France

(Received 4 April 1972)

Accurate flux densities, precise positions of unresolved sources, and structures of resolved sources have been derived from full-beam and interferometric observations of intense sources at 1400 MHz. Results are given for 424 sources in the area of sky $-5°<\delta<+70°$, $|b|>5°$ whose 1400-MHz integrated flux densities S_{1400} exceed 1.70 f.u. [1 flux unit (f.u.) $=10^{-26}$ w.m^{-2}.Hz^{-1}]. The 234 sources with $S_{1400}\geqslant 2.00$ f.u., equivalent diameters <10 arc min, and $|b|>20°$ form a $98\pm2\%$ complete sample comparable in number to the 178-MHz *Revised Third Cambridge Catalogue* in this 4.30-sr area of sky, but selected at 1400 MHz. This sample is suitable for statistical studies of the properties of extragalactic radio sources. To facilitate its use, and that of other samples which may be drawn from these data, references to other studies of the positions, fine and extended structure, polarization, and variability of the sources have been assembled in the principal table of this paper (Table II). A comparison is made with other 1400-MHz flux-density data (Sec. III), and the spectral content of the complete sample is discussed (Sec. IV).

IT has been recognized for over 15 years that the study of the powerful extragalactic radio sources presents both one of the most extreme problems of energetics in astrophysics, and an important means of testing cosmological models. Progress in understanding the formation and evolution of these sources, and interpreting their implications for cosmology, has stemmed mainly from detailed studies of their structures, continuum spectra, polarizations, and optical identifications. Such data can generally be obtained only for the more intense sources at any given frequency. Observationally unbiased and reliably defined samples of such intense sources are therefore essential to both extragalactic astrophysics and observational cosmology.

Statistically complete catalogues of the most intense sources at decimetric and centimetric wavelengths are particularly needed for two reasons: measurements made at such wavelengths are more precise than those presently possible at longer or shorter wavelengths, and the dispersion of the spectral indices of extragalactic sources makes the spectral composition of complete samples strongly dependent on the observing frequency. Samples selected at decimetric or centimetric wavelengths will contain significant proportions both of the 'transparent' sources recognized in early radio surveys and of the 'opaque' sources discovered by more recent studies at short wavelengths.

A substantially complete and unbiased catalogue of intense radio sources at 1400 MHz could in principle (e.g., Witzel *et al.* 1971) be compiled to a limiting surface density of ~50 sources per steradian from recent surveys at this frequency (Kellermann and Read 1965; Höglund 1967; Davis 1967; Galt and Kennedy 1968; Scheer and Kraus 1967; Dixon and Kraus 1968; Fitch *et al.* 1969; Ehman *et al.* 1970). The positions and flux densities given by these survey observations are, however, very imprecise for most of the sources and cannot be used directly for meaningful astronomical analyses. The survey observations also provide little useful data on structures of the sources.

This paper presents measurements of accurate flux densities, positions, and structures of 424 intense sources

* Operated by Associated Universities, Inc. under contract with the National Science Foundation.

at 1400 MHz, derived from reobservations of sources from 1400-MHz surveys and other literature with both the National Radio Astronomy Observatory (NRAO) 300-ft paraboloid and the California Institute of Technology (CIT) twin 90-ft element interferometer. The resulting source list (Table II) contains a statistically complete and unbiased sample of 234 sources with 1400-MHz flux densities $S_{1400} \geqslant 2.00$ f.u. in the area of sky defined by $-5° < \delta < +70°$, $|b| > 20°$. This sample provides a set of data suitable for many statistical studies of intense extragalactic sources.

Section I of the paper describes the observations made at the NRAO and at CIT and discusses the intercomparison of the full-beam and interferometric data. The source list, and data on weak sources confusing those in the list, are presented in Sec. II. Section III describes the computation of the completeness of the sample referred to above, assesses the quality of the data in the other 1400-MHz studies on which this work was based, and presents data on those sources rejected from the list as a result of our observations. Section IV summarizes results on the spectra of sources in the statistically complete sample.

I. OBSERVATIONS

A. Selection of the Sources to be Studied

The selection from the literature of the 650 sources reobserved with the NRAO 300-ft telescope determines the final completeness of our work at any given flux-density level. This selection was made with a view to ensuring substantial final completeness at $S_{1400} \geqslant 2.00$ f.u.; the completeness achieved is derived in Sec. III. Two distinct classes of earlier observations provided sources for the present study: surveys initially conducted at 1400 MHz, and measurements of 1400-MHz flux densities for sources initially discovered in surveys at lower frequencies.

The area of sky covered in this program had previously been surveyed fully by Galt and Kennedy (1968). Their DA survey suffers, however, from two serious limitations. The precision of the flux densities is low, and the published source list is biased towards the inclusion of previously catalouged sources. In particular, sources detected only marginally in the DA observations were included in the published list if their positions agreed with those of previously catalogued objects, but were excluded if they did not. The first limitation made it necessary to reobserve every field in the DA catalogue within the area of sky covered in our work, with the exception of those studied with the 300-ft telescope by Pauliny-Toth *et al.* (1966) whose data are of a precision and reliability comparable to our own. The second limitation, which would lead to spectral bias and incompleteness in the resulting source list, was overcome by supplementing the published DA survey with a list of 85 objects marginally detected in the DA observations but excluded from their publication by the identification criterion. This supplementary list, kindly made available to us by the authors of the survey, also gave the observed positions for all sources detected in the DA survey. In contrast, the published list gives the previously published positions for the presumed identifications. The availability of the observed DA positions enabled us in some instances to displace the center of the field studied at NRAO towards a more appropriate 1400-MHz position. This assisted us in detecting sources which confused the DA observations, and in some cases provided new identifications of the lower-frequency sources responsible for the 1400-MHz emission. Such a case is illustrated in Sec. I.B (Fig. 2).

Sources whose equivalent Gaussian diameters were shown by the DA observations to be greater than 40 arc min were not reobserved, as they are mostly galactic objects. Such sources are so fully resolved by the 300-ft telescope that it is difficult to derive their integrated flux densities reliably.

An initial comparison of the DA survey with other 1400-MHz surveys showed that a significant number of sources with $S_{1400} > 2.0$ f.u. in other surveys were absent from the DA list. (A final estimate of the completeness of the DA survey is derived in Sec. III.) We therefore included in our observing program sources from all the OSU surveys then available (Kraus 1964; Kraus and Dixon 1965; Kraus *et al.* 1966; Scheer and Kraus 1967; Dixon and Kraus 1968; Fitch *et al.* 1969; Ehman *et al.* 1970), and from the DW (Davis 1967), Höglund (1967), and CTD (Kellermann and Read 1965) surveys whose published flux densities were $\geqslant 1.5$ f.u. at 1400 MHz. In the case of the DW survey, a lower limit of 1.0 f.u. was adopted for those observations consisting of less than three drift scans in the verification study made at NRAO (Davis 1967).

The completeness of the above source selection was assessed, and 16 further sources were consequently added to our sample at $S_{1400} \geqslant 2.00$ f.u., by remeasuring 1400-MHz flux densities for sources in lower-frequency surveys which had been observed at 1400 MHz in studies of radio continuum spectra. We observed all sources with published 1400-MHz flux densities $\geqslant 1.5$ f.u. in the Parkes studies (Shimmins and Day 1968; Ekers 1969) and in the CIT study by Olsen (1967). We also observed all sources with quoted 1400-MHz flux densities $\geqslant 1$ f.u. in the Jodrell Bank/Cambridge studies of the spectra of 4C and VRO sources (Long *et al.* 1966; Williams and Stewart 1967), and all sources with 1400-MHz flux densities > 1.5 f.u. in two unpublished spectral studies, of Parkes sources (I.I.K. Pauliny-Toth and K. I. Kellermann, private communication) and of 4C sources (A. E. Niell, private communication). Finally, we included 13 further sources which were noted by Pauliny-Toth *et al.* (1966) as confused, or whose flux densities were poorly determined by their data. Additional sources from this list, and fainter sources from the OSU catalogues, were observed as time permitted.

B. The Full-Beam Observations

Four independent load-switched radiometers with system temperatures of 150 K and bandwidths of 60 MHz centered on 1400 MHz were mounted around the focus of the NRAO 300-ft transit telescope. Four rectangular feed horns with E-vectors in position angle 0° were mounted so as to provide four beams each 16 arc min (1.5 half-power beamwidth) off the electrical axis. The orientation of the four beams on the sky was such that by interleaving observations from two transits of a source at telescope settings 5 arc min apart in declination, eight independent drift scans were obtained at 5-arc min intervals in declination through the field surrounding the source (Fig. 1). On the basis of such observations, additional transits were recorded with the telescope set further north or south, when necessary to define more fully the structure of an extended source or to obtain more accurate positions and flux densities of nearby sources. The original data and a contour map of one such field are shown in Fig. 2. The area normally mapped around each source position was ~70 arc min in right ascension by ~35 arc min in declination.

The gain of the radiometer in each channel was monitored once every minute by injecting a noise signal from a discharge tube for 4 sec. Repeated observations of eight intense sources were used to monitor the overall response of the instrument in each of the four channels at intervals of ~12 h. Values of the ambient temperature recorded hourly were used to correct all the observations for a variation of the system response with ambient temperature amounting to about 0.1% per °C. After correction for this and for the small variations in radiometer gain, the rms deviations from the mean of the twice-daily determinations of the system response were from 0.3% to 0.9% depending on the channel.

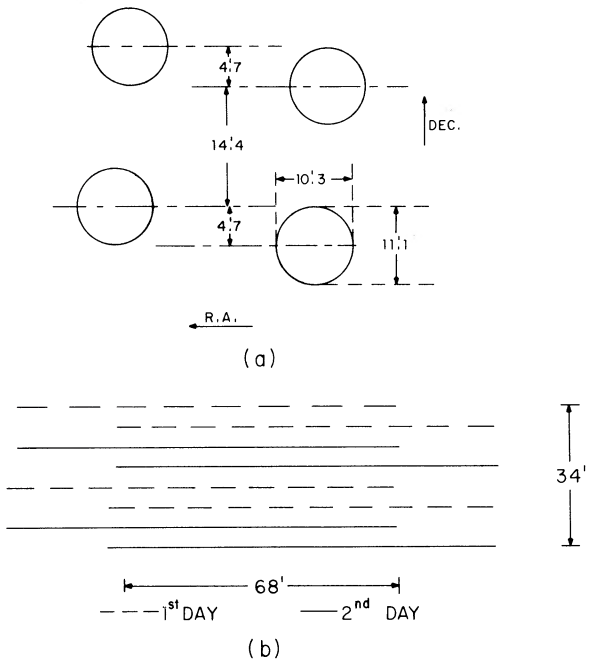

FIG. 1. (a) Orientation of the four beams used for the full-beam 300-ft telescope observations. (b) Resulting sky coverage using two transits separated by 5 arc min in declination.

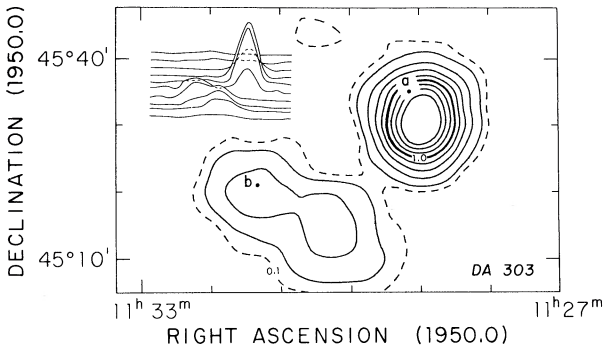

FIG. 2. Original data (insert, upper left) and resultant contour plot for the field of DA 303. Three transits were used to obtain these data. The contours are at intervals of 0.2 f.u. per beam area, with an additional dashed contour at the 0.1-f.u. level. The source position (a) found in the DA survey was shifted to that of a nearby 4C source (b) in their published catalogue. The more extensive unpublished list (Galt and Kennedy, private communication) was used in compiling the present finding list.

Most of the observations were made at night during August–September 1969 and February–March 1970. The 1969 observations of 15 unresolved isolated sources were repeated in 1970; the measured differences in flux density were consistent with random errors of 2.0% in the individual measurements. Observations of 54 sources which were neither resolved nor confused were used to determine the variation of the aperture efficiency of the telescope with declination, and to normalize the flux-density scale to that of Kellermann *et al.* (1969). The sources used for these purposes, and the flux densities adopted for them in linear polarization at position angle 0°, are listed in Table I.

Uncertainties in the flux densities due to confusion have been investigated quantitatively for this system by Monte Carlo analysis of a survey made with the same equipment to a limiting flux density of 0.20 f.u. (M. M. Davis, in preparation). It was deduced that the standard error in the flux density at position angle 0° for an unresolved source, including the effects of noise, confusion, and uncertainty in the normalization to the scale of Kellermann *et al.* (1969), is $[(0.035)^2+(0.02S)^2]^{\frac{1}{2}}$ f.u., where S is the flux density in f.u. For those sources whose polarization at 1400 MHz is known, the ratio of the total flux density to that measured in position angle 0° has an rms deviation of 2.8% about the mean of 1.00. The standard error in our measurements, if used as total flux densities, should therefore be taken as the combination of these errors in quadrature.

In each field, all sources having peak flux densities $\geqslant 0.1$ f.u. were fitted with two-dimensional Gaussian responses using an iterative least-squares procedure. In crowded fields up to seven sources were fitted. Posi-

TABLE I. Flux densities from KPW adopted for calibration of the full-beam observations at NRAO.

Source	Flux density*	Source	Flux density*
3C 16	1.75	3C 245	3.10
3C 19	3.13	3C 249	2.51
3C 63	3.31	3C 249.1	2.24
3C 76.1	2.53	3C 254	3.02
3C 78	7.00	PK 1138+01	2.55
3C 89	2.74	3C 268.3	3.59
3C 91	3.26	3C 270.1	2.50
3C 93.1	2.23	3C 274.1	2.95
3C 95	2.83	3C 275	3.38
3C 105	5.11	3C 286	14.90
3C 109	3.99	3C 289	2.32
3C 153	4.13	3C 299	2.78
3C 166	2.38	3C 303	2.22
3C 180	2.52	3C 305	3.09
3C 181	2.23	3C 309.1	8.02
3C 190	2.48	3C 313	3.56
3C 194	2.08	3C 315	3.83
3C 196	13.99	3C 319	2.36
3C 205	2.29	3C 327.1	4.07
3C 212	2.48	3C 330	7.13
3C 216	3.69	3C 332	2.44
3C 218	42.55	3C 338	3.51
3C 219	7.79	3C 341	2.10
3C 226	2.11	PK 1645+17	2.10
3C 228	3.56	3C 410	10.15
3C 234	5.15	3C 411	3.20
3C 244.1	3.63	3C 435	2.01

* Position angle 0° (cf. text).

tions, integrated flux densities, and equivalent Gaussian diameters were computed for all sources. Upper limits based on a 2σ criterion (von Hoerner 1965) were placed on the equivalent diameters of unresolved sources; this criterion implies that the diameter will be less than the quoted limit for 95% of the sources. With the 10.3-arc min by 11.1-arc min resolution of this instrument in right ascension and declination, diameter assignments are only significant in general for sources with angular extents >4 arc min.

Pointing corrections were determined with reference to precise positions determined at 11 cm by Wade (1970) and by Adgie, Crowther, and Gent (private communication).

For each field observed, the entire primary beam of the 90-ft elements of the CIT interferometer has been mapped with the 300-ft telescope. This mapping was used to assist reduction of the CIT data in some confused fields. Similar, although less extensive, data are available in the list of Pauliny-Toth *et al.* (1966) for 128 3C and NRAO sources which were not reobserved at the 300-ft telescope. The consistency of the new NRAO observations with those of Pauliny-Toth *et al.* (1966), which were also used in compiling our final source list where necessary, was evaluated by reobserving 44 unresolved sources from their study. The rms deviation of the flux densities measured for these sources by Pauliny-Toth *et al.* from those measured by us was 3.1%. There was no systematic discrepancy between the two sets of measurements after applying the corrections to the flux-density scale of Pauliny-Toth *et al.* derived by Kellermann *et al.* (1969).

C. The Interferometric Observations

Of the 424 sources included in our final list, 362 were also observed with the CIT twin 90-ft element interferometer. Many of the interferometric observations have been described elsewhere. In 1965 a program was begun at CIT to determine the structures of a large number of intense extragalactic sources at 1425 MHz, using a source list estimated from the present work to be about 70% complete above $S_{1400}=2.00$ f.u. The instrument and observing procedures are described by Fomalont (1967), and the reduction process, Fourier inversion, and model-fitting techniques by Fomalont (1968). Positions, flux densities, and diameters of most of the sources in the original list with diameters less than 50 arc sec are given by Fomalont and Moffet (1971), and structures for the more resolved sources by Fomalont (1971a). Some data have also been taken from Maltby and Moffet (1962), Fomalont *et al.* (1967), Olsen (1967), and Fomalont (1971b).

New observations were obtained in 1968 and 1969 for 171 sources not in Fomalont's original list. Results for the 90 such sources with $S_{1400}\geqslant 1.70$ f.u. are included in Tables II and IV. The instrument, observing procedures, calibration, and reduction were identical to those of the earlier observations. Most of the sources, including those which were not resolved, were observed with the two elements at east–west spacings of 100, 200, 400, 800, 1200, and 1600 ft (100 ft $=144\lambda$), once or twice at each spacing. In addition, 116 of these sources were also observed at a north–south spacing of 400 ft; these observations provided declinations and limits to the north–south diameters for about 60 of the sources in our final list.

The positions obtained for unresolved sources not used as position calibrators were compared with their precise positions obtained at 11 cm by Wade (1970) and by Adgie, Crowther, and Gent (private communication). No systematic discrepancies were found. The rms deviation in right ascension of the CIT positions from those determined at 11 cm is 1.65 arc sec for the data of Fomalont and Moffet (1971), and 2.1 arc sec for the new CIT data. The corresponding rms deviations in declination are 1.7 and 4.2 arc sec respectively; the greater accuracy of the data of Fomalont and Moffet is due to their use of a longer north–south baseline.

D. Intercomparison of Full-Beam and Interferometric Data

The flux density, positional, and structural data from the full-beam and interferometric studies were compared for sources with $S_{1400}\geqslant 1.70$ f.u. in either set of observations. Good agreement was found in all parameters within the estimated errors for nearly all sources; the few apparent discrepancies could all be explained

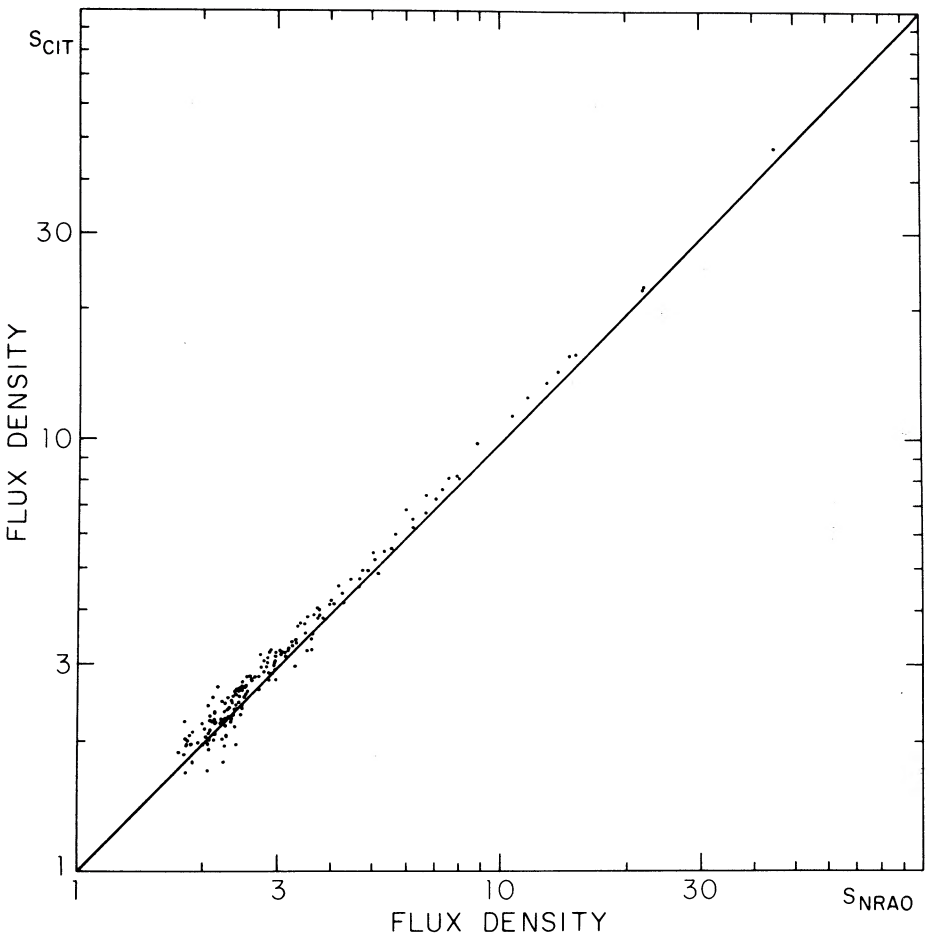

FIG. 3. Comparison of the full-beam flux density S_{NRAO} and the interferometer flux density S_{CIT} for 174 small-diameter sources. A line through the origin of slope unity is shown.

by the effects of confusion, source structure, or variability, and are noted in Table II (Sec. II).

Figure 3 compares the interferometric and full-beam flux densities for 175 unresolved, isolated, nonvariable sources. The CIT flux densities have been corrected from 1425 to 1400 MHz. A least-squares fit to the relation between the two sets of flux-density measurements gives $S_{CIT}=(1.042\pm0.006)S_{BDFL}-(0.01\pm0.04)$ where S_{BDFL} is the flux density obtained in the present observations. The value 1.042 is close to the expected value of 1.021 due to the standardization of CIT flux densities with Conway, Kellermann, and Long (1963). The rms deviation between the two sets of data is 4.4%. Figure 4 shows histograms of the positional discrepancies between the interferometric and the new full-beam observations. For sources with equivalent Gaussian diameters less than 3 arc min in the appropriate coordinate, the rms deviations between the two sets of measurements are 12 arc sec in right ascension and 15 arc sec in declination. For sources with larger equivalent Gaussian diameters the corresponding values are 18 and 20 arc sec. As the errors in the interferometric positions are much smaller (Sec. I.C), these errors are effectively those in the new full-beam positions.

II. RESULTS

In this section we present a catalogue of the results obtained for all sources in the area of sky $-5°<\delta<+70°$, $|b|>5°$ for which our observations gave integrated flux densities $S_{1400}\gtrsim 1.70$ f.u. The full-beam integrated flux densities have been used to establish membership of the catalogue, except for three sources: 3C 26, for which the NRAO measurement was unreliable, and 3C 135 and 3C 165, for which the interferometer detected faint confusing neighbors not fully separated by the full-beam observations. The source M 31, which was not observed due to its large angular size, is not included in the catalogue.

Because of the double structure of most radio sources, it is difficult to determine whether individual pairs of widely separated sources are physical doubles. In some cases optical identifications or details of the radio structure of the suspected double can be of help. To evaluate the probability that pairs of sources resolved by the full-beam observations (>5-arc min separation) are physical associations, the number-flux density relationships derived from this catalogue (Bridle *et al.* 1972) and from a survey to 0.2 f.u. with the 300-ft telescope (M. M. Davis, in preparation) were used to

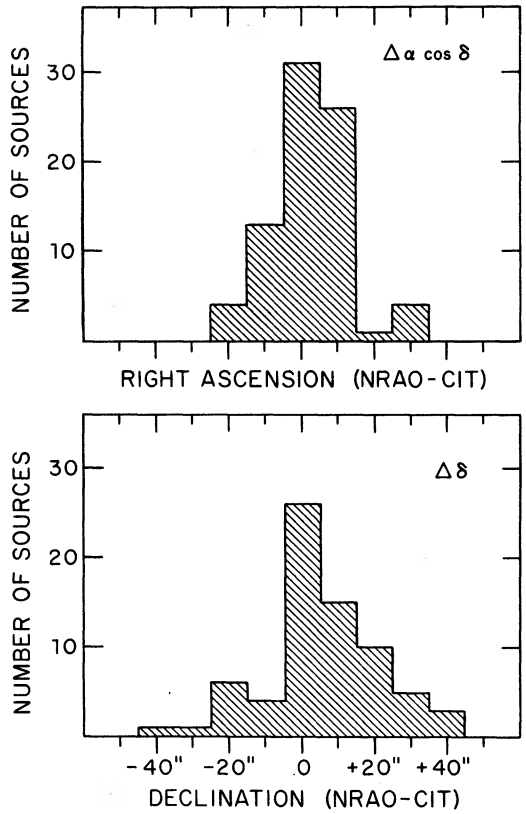

FIG. 4. Comparison of the full-beam and interferometer positions for 174 small-diameter sources.

determine the probability that close pairs of radio sources were chance associations. We restricted the calculation to pairs of sources whose flux densities differ by less than a factor of 2. We found, for example, that there is a 0.5% chance that a source of 1.5 f.u. has a weaker neighbor within a radius of 10 arc min with a flux density greater than 0.75 f.u. Although this probability is low, several such occurrences are expected by chance in a catalogue of ~400 sources.

The three most doubtful cases of close pairs have been included in the catalogue (Table II) with the combined flux density of both components, but are distinguished from the other entries by the symbol #. The probability of physical association for each of these cases is less than 99%. Conversely, three possible pairs of sources (3C 208−3C 208.1, 3C 343−3C 343.1, PK2147+14 −PK2148+14) have been listed as separate sources although the probability is less than 1% that each of these pairs is accidental: tentative optical identifications have been suggested for the individual sources of the first two pairs, but not for the third. PK1233+16, which consists of two sources each identified with a galaxy, has been considered as two sources with flux densities of 1.5 and 0.6 f.u. (Fomalont 1971a), and is therefore not included in the catalogue (cf. Table V, DA 327).

The catalogue is presented in Table II. The positions given are those from the interferometric observations where possible: if the full-beam observations showed the interferometric data to be seriously confused, the full-beam positions are given. Also, for sources with equivalent Gaussian diameters greater than 4 arc min, which are heavily resolved even at the closest interferometer spacing, the more reliable full-beam positions have been used.

Table II is arranged as follows:

Column 1. Source designation. Sources for which contour maps are given in Fig. 5 are denoted by asterisks (*) in this column. A dagger (†) signifies that there is a nearby weak source within a radius of about 20 arc min. The flux density, separation, and position angle (defined from the catalogued source towards the weaker source) are given in a footnote, and a more detailed listing is given in Table III. A number sign (#) denotes a source which is composed of two widely separated components and which is likely to be an accidental, rather than physical, double.

Column 2. Common source name. LS indicates a lobe shift in the original survey.

Column 3. Right ascension (1950.0) and standard error.

Column 4. Reference for the right ascension.

Column 5. Declination (1950.0) and standard error.

Column 6. Reference for the declination.

Column 7. Galactic latitude truncated to nearest degree.

Column 8. Flux density and standard error at 1400 MHz in units of 10^{-26} W m^{-2} Hz^{-1}.

Column 9. Reference for the flux density.

Column 10. Source designation.

Column 11. Structure type: D=double, T=triple, H=core-halo, C=complex.

Column 12. East–west extent in arc minutes.

Column 13. Reference for east–west extent.

Column 14. North–south extent in arc minutes.

Column 15. Reference for north–south extent.

Column 16. Brightness classification. H=high brightness, L=low brightness. See Bridle *et al.* (1972). This classification is given only for those sources in the complete sample: $-5° < \delta < 70°$, angular extent $< 10'$ with $S \geq 2.00$ f.u. for $|b| \geq 20°$ (234 sources) or $S > 6.00$ f.u. for $5° \leq |b| < 20°$ (18 sources).

Column 17. Integrated degree of polarization at 1400 MHz.

Column 18. Position angle of electric vector at 1400 MHz.

Column 19. Reference for polarization.

Column 20. Other references to information concerning the source. For sources resolved by the 300-ft observations, peak flux densities are given in this column.

Asterisks (*) in columns 2–20 refer to notes at the bottom of the page. The references used are summarized below. The information contained in Table II is available in punched card format.

References to data presented in Table II.

N: NRAO 300-ft telescope data
- N1 Pauliny-Toth *et al.* 1966
- N2 The present observations

C: CIT Interferometer data
- C1 Fomalont and Moffet 1971
- C2 Fomalont 1968
- C3 Fomalont 1971a
- C4 The present observations
- C5 Fomalont *et al.* 1967
- C6 Olsen 1967
- C7 Fomalont 1971b
- C8 Maltby and Moffet 1962

KPW: Kellermann *et al.* 1969

Polarization data
- 1 Bologna *et al.* 1969
- 2 Gardner *et al.* 1969
- 3 Morris and Berge 1964
- 4 Morris and Radhakrishnan 1963
- 5 Weighted vector average of Refs. 1 and 2.
- 6 Weighted vector average of Refs. 2 and 3.

Other References in Table II.

A: Accurate positions for unresolved sources.
- A1 Wade *et al.* 1970
- A2 Elsmore and Mackay 1969
- A3 Clark and Hogg 1966
- A4 Hogg 1969
- A5 Hazard *et al.* 1964
- A6 Clarke and Batchelor 1965
- A7 Hazard *et al.* 1968
- A8 Taylor 1966
- A9 Parker *et al.* 1966
- A10 Cohen and Shaffer 1971
- A11 Wade and Miley 1971
- A12 Moseley *et al.* 1970
- A13 Miley *et al.* 1970

M: Accurate positions and structures and/or maps of extended sources.
- M1 MacDonald *et al.* 1968
- M2 Mackay 1969
- M3 Clark and Hogg 1966
- M4 Hogg 1969
- M5 Mitton 1970a
- M6 Mitton and Ryle 1969
- M7 Mitton 1970b
- M8 Graham 1970
- M9 Miley *et al.* 1967
- M10 Mitton 1970c
- M11 Occultations; cf Cohen 1969 for references.
- M12 Hazard 1962
- M13 Hazard *et al.* 1964
- M14 Gulkis *et al.* 1969
- M15 De Jong 1967
- M16 Taylor 1966
- M17 Taylor 1967
- M18 Taylor and De Jong 1968
- M19 Talen 1965
- M20 Moffet *et al.* 1967
- M21 Ryle *et al.* 1965
- M22 Ryle and Windram 1968
- M23 Branson 1965
- M24 MacDonald and Kenderdine 1967
- M25 Parker and Kenderdine 1967
- M26 Mackay 1970
- M27 MacDonald *et al.* 1966
- M28 Clark and Miley 1969
- M29 Fomalont 1971a
- M30 Miley and Wade 1971

P: Positions only, structures unknown in these measurements.
- P1 Clarke, T. W. *et al.* 1969
- P2 Wills 1967
- P3 Bailey and Pooley 1968
- P4 Thomson *et al.* 1968
- P5 Merkelijn 1969
- P6 Wills and Bolton 1969
- P7 Olsen 1967
- P8 Moseley *et al.* 1970
- P9 Backer *et al.* 1970

S: Structures only.
- S1 Hogg 1969
- S2 Bash 1968, unresolved sources
- S3 *ibid.*, resolved sources
- S4 Palmer *et al.* 1967
- S5 Anderson and Donaldson 1967
- S6 Ekers (Ed.) 1969
- S7 Sutton *et al.* 1967
- S8 Biraud *et al.* 1960
- S9 MacDonald and Miley 1971

VLB: Long baseline interferometry.
- VLB1 Broten *et al.* 1969 and Clarke, R. W. *et al.* 1969
- VLB2 Jauncey *et al.* 1970
- VLB3 Kellermann *et al.* 1970
- VLB4 Kellermann *et al.* 1971
- VLB5 Broderick *et al.* 1972
- VLB6 Cohen *et al.* 1972

SC: Interplanetary scintillation data.
- SC1 Little and Hewish 1968
- SC2 Cohen *et al.* 1967
- SC3 Harris and Gundermann-Hardebeck 1969
- SC4 J. Ekers (Ed.) 1969 and R. Ekers, private communication

VAR: Variable Radio sources.
- VAR1 Kellermann and Pauliny-Toth 1968
- VAR2 W. J. Medd, private communication
- VAR3 D. E. Hogg, private communication

TABLE II. A complete catalogue of intense sources at 1400 MHz.

Source		Coordinates (1950.0) Right Ascension	Ref.	Declination	Ref.	Galactic Latitude	Flux Density	Ref.
1	2	3	4	5	6	7	8	9
0002+12	PK0002+12	$00^h02^m16^s.3 \pm 0^s.6$	C3	12°32'02" ±5"	C3	-48°	1.93 ± 0.06	N2
0003-00	3C2.0	00 03 48.8 0.1	C1	-00 21 06 1	C1	-60	3.54 0.12	N1
0007+12	PK0007+12	00 07 17.5 0.4	C3	12 27 48 6	C3	-48	1.77 0.06	N2
0010+40†	4C40.01	00 10 53.9 1.1	N2	40 35 32 15	N2	-21	1.73 0.05	N2
0017+15	3C9.0	00 17 49.8 0.2	C1	15 24 16 2	C1	-46	1.98 0.12	N1
0019-00	PK0019-00	00 19 51.9 0.1	C1	-00 01 46 3	C1	-61	2.73 0.07	N2
0026+34	OB343	00 26 34.8 1.0	N2	34 39 46 15	N2	-27	1.85 0.06	N2
0031+39	3C13.0	00 31 32.9 0.2	C2	39 07 43 12	C5	-23	1.79 0.08	N1
0033+18	3C14.0	00 33 29.4 0.2	C1	18 21 28 2	C1	-44	1.82 0.10	N1
0034-01	3C15.0	00 34 30.6 0.2	C1	-01 25 28 15	N1	-63	4.30 0.20	N1
0035-02	3C17.0	00 35 47.1 0.2	C1	-02 24 19 15	N1	-64	6.25 0.17	N1
0036+03	PK0036+03	00 36 43.6 1.2	N2	03 03 08 15	N2	-59	1.76 0.09	N2
0038+32	3C19.0	00 38 14.0 0.3	C1	32 53 42 2	C1	-29	3.12 0.08	N2
0038+09	3C18.0	00 38 14.6 0.2	C1	09 46 56 4	C1	-52	4.26 0.14	N1
0040+51	3C20.0	00 40 19.6 0.4	C1	51 47 09 2	C1	-10	10.79 0.31	N2
0048+50†	3C22.0	00 48 04.9 0.3	C1	50 55 45 2	C1	-11	2.27 0.15	N1
0050+56	CTA 6	00 50 00.7 5.9	N2	56 20 41 50	N2	-6	18.85 1.00	N2
0051-03	3C26	00 51 35.7 0.4	C1	-03 50 14 3	C1	-66	2.11 0.09	C1
0052+68	3C27.0	00 52 44.9 0.9	C1	68 06 06 2	C1	5	7.10 0.27	N1
0053-01*	PK0053-01	00 53 46.8 4.0	N1	-01 36 01 40	N1	-64	2.36 0.39	N1
0055-01*	3C29.0	00 55 00.7 2.0	N1	-01 40 30 40	N1	-64	5.22 0.14	N1
0055+30*†	DW0055+30	00 55 01.0 1.4	N2	30 04 49 20	N2	-32	1.95 0.11	N2
0056-00	PK0056-00	00 56 32.4 0.1	C1	-00 09 23 3	C1	-62	2.16 0.07	N2
0059+14*#	3C30 + PK	00 59 46.7 1.5	N2	14 31 57 25	N2	-47	2.45* 0.07	N2
0104+32†	3C31.0	01 04 41.9 0.3	C2	32 08 44 20	N2	-30	5.22 0.22	N2
0106+13	3C33.0	01 06 14.2 0.6	C3	13 03 37 15	C3	-49	12.59 0.27	N1
0107+56†	4C56.02	01 07 54.3 1.5	N2	56 16 05 30	N2	-6	1.88 0.07	N2
0109+49*†	3C35.0	01 09 05.9 0.7	C4	49 14 25 30	N2	-13	2.20 0.08	N2
0116+08	PK0116+08	01 16 24.2 0.2	C1	08 14 10 2	C1	-53	2.38 0.06	N2
0116+31	DW0116+31	01 16 47.5 0.2	C4	31 55 10 4	C4	-30	2.54 0.07	N2
0123-01	3C40.0	01 23 27.0 0.8	C2	-01 37 07 30	N2	-62	6.42 0.28	N2
0123+32	3C41.0	01 23 54.8 0.1	C1	32 57 36* 2	C1	-29	3.49 0.10	N1
0125+28	3C42.0	01 25 42.9 0.2	C1	28 47 29 2	C1	-33	2.64 0.08	N1
0127+23	3C43.0	01 27 15.1 0.2	C1	23 22 53 2	C1	-38	2.78 0.08	N1
0128+25	PK0128+25	01 28 33.3 0.6	C6	25 05 16 9	C6	-36	1.72 0.05	N2
0128+03†	PK0128+03	01 28 38.5 0.6	C3	03 58 40 20	N2	-57	2.52 0.07	N2
0130+30	M33	01 30 59.4 5.6	N2	30 25 04 90	N2	-31	3.79 0.27	N2
0132+07	3C45	01 32 37.5 0.2	C1	07 55 46 3	C1	-53	2.33 0.07	N1
0133+20	3C47.0	01 33 40.0 0.2	C2	20 41 55 15	N1	-40	3.68 0.09	N1
0133+47	DA,UNPUBL.	01 33 54.8 1.2	N2	47 36 06 30	N2	-14	2.17 0.06	N2
0134+32	3C48.0	01 34 49.8 0.1	C1	32 54 21 2	C1	-28	15.29 0.35	N1
0138+13	3C49.0	01 38 28.5 0.2	C1	13 38 21 2	C1	-47	2.69 0.08	N1
0145+53	3C52.0	01 45 15.3 0.3	C1	53 17 45 6	C1	-8	3.72 0.10	N1
0152+43	3C54.0	01 52 26.2 0.2	C4	43 31 12 10	C5	-17	1.79 0.07	N1
0154+28	3C55.0	01 54 19.3 0.3	C2	28 37 03 3	C7	-31	2.50 0.12	N1
0201+08	OD003	02 01 55.5 0.8	N2	08 49 28 30	N2	-49	1.72 0.06	N2
0202+14	PK0202+14	02 02 07.3 0.2	C1	14 59 51 3	C1	-44	3.40 0.08	N2
0204+29	3C59	02 04 10.8 0.6	C3	29 16 51 5	C3	-30	2.26 0.08	N1
0206+35	4C35.03	02 06 39.4 0.2	C4	35 33 41 4	C4	-24	2.15 0.06	N2
0218-02	3C63.0	02 18 21.9 0.2	C1	-02 10 36 3	C1	-56	3.32 0.08	N2
0219+08	3C64	02 19 19.5 0.4	C3	08 13 19 4	C3	-48	2.51 0.08	N1
0219+42	3C66.0	02 19 57.6 1.9	C2	42 45 58 20	N2	-16	10.25 0.38	N2
0220+39	3C65.0	02 20 36.8 0.3	C1	39 47 16 4	C1	-19	3.13 0.21	N1
0221+27	3C67.0	02 21 18.0 0.2	C1	27 36 36 2	C1	-30	2.94 0.23	N1
0223+34†	4C34.07	02 23 09.8 0.2	C4	34 08 05 4	C4	-24	2.17 0.06	N2

Notes to Table II

0010+40. 0.43-f.u. source, SEP=20′, PA=200°.
0033+18. A2 gives <7″ EW by <23″ NS.
0048+50. 0.29-f.u. source=NRAO 43, SEP=18′, PA=70°.
0053−01 & 0055−01. SEP=19′, PA=104°.
0055+30. 0.72-f.u. source, SEP=16′, PA=305°. See Fig. 5.
0059+14. 1.41-f.u.+1.04-f.u. double. See Fig. 5.
0104+32. M1 contour map in agreement with our structure; M1 table excludes northern extension of source. There is also an 0.17-f.u. source, SEP=18′, PA=55°.

TABLE II (*continued*)

Source	Class	Structure EW	Ref.	Structure NS	Ref.	T_B	Polarization %	PA(°)	Ref.	References
10	11	12	13	14	15	16	17	18	19	20
0002+12	T	4.'0	C3	1.'0	C3					M29
0003-00		<0.25	C1	<0.35	C1	H	<1.1		5	A3,12 S3,9 SC1,2,3
0007+12	D	0.73	C3	1.9	C3					M29
0010+40		<2.1	N2	<2.8	N2					
0017+15		<0.25	C1	<0.30	C1		5.8	159	5	A2 M9,28 S3 SC3
0019-00		<0.35	C1	<0.35	C1	H				P5 VLB2,4
0026+34		<3.4	N2	<4.1	N2					P4
0031+39	H	1.6	C2	<2.0	C5					M1 S3
0033+18		0.29*	C1	0.33*	C1					A2 SC3
0034-01		<0.25	C1	<0.60	C8	H	4.4	15	2	M13 S3,7 P8
0035-02		0.30	C1	<0.50	C8	H	0.8	159	5	M16,19,20 S3
0036+03		5.3	N2	<5.3	N2					PEAK = 1.56
0038+32		<0.25	C1	<0.25	C1	H				A2 S3
0038+09		0.28	C1	0.68	C1	H	1.6	118	2	S3
0040+51		0.70	C1	<0.30	C1	L	1.8	118	1	A12 M1 P3
0048+50		0.42	C1	<0.25	C1					A12 M1 P3
0050+56		16.3	N2	16.9	N2					PEAK = 5.51
0051-03		<0.25	C1	<0.67	C1	H				
0052+68		0.52	C1	0.37	C1	L	5.7	128	1	
0053-01	D	6.0	C2			L	<4.7		2	PEAK = 1.67
0055-01		1.1	C2	2.5	C8	L	9.4	163	2	S3 SC3
0055+30		5.6	N2	6.2	N2					PEAK = 1.50
0056-00		<0.25	C1	<0.35	C1	H	4.1	78	2	S9 SC3
0059+14	D	10.4	N2	9.3	N2					
0104+32	D	2.2	C2	6.1*	C7	L	3.1	53	1	M1,25 PEAK = 4.35
0106+13	T	1.4	C3	3.8	C3	L	8.3	60	5	M1,7,29 SC2,3 PEAK = 11.49
0107+56		<2.8	N2	<5.3	N2					
0109+49	C	2.1	C4	9.6	N2					M2 PEAK = 1.66
0116+08		<0.25	C1	<0.30	C1	H				SC3
0116+31		<0.25	C4	<1.0	C4	H				P4
0123-01	D	4.0	C2	10.3	N2	L	1.5	173	2	PEAK = 4.35
0123+32		<0.25*	C1	<0.25*	C1	H	7.6	54	1	M2 S3
0125+28		0.37	C1	0.38	C1	L				M2 S3
0127+23		<0.25	C1	<0.30	C1	H				A2 S2 SC1,2,3
0128+25		<3.7	N2	<4.6	N2					SC3
0128+03	D	3.1	C3	5.1	C3	L				M29 SC2,3 PEAK = 2.05
0130+30		23.9	N2	29.7	N2					PEAK = 0.52
0132+07		<0.25	C1	<0.30	C1	H				M14 S3 SC3
0133+20		0.64	C2	1.3	C8	L	2.5	3	5	M1,10,21 S3 SC3
0133+47		<3.6	N2	<3.1	N2					VAR2
0134+32		<0.25	C1	<0.25	C1	H	<0.7		1	A1,2,3,12 S4,5 SC1,2,3 VLB1
0138+13		<0.25	C1	<0.30	C1	H	<2.1		1	A2 S2 SC1,2,3
0145+53		0.42	C1	0.92	C1					
0152+43		0.30	C4	<2.0	C5		4.4	35	1	M1 S3
0154+28	D	1.0	C2	<0.42	C7	L	4.8	119	1	M1 S3 SC2,3
0201+08		<2.8	N2	<5.6	N2					
0202+14		<0.25	C1	<0.50	C1	H				S2,4 SC2,3 VLB(1),2,4
0204+29	T	2.5	C3	1.6	C3	L				M29 S3
0206+35		0.70	C4	<1.0	C4	L				P7
0218-02		<0.25	C1	<0.67	C1	H	2.9	42	5	A12 S3
0219+08	D	2.2	C3	0.54	C3	L	5.2	6	2	M29 S3
0219+42	C	7.3	C2	3.8	C7	L	2.8	91	1	M1,27 PEAK = 7.60
0220+39		<0.25	C1	<0.42	C1					A12 M2
0221+27		<0.25	C1	<0.25	C1	H				A2,3 S2 SC1,2,3
0223+34		<0.25	C4	<1.0	C4	H				P7 SC3

0107+56. 0.15-f.u. source, SEP=17′, PA=110°.
0109+49. 0.48-f.u. source, SEP=21′, PA=40°. See Fig. 5.
0123+32. M2 gives extension 26″ in PA=146°, and declination 7″ N of our position.
0128+03. 0.20-f.u. source, SEP=19′, PA=80°.
0223+34. 0.49-f.u. source, SEP=18′, PA=295°.

TABLE II (*continued*)

Source		Coordinates (1950.0) Right Ascension	Ref.	Declination	Ref.	Galactic Latitude	Flux Density	Ref.
1	2	3	4	5	6	7	8	9
0229+34	3C68.1	$02^h29^m27^s0 \pm 0^s3$	C1	34° 10' 56" ± 2"	C1	-23°	2.42 ± 0.16	N1
0240-00	3C71.0	02 40 07.1 0.1	C1	-00 13 32 2	C1	-51	4.87 0.13	N1
0246+42	4C42.08	02 46 15.8 0.5	C4	42 52 46 15	N2	-14	1.79 0.06	N2
0247+39	3C73	02 47 05.0 0.5	C3	39 22 12 4	C3	-17	1.83 0.07	N1
0255+05	3C75.0	02 55 05.1 0.6	C3	05 50 44 8	C3	-44	6.22 0.16	N1
0258+35	4C34.09	02 58 35.6 0.2	C4	35 00 36 4	C4	-20	1.88 0.06	N2
0300+16	3C76.1	03 00 27.1 0.3	C2	16 14 31 5	C7	-35	2.60 0.07	N2
0305+03	3C78.0	03 05 48.9 0.4	C3	03 55 17 6	C3	-44	7.24 0.15	N2
0307+16	3C79.0	03 07 11.4 0.3	C2	16 54 34 15	N1	-34	4.59 0.40	N1
0309+39	4C39.11	03 09 12.4 0.2	C4	39 05 22 4	C4	-15	1.73 0.05	N2
0315+41	3C83.1	03 15 00.4 1.6	N2	41 43 08 20	N2	-13	9.35 0.42	N2
0316+16	CTA 21	03 16 09.1 0.3	C1	16 17 41 2	C1	-33	7.60 0.16	N2
0316+41	3C84.0	03 16 28.8 0.7	C3	41 19 37 8	C3	-13	12.76 0.62	N2
0319+12	PK0319+12	03 19 08.0 0.5	C1	12 10 33 2	C1	-36	1.82 0.06	N2
0320+05	PK0320+05	03 20 41.5 0.2	C1	05 23 34 2	C1	-40	2.86 0.07	N2
0325+02	3C88.0	03 25 18.9 0.4	C3	02 23 22 4	C3	-42	4.85 0.20	N1
0326+39†	OA132	03 26 00.0 1.6	N2	39 36 34 15	N2	-13	1.74 0.06	N2
0327+40†	4C40.11	03 27 07.8 0.2	C4	40 51 09 20	N2	-12	1.70 0.05	N2
0331-01	3C89.0	03 31 42.1 0.2	C2	-01 21 16 3	C7	-43	2.72 0.07	N2
0333+32	NRAO140	03 33 22.6 0.2	C4	32 08 37 4	C4	-18	3.91 0.14	N1
0333+12	3C90	03 33 40.6 0.2	C1	12 52 40 2	C1	-33	1.80 0.07	N1
0336-01†	CTA 26	03 36 58.9 0.2	C1	-01 56 18 2	C1	-42	2.30 0.06	N2
0340+04	3C93.0	03 40 51.6 0.2	C1	04 48 24 2	C1	-37	2.84 0.07	N2
0341+67	DW0341+67	03 41 52.5 7.5	N2	67 56 44 46	N2	10	2.82 0.23	N2
0345+33	3C93.1	03 45 35.5 0.4	C1	33 44 06 2	C1	-15	2.25 0.14	N2
0347+05	PK0347+05	03 47 07.3 0.2	C2	05 42 34 15	N2	-35	3.25 0.08	N2
0356+10	3C98.0	03 56 11.0 0.4	C2	10 17 41 10	C7	-31	9.56 0.29	N1
0400+25	DW0400+25	04 00 03.5 0.2	C4	25 51 47 4	C4	-19	1.82 0.06	N2
0402+37	4C37.11	04 02 30.0 0.2	C4	37 55 18 15	N2	-10	1.73 0.05	N2
0404+42	3C103.0	04 04 35.1 0.5	C3	42 52 27 6	C3	-6	5.22 0.37	N1
0404+03	3C105.0	04 04 44.8 0.7	C3	03 33 26 8	C3	-33	4.93 0.11	N2
0406+38	4C38.13	04 06 02.5 0.3	C4	38 40 37 4	C4	-9	1.70 0.05	N2
0410+11	3C109.0	04 10 55.0 0.2	C2	11 04 36 15	N2	-27	4.09 0.09	N2
0411+14	PK0411+14	04 11 41.2 0.2	C2	14 08 42 20	N2	-25	2.15 0.06	N2
0411+05†	PK0411+05	04 11 58.4 0.2	C4	05 27 20 15	N2	-31	1.71 0.05	N2
0415+37	3C111.0	04 15 01.1 0.6	C2	37 54 37 5	C7	-8	14.58 0.65	N1
0420+41	4C41.11	04 20 28.7 0.3	C4	41 43 12 4	C4	-5	1.71 0.05	N2
0428+20†	PK0428+20	04 28 06.6 0.2	C4	20 31 12 4	C4	-18	3.81 0.09	N2
0430+05	3C120	04 30 31.5 0.2	C1	05 14 59 2	C1	-27	5.48 0.31	N1
0433+29	3C123.0	04 33 55.2 0.2	C1	29 34 14 2	C1	-11	45.67 0.78	N1
0440-00	NRAO190	04 40 05.3 0.2	C4	-00 23 15 4	C4	-28	3.18 0.08	N2
0448+52†	3C130.0	04 48 53.8 0.7	C3	52 00 00 10	C3	5	2.89 0.07	N2
0450+31	3C131.0	04 50 10.6 0.2	C1	31 24 32 3	C1	-7	2.90 0.15	N1
0453+22	3C132.0	04 53 42.4 0.2	C1	22 44 42 2	C1	-12	3.25 0.09	N1
0458-02†	PK0458-02	04 58 41.4 0.2	C4	-02 03 31 5	C4	-25	1.87 0.06	N2
0459+25	3C133.0	04 59 54.2 0.2	C1	25 12 12 2	C1	-9	5.55 0.14	N1
0500+01	OG003	05 00 46.5 0.8	N2	01 58 54 15	N2	-22	2.21 0.06	N2
0507+29	4C29.17	05 07 30.4 1.0	N2	29 05 11 15	N2	-6	1.90 0.06	N2
0511+00†	3C135.0	05 11 33.3 0.7	C3	00 53 01 10	C3	-21	2.80 0.20	C3
0512+24	3C136.1	05 12 57.5 0.4	C4	24 55 15 15	N1	-7	2.95 0.23	N1
0515+50	3C137.0	05 15 38.0 0.3	C1	50 51 30 3	C1	7	2.22 0.14	N1
0516+27†	4C27.15	05 16 27.0 0.9	N2	27 40 55 30	N2	-5	1.84 0.06	N2
0518+16	3C138.0	05 18 16.5 0.1	C1	16 35 26 2	C1	-11	8.88 0.19	N2
0528+06	3C142.1	05 28 48.0 0.2	C1	06 28 16 3	C1	-14	3.61 0.33	N1
0529+07†	OG050	05 29 57.4 1.2	N2	07 30 16 15	N2	-13	2.12 0.06	N2

0229+34. Corresponds to northern component of M2.
0330+16. M1 and M18 give smaller component separation.
0326+39. 0.33-f.u. source, SEP=14′, PA=195°.
0327+40. 0.15-f.u. source, SEP=18′, PA=125°.
0336−01. 0.58-f.u. source, SEP=15′, PA=330°, and 0.30-f.u. source, SEP=14′, PA=125°.
0356+10. M2 gives larger component separation.
0404+03. All position refers to the unresolved south-following component.

TABLE II (*continued*)

Source	Structure Class	EW	Ref.	NS	Ref.	T_B	Polarization %	PA(°)	Ref.	References
10	11	12	13	14	15	16	17	18	19	20
0229+34		<0.25	C1	<0.42	C1	H				M2*S3 SC3
0240-00		<0.25	C1	<0.35	C1	H	<1.0		5	A12 S3 SC2
0246+42	D	1.4	C4	<3.6	N2					
0247+39	D	2.1	C3	<0.50	C3					M29
0255+05	C	2.9	C3	2.2	C3	L	<0.9		5	M29 S2 SC3 PEAK = 5.64
0258+35		<0.25	C4	<1.0	C4					P2,7
0300+16	D	1.2*	C2	0.9*	C7	L	12.7	61	2	M1,18 S3
0305+03	H	1.3	C3	0.9	C3	L	2.9	123	5	M29 S2 SC3
0307+16	D	0.94	C2	<0.7	C8	L	6.9	159	2	M1 S3 SC2,3
0309+39		0.70	C4	<1.0	C4					
0315+41	D	4.2	C2	7.0	C7	L				M22 PEAK = 6.34
0316+16		<0.25	C1	<0.30	C1	H	<0.6		2	A1,6,8 S4,5 SC1,2,3 VLB1,2,4
0316+41	H	6.3	C3	3.8	C3	L	0.8	99	1	M3,22,29 S4 P8 VLB1,4 VAR1,2 PEAK = 11.81
0319+12		<0.25	C1	<0.30	C1					SC3
0320+05		<0.25	C1	<0.30	C1	H	0.9	174	2	SC3,4
0325+02	D	2.3	C3	1.1	C3	L	4.1	146	5	M29 S3 PEAK = 4.45
0326+39		7.1	N2	<4.0	N2					PEAK = 1.44
0327+40		<0.25	C4	4.6	N2					PEAK = 1.57
0331-01	D	0.79	C2	0.90	C7	L	<1.0		2	S3
0333+32		<0.25	C4	<1.0	C4					A1 S4 SC2,3 VLB1,2,3,4 VAR1,2
0333+12		<0.25	C1	<0.30	C1					SC1,3,4
0336-01		<0.30	C1	<0.35	C1	H	2.0	16	2	A10 S9 VLB3,4 VAR1,2
0340+04		0.27	C1	0.32	C1	H	2.7	162	2	S3
0341+67		14.1	N2	15.4	N2					PEAK = 0.97
0345+33		<0.25	C1	<0.25	C1		2.5	78	1	A2 SC1,2,3
0347+05		<0.25	C2	<4.2	N2	H	2.9	137	2	SC2,3,4
0356+10	D	1.3*	C2	3.1*	C7	L	5.4	74	5	M2 S3 PEAK = 8.62
0400+25		0.50	C4	<1.1	C4					
0402+37		0.60	C4	<4.3	N2					
0404+42	H	4.0	C3	6.0	C3		3.9	142	1	M1,21,29 PEAK = 4.59
0404+03	C?	3.5	C3	2.7	C3	L	4.3	60	2	A11*M29 S3 SC(3)
0406+38		<0.25	C4	<1.0	C4					
0410+11	D	0.71	C2	1.3	C8	L	5.5	19	2	M1 S3 SC3
0411+14		0.87	C2	<3.6	N2	L	9.0	61	2	
0411+05		<0.25	C4	<3.9	N2					SC3 VAR3
0415+37	T	2.8	C2	1.6	C7	L	1.9	80	1	M2,10 S3 SC3 VLB5,6
0420+41		<0.25	C4	<1.0	C4					
0428+20		0.40	C4	<1.0	C4					A11 VLB4
0430+05		<0.25	C1	<0.25	C1	H	3.3	9	2	A1 S2,3,4 SC2,3,4 VLB(1),2,3,4 VAR1,2
0433+29		<0.25	C1	0.45	C1	H	<1.2		6	A12 M2,5 S3 SC2,3
0440-00		<0.25	C4	<1.3	C4	H	<0.5		2	A1 S2,4 VLB2,3,4 VAR1,2
0448+52	C	1.6	C3	2.9	C3		1.7	176	1	M29 PEAK = 2.66
0450+31		<0.25	C1	<0.50	C1					SC3
0453+22		<0.25	C1	<0.35	C1		2.6	112	2	M2,15,16
0458-02		<0.25	C4	<1.3	C4					VAR2,3
0459+25		<0.25	C1	<0.25	C1		2.2	112	1	M2,18 SC3
0500+01		<4.6	N2	<4.1	N2	(H)				
0507+29		<3.3	N2	<3.1	N2					SC3 P9
0511+00	D	1.4	C3	0.83	C3	L	2.8	13	2	M29 S3
0512+24	C	4.7	C4				8.2	26	2	
0515+50		0.70	C1	0.33	C1					P3
0516+27		<3.4	N2	<5.1	N2					P9 SC(3)
0518+16		<0.25	C1	<0.30	C1	H	6.4	167	5	A1,2,3 S2,4,5 SC1,2,3,4 VLB1,4
0528+06		0.52	C1	0.52	C1		3.3	83	2	PEAK = 3.07
0529+07		4.4	N2	<3.1	N2					PEAK = 1.95

0411+05. 0.58-f.u. source, SEP=11′, PA=280°.
0428+20. 0.26-f.u. source, SEP=18′, PA=90°.
0448+52. 0.34-f.u. source, SEP=19′, PA=5°.
0458−02. 0.22-f.u. source, SEP=14′, PA=210°.
0511+00. 0.60-f.u. source, SEP=8′, PA=300°.
0516+27. 0.30-f.u. source, SEP=18′, PA=160°, and 0.32-f.u. source, SEP=19′, PA=110°.
0529+07. 0.36-f.u. source, SEP=18′, PA=140°.

TABLE II (*continued*)

Source		Coordinates (1950.0) Right Ascension	Ref.	Declination	Ref.	Galactic Latitude	Flux Density	Ref.
1	2	3	4	5	6	7	8	9
0530+04†	PK0530+04	$05^h30^m25^s.4 \pm 0^s.3$	C1	04° 03' 51" ±2"	C1	-15°	1.93 ± 0.06	N2
0531+21	CRAB NEB.	05 31 31.0 1.0	C2	21 59 17 15	N1	-5	930	KPW
0531+19	PK0531+19	05 31 47.4 0.2	C4	19 25 18 4	C4	-7	6.73 0.14	N2
0538+49	3C147.0	05 38 43.6 0.3	C1	49 49 43 2	C1	10	22.05 0.40	N1
0539-01	3C147.1	05 39 11.0 0.8	C2	-01 55 36 10	C7	-16	58.20 1.16	N2
0540+18	4C18.16	05 40 30.9 0.3	C4	18 44 23 4	C4	-5	2.24 0.06	N2
0548+16	4C16.14	05 48 25.1 0.2	C4	16 35 51 4	C4	-5	2.13 0.06	N2
0605+48	3C153.0	06 05 44.6 0.2	C1	48 04 50 2	C1	13	4.01 0.09	N2
0621+40†	3C159	06 21 34.3 0.3	C1	40 05 32 3	C1	12	1.98 0.06	N2
0640+23	3C165.0	06 40 04.9 0.4	C3	23 22 08 5	C3	8	2.40 0.20	C3
0640+59*#	DA,UNPUBL.	06 40 37.0 3.0	N2	59 54 15 25	N2	22	2.64* 0.07	N2
0642+29	4C29.24	06 42 00.5 0.3	C4	29 32 04 15	N2	11	1.73 0.05	N2
0642+21	3C166.0	06 42 24.7 0.2	C1	21 24 54 4	C1	8	2.43 0.06	N2
0648+19*	H0648+19	06 48 22.3 1.8	N2	19 38 30 45	N2	8	1.70 0.08	N2
0651+54	3C171.0	06 51 10.8 0.2	C1	54 12 50 2	C1	22	3.66 0.14	N1
0655+69†	4C69.10	06 55 56.4 0.6	C4	69 56 33 25	N2	26	1.70 0.11	N2
0658+38	3C173.0	06 58 56.4 2.5	N1	38 01 25 15	N1	18	1.76 0.11	N1
0659+25†	3C172.0	06 59 04.0 0.3	C2	25 18 06 5	C7	13	2.89 0.07	N2
0659+44†	4C44.15	06 59 16.4 0.2	C4	44 35 33 4	C4	20	2.47 0.07	N2
0703+42†	4C42.23	07 03 12.5 0.7	C4	42 36 10 15	N2	20	2.85 0.07	N2
0710+11	3C175.0	07 10 15.6 0.4	C1	11 51 20 3	C1	10	2.40 0.06	N2
0711+35	OI318	07 11 07.7 1.5	N2	35 40 35 15	N2	19	1.87 0.06	N2
0711+14	3C175.1	07 11 14.5 0.4	C1	14 41 33 2	C1	11	2.04 0.06	N2
0723+67	3C179	07 23 04.9 0.8	C1	67 54 53 2	C1	28	2.38 0.06	N2
0723-00	DW0723-00	07 23 18.0 0.8	N2	-00 49 01 30	N2	7	3.10 0.08	N2
0724-01	3C180.0	07 24 33.5 0.2	C3	-01 58 36 6	C3	6	2.65 0.07	N2
0725+14	3C181.0	07 25 20.3 0.2	C1	14 43 46 2	C1	14	2.29 0.06	N2
0732+33	4C33.21	07 32 42.0 0.2	C4	33 14 55 30	N2	23	2.32 0.06	N2
0735+17	PK0735+17	07 35 14.1 0.3	C1	17 49 11 3	C1	18	1.92 0.06	N2
0736+01	PK0736+01	07 36 42.6 0.2	C1	01 44 00 2	C1	11	2.89 0.07	N2
0738+31	OI363	07 38 00.0 0.2	C4	31 18 48 15	N2	23	2.20 0.06	N2
0742+10	DW0742+10	07 42 48.2 0.2	C4	10 18 33 4	C4	16	3.17 0.08	N2
0744+55*	DA 240	07 44 55.5 3.0	N2	55 58 43 30	N2	30	4.74* 0.15	N2
0755+37†	4C37.21LS	07 55 10.6 1.0	N2	37 54 52 15	N2	28	2.54 0.07	N2
0758+14	3C190.0	07 58 45.1 0.2	C1	14 23 02 2	C1	21	2.47 0.07	N2
0802+10	3C191.0	08 02 03.6 0.2	C4	10 24 10* 4	C4	20	1.79 0.08	N2
0802+24	3C192.0	08 02 35.1 0.4	C2	24 18 34 5	C7	26	4.89 0.11	N2
0806+42	3C194.0	08 06 38.0 0.3	C1	42 36 56 2	C1	31	2.05 0.06	N2
0809+48	3C196.0	08 09 59.4 0.2	C1	48 22 07 2	C1	33	13.85 0.28	N2
0812+02†	PK0812+02	08 12 47.2 0.2	C1	02 04 13 5	C1	19	1.87 0.06	N2
0812-02	3C196.1	08 12 57.2 0.2	C1	-02 59 16 2	C1	17	1.82 0.07	N1
0814+42	VR042.08.2	08 14 52.3 1.1	N2	42 32 11 15	N2	33	2.48 0.08	N2
0818+47	3C197.1	08 18 01.4 0.7	C4	47 12 12 4	C4	34	1.87 0.07	N1
0819+06	3C198.0	08 19 51.9 0.4	C3	06 06 31 10	C3	22	2.08 0.10	N1
0820+22	PK0820+22	08 20 28.3 0.2	C4	22 32 46 4	C4	29	2.31 0.06	N2
0821+39	4C39.23	08 21 48.7 1.8	C4	39 27 51 20	N2	34	2.65* 0.08	N2
0824+29	3C200.0	08 24 21.6 0.2	C4	29 28 36 10	C5	32	2.00 0.11	N1
0827+37†	4C37.24	08 27 55.1 0.2	C1	37 52 17 2	C1	35	2.22 0.06	N2
0828+32†	4C32.25LS	08 28 17.8 1.4	N2	32 29 38 20	N2	34	2.06 0.06	N2
0831+55	4C55.16	08 31 04.4 0.3	C4	55 44 42 4	C4	36	8.04 0.17	N2
0831+17†	3C202	08 31 58.5 0.3	C1	17 11 11 2	C1	30	2.23 0.15	N1
0835+58	3C205.0	08 35 09.6 1.0	C1	58 04 48 2	C1	36	2.34 0.07	N2
0838+13	3C207.0	08 38 01.8 0.2	C1	13 23 06 2	C1	30	2.46 0.08	N2
0850+14*	3C208.0	08 50 23.4 0.5	C1	14 04 16 2	C1	33	2.29 0.06	N2
0851+14*	3C208.1	08 51 54.0 0.5	C1	14 17 16 3	C1	33	2.06 0.06	N2

0530+04. 0.22-f.u. source, SEP=17′, PA=10°.
0531+21. Integrated polarization. Detailed 1407-MHz polarization map in Wright (1970).
0621+40. 1.13-f.u. source=4C40.16, SEP=17′, PA=10°.
0640+59. See Fig. 5. North-preceding component of 1.5 f.u. is 4C60.10; the south-following component of 1.1 f.u. is 4C59.07 lobe shifted.
0642+21. A2 gives 13″×9″ in PA=8°.
0648+19. See Fig. 5.
0655+69. 0.43-f.u. source, SEP=15′, PA=180°.
0659+25. 0.17-f.u. source, SEP=17′, PA=30°.
0659+44. 0.16-f.u. source, SEP=19′, PA=105°.
0703+42. 0.34-f.u. source, SEP=13′, PA=25°.

TABLE II (*continued*)

Source	Structure Class	EW	Ref.	NS	Ref.	T_B	Polarization %	PA(°)	Ref.	References
10	11	12	13	14	15	16	17	18	19	20
0530+04		<0.'25	C1	<0.'30	C1					
0531+21		3.4	C2	3.7	C8		1.6*	86	2	M16,23 SC3
0531+19		<0.25	C4	<1.0	C4	H	1.2	125	2	
0538+49		<0.25	C1	<0.25	C1	H	0.8	83	1	A1,2,3,12 S4,5 SC1 VLB1,4
0539-01		3.7	C2	3.4	C7					PEAK = 56.54
0540+18		<0.6	C4	<3.6	N2					SC3
0548+16		<0.25	C4	<1.1	C4					SC3
0605+48		<0.25	C1	<0.25	C1		1.6	112	1	A2 S3 P3 SC(1)
0621+40		0.45	C1	0.45	C1					S3
0640+23	D	0.43	C3	0.81	C3					M29 S3 SC3
0640+59	D	17.4	N2	9.7	N2					
0642+29		<0.25	C4	<3.4	N2					SC3
0642+21		<0.25	C1	0.57*	C1		6.2	76	1	A2 SC3
0648+19		8	N2	15	N2					PEAK = 0.78
0651+54		<0.25	C1	<0.30	C1	H	3.5	48	1	A2,12 S3
0655+69		<0.25	C4	<6.8	N2					
0658+38										A2 S3 PEAK = 1.51
0659+25	D	0.45	C2	1.3	C7		6.8	145	5	M2,4
0659+44		<0.25	C4	<1.0	C4	H				P2
0703+42	T	4.2	C4	<4.3	N2	L				PEAK = 2.53
0710+11		0.80	C1	0.38	C1		3.7	38	5	M2 S1 SC3
0711+35		3.0	N2	<4.0	N2					P4 SC3 PEAK = 1.79
0711+14		<0.25	C1	<0.30	C1		2.6	90	1	A2 SC3
0723+67		0.27	C1	<0.30	C1	H				S3
0723-00		<2.4	N2	<3.7	N2					VAR2
0724-01	D	<0.41	C3	1.2	C3		<2.1		1	M29
0725+14		<0.25	C1	<0.30	C1		1.3	142	1	A2,12 M4 S3 SC1,2,3,4
0732+33		<0.25	C4	<4.0	N2	H				SC1,3
0735+17		<0.25	C1	<0.50	C1		3.2	31	2	A10 P8 SC2,3,4 VLB2,3 VAR1,2
0736+01		<0.25	C1	<0.35	C1		5.2	125	2	A10 S9 SC3 VLB3 VAR1,2
0738+31		<0.25	C4	<3.4	N2	H				P4 SC3 VAR2
0742+10		<0.25	C4	<1.1	C4					A10 VLB3,4
0744+55	D	17.2	N2	8.0	N2					
0755+37		<2.2	N2	<4.0	N2	*				S3
0758+14		<0.25	C1	<0.35	C1	H	<2.3		5	A2,12 S3 SC2,3,4
0802+10		<0.25	C4	<1.1	C4					A1,2,3,12 S2 SC1,2,3,4
0802+24	D	1.4	C2	1.3	C7	L	1.0	141	5	M2,17,18 S2
0806+42		<0.25	C1	<0.35	C1	H				M2 S3
0809+48		<0.25	C1	<0.25	C1	H	<1.2		1	A2,12 M5 S1,3 SC1
0812+02		<0.30	C1	0.65	C1					S9 SC3
0812-02		<0.25	C1	<0.35	C1		<6.3		1	
0814+42		<3.2	N2	<4.8	N2	(H)				
0818+47		<0.25	C4	<1.0	C4					A2
0819+06	D	2.0	C3	2.6	C3	L				M29 S3
0820+22		<0.25	C4	<1.0	C4	H				P7 SC3
0821+39	D	5.2	C4	4.2	N2	L				P7
0824+29		<0.25	C4	<2.0	C5	H				A2
0827+37		<0.25	C1	<0.35	C1	H				S9 SC3
0828+32		5.0	N2	3.0	N2	L				PEAK = 1.78
0831+55		<0.25	C4	<1.0	C4	H				VLB5
0831+17		<0.25	C1	<0.42	C1	H				M2 SC1,3 PEAK = 1.65*
0835+58		<0.25	C1	0.35	C1	H	6.9	42	1	M2,4 S3
0838+13		<0.25	C1	<0.30	C1	H	1.8	93	2	A2,12 M4 S3 SC3
0850+14		<0.30	C1	<0.42	C1	H	<1.9		5	A2,12 M4 S3,6 SC1,2,3,4
0851+14		<0.30	C1	<0.42	C1	H				A2 S3 SC3

0744+55. 2.98-f.u.+1.76-f.u. double; both components are extended. See Fig. 5.
0755+37. 1.60-f.u. source, SEP=18′, PA=120°. Brightness classification unknown.
0802+10. Our position is 12″.5 north of A1, 15″.5 north of A12.
0812+02. 0.40-f.u. source, SEP=11′, PA=85°.
0821+39. 1.5-f.u.+1.2-f.u. double, SEP=6′.7, PA=51°, from CIT data (see Table IV).
0827+37. 0.15-f.u. source, SEP=16′, PA=25°.
0828+32. 0.17-f.u. source, SEP=14′, PA=55°.
0831+17. 5′.9 extent of source found in 300-ft. data may be spurious. 0.59-f.u. source=3C201, SEP=19′, PA=335°.
0850+14 & 0851+14. SEP=26′, PA=60°.

TABLE II (*continued*)

Source		Coordinates (1950.0) Right Ascension	Ref.	Declination	Ref.	Galactic Latitude	Flux Density	Ref.
1	2	3	4	5	6	7	8	9
0855+28†	3C210.0	$08^h55^m12^s.0 \pm 0^s.5$	C5	28° 02′ 33″ ±9″	C5	38°	1.74 ± 0.06	N2
0855+14	3C212.0	08 55 55.7 0.2	C1	14 21 24 3	C1	34	2.47 0.07	N2
0858+29	3C213.1	08 58 05.2 0.4	C1	29 13 33 2	C1	39	1.89 0.07	N1
0904+41*†	4C41.19	09 04 20.9 1.6	N2	41 46 07 20	N2	42	1.85 0.07	N2
0905+38	3C217.0	09 05 41.1 0.2	C1	38 00 30 2	C1	42	2.12 0.06	N2
0906+43	3C216.0	09 06 17.3 0.2	C1	43 05 59 2	C1	42	3.76 0.09	N2
0917+45	3C219.0	09 17 50.7 0.4	C2	45 51 47 5	C7	44	8.02 0.26	N2
0923+39	4C39.25	09 23 55.4 0.2	C4	39 15 21 4	C4	46	2.52 0.07	N2
0927+36	3C220.2	09 27 30.0 0.3	C1	36 14 39 2	C1	46	1.75 0.08	N1
0936+36	3C223.0	09 36 50.6 0.4	C2	36 07 41 10	C7	48	3.35 0.08	N2
0938+39	3C223.1	09 38 18.2 0.2	C2	39 58 12 8	C5	48	1.86 0.14	N1
0939+14	3C225.0	09 39 30.3 0.4	C2	14 00 54 20	N2	44	4.34 0.12	N2
0941+10	3C226.0	09 41 36.2 0.2	C1	10 00 08 3	C1	42	2.25 0.06	N2
0945+07*†	3C227.0	09 45 07.8 0.6	C3	07 39 09 5	C3	42	7.40 0.16	N2
0945+40	4C40.24	09 45 50.1 0.5	C4	40 53 46 20	N2	50	1.96 0.06	N2
0947+14	3C228.0	09 47 27.6 0.2	C1	14 34 00 3	C1	45	3.47 0.08	N2
0949+24	3C229	09 49 10.5 0.2	C4	24 36 40 8	C6	49	1.78 0.08	N1
0949+00†	3C230.0	09 49 25.2 0.3	C1	00 12 35 3	C1	39	3.03 0.08	N1
0951+69	3C231.0	09 51 43.0 0.7	C1	69 54 59 3	C1	40	7.94 0.17	N2
0954+55	4C55.17	09 54 15.5 1.4	N2	55 37 06 15	N2	47	3.52 0.08	N2
0958+29	3C234.0	09 58 56.8 0.4	C2	29 01 40 4	C7	52	5.35 0.12	N2
1003+35*†	3C236.0	10 03 05.5 0.2	C1	35 08 49 2	C1	53	3.24 0.08	N2
1005+07	3C237.0	10 05 22.1 0.1	C1	07 44 58 2	C1	46	6.25 0.15	N1
1008+06	3C238.0	10 08 23.1 0.3	C1	06 39 28 2	C1	46	2.93 0.09	N2
1030+58	3C244.1	10 30 19.5 0.4	C1	58 30 06 4	C1	50	3.74 0.09	N2
1039+02	PK1039+02	10 39 04.1 0.3	C1	02 58 16 2	C1	50	2.84 0.07	N2
1040+12	3C245.0	10 40 06.1 0.2	C1	12 19 15 2	C1	56	3.06 0.08	N2
1055+20†	PK1055+20	10 55 37.4 0.2	C4	20 08 02 15	N2	63	2.19 0.06	N2
1055+01	PK1055+01	10 55 55.4 0.2	C1	01 50 05 3	C1	52	3.10 0.08	N2
1056+43	3C247.0	10 56 08.3 0.2	C2	43 17 29 4	C7	62	2.82 0.12	N1
1059-01	3C249.0	10 59 30.6 0.2	C1	-01 00 08 4	C1	51	2.56 0.07	N2
1106+37	4C37.29	11 06 58.6 1.2	C4	37 56 14 20	N2	66	3.22 0.14	N2
1107+11	PK1107+10	11 07 12.6 1.3	N2	11 00 14 15	N2	61	1.71 0.05	N2
1111+40	3C254.0	11 11 53.2 0.1	C1	40 53 41 2	C1	65	3.05 0.13	N2
1113+29	4C29.41	11 13 53.9 0.3	C2	29 31 36 15	N2	69	1.97 0.06	N2
1116+12	PK1116+12	11 16 20.8 0.2	C1	12 51 09 2	C1	63	2.25 0.06	N2
1117+14	PK1117+14	11 17 51.0 0.2	C1	14 37 22 2	C1	65	2.35 0.06	N2
1128+45*	DA,UNPUBL.	11 28 56.3 1.2	N2	45 31 44 15	N2	65	2.00 0.06	N2
1137+66†	3C263.0	11 37 10.8 0.3	C2	66 04 28 5	C7	49	2.98 0.11	N2
1138+01	PK1138+01	11 38 34.4 0.3	C1	01 30 57 2	C1	59	2.47 0.07	N2
1140+22	3C263.1	11 40 49.2 0.1	C1	22 23 37 2	C1	73	2.96 0.07	N2
1141+37	4C37.32	11 41 49.6 0.8	C4	37 25 50 15	N2	72	2.11 0.06	N2
1142+19	3C264.0	11 42 32.1 0.6	C3	19 53 56 10	C3	73	5.78 0.29	N1
1142+31	3C265.0	11 42 52.6 0.3	C2	31 50 25 7	C7	74	2.80 0.08	N1
1147+13	3C267.0	11 47 22.1 0.2	C2	13 04 00 4	C7	69	2.16 0.07	N1
1148-00†	PK1148-00	11 48 10.1 0.2	C4	-00 07 11 4	C4	58	3.06 0.08	N2
1150+49†	4C49.22	11 50 48.6 1.3	N2	49 48 14 20	N2	64	1.97 0.08	N2
1152+55*†	4C55.22	11 52 46.9 1.3	C4	55 10 44 30	N2	60	2.24 0.08	N2
1153+31	4C31.38	11 53 44.1 0.2	C4	31 44 45 4	C4	77	2.77 0.07	N2
1201-04	PK1201-041	12 01 28.5 0.2	C1	-04 06 00 3	C1	56	2.10 0.06	N2
1203+64	3C268.3	12 03 54.0 0.7	C1	64 30 20 2	C1	52	3.53 0.15	N2
1206+43	3C268.4	12 06 42.3 0.2	C4	43 55 56 4	C4	71	2.04 0.09	N2
1213+53	4C53.24	12 13 00.9 0.7	C4	53 53 07 15	N2	62	2.65 0.07	N2
1215+03†	PK1215+03	12 15 01.2 0.5	C3	03 54 57 15	C3	65	2.34 0.06	N2
1216+06	3C270.0	12 16 51.2 1.0	C3	06 06 13 6	C3	67	17.50 0.45	N1

0855+28. 0.25-f.u. source, SEP=16′, PA=335°.
0855+14. Corresponds to early component of M2. Two discrepant polarization measures: 5.7%±1.7% in PA=94° (Ref. 1) and <1.0% (Ref. 2).
0858+29. A2 gives <7″ EW by <14″ NS.
0904+41. 0.41-f.u. source, SEP=20′, PA=45°. See Fig. 5.
0938+39. M1 gives 71″ separation in PA=13°.
0945+07. 0.48-f.u. source, SEP=18′, PA=80°. See Fig. 5.
0949+00. 0.77-f.u. source=NRAO 340=PK0950+00, SEP=12′, PA=80°.
1003+35. 1.33-f.u. source, SEP=12′, PA=305°; and 0.88-f.u. source=NRAO 346, SEP=22′, PA=125°. See Fig. 5.

TABLE II (*continued*)

Source	Class	Structure EW	Ref.	Structure NS	Ref.	T_B	Polarization %	PA(°)	Ref.	References
10	11	12	13	14	15	16	17	18	19	20
0855+28		<3.1	N2	<5.1	N2		<4.1		1	A2,12 S3 SC2
0855+14		<0.25	C1	0.50	C1	H	*			A12 M2*,12,13 S3 SC3,4
0858+29		<0.25	C1	0.42*	C1					A2 SC3
0904+41		4.7	N2	5.9	N2					PEAK = 1.49
0905+38		0.27	C1	<0.25	C1	L				M2 S3
0906+43		<0.25	C1	<0.25	C1	H	1.0	96	3	A2,3,12 S3 SC1
0917+45	D	1.0	C2	1.6	C7	L	3.0	114	3	M1 S3
0923+39		<0.25	C4	<1.0	C4	H				A10 S9 P2,7 VLB3,4 VAR2
0927+36		<0.25	C1	<0.30	C1					A2,12 S3
0936+36	D	1.0	C2	3.6	C7	L	7.5	114	1	M2 S3 PEAK = 3.16
0938+39		0.65*	C2	<2.0*	C5					M1
0939+14	D	1.6	C2	6.1	C7	L	1.5	44	2	M1,24 S3 P8 SC1,2,3,4 PEAK = 3.78
0941+10		<0.35	C1	0.55	C1	L				M2 S3 SC3
0945+07	T	3.0	C3	<0.50	C3	L	5.3	140	5	M29 S3 SC(3)
0945+40	D	2.5	C4	3.1	N2					PEAK = 1.89
0947+14		<0.25	C1	0.90	C1	H	2.7	124	2	M2 S3 SC3,4
0949+24		0.75	C4							
0949+00		<0.30	C1	<0.35	C1	H	1.4	31	2	A1,4,12 S3 SC1,2,3,4
0951+69		0.58	C1	0.45	C1	L	1.0	161	1	M1 S3
0954+55		<2.2	N2	<3.0	N2	(H)				
0958+29	D	1.2	C2	0.7	C7	L	3.9	133	1	M1 S3 P8 SC(3)
1003+35		<0.25	C1	<0.25	C1	H				A2,3 P8
1005+07		<0.25	C1	<0.30	C1	H	<1.5		5	A3,12 S3,4,5 SC1,2,3,4 VLB1
1008+06		<0.25	C1	<0.42	C1	H	1.2	10	2	A3,12 S3 SC1,2,3,4
1030+58		<0.25	C1	1.1	C1	H	3.8	112	1	M1 S3
1039+02		<0.25	C1	<0.35	C1	H	1.6	25	2	P8*SC3
1040+12		<0.25	C1	<0.30	C1	H	4.3	99	5	A2 M3,13 S3,7 P1 SC1,2,3,4
1055+20		<0.25	C4	<3.1	N2	H				S9 P2 SC3 VLB(1)
1055+01		<0.25	C1	<0.50	C1	H	4.6	1	2	A1,12 S4 P1 SC2,3,4 VLB1,3,4 VAR1,2
1056+43		<0.30	C2	<0.40	C7	H*	<2.0		1	M2,4,5 S3 PEAK = 2.56*
1059-01		0.30	C1	<0.67	C1	L	5.6	76	5	A12 S3 SC2,3
1106+37	T	5.2	C4	6.7*	N2	L				PEAK = 2.51
1107+11		5.9	N2	<3.0	N2					A7 SC3 PEAK = 1.48
1111+40		0.23	C1	<0.25	C1	H	4.0	77	1	A12 M2,3 S3
1113+29	D	0.74	C2	<3.7	N2					M21 P7
1116+12		<0.25	C1	<0.30	C1	H	<2.6		2	A1,12 M9 S9 P1 SC2,3,4 VLB3
1117+14		<0.25	C1	<0.35	C1	H				P1 SC3,4
1128+45		<3.1	N2	<3.3	N2	*				
1137+66	D	0.66	C2	<0.30	C7	L	1.5	140	1	M1,4,10 S3
1138+01		<0.25	C1	<0.35	C1	H				S3 P1,8
1140+22		<0.30	C1	<0.30	C1	H	<1.5		2	A2,12 S3 SC1,2,3
1141+37	D	3.1	C4	<4.6	N2	L				
1142+19	C	2.2	C3	2.4	C3	L	<1.4		5	M1,29 S2 P5 PEAK = 5.30
1142+31	D	1.1	C2	0.50	C7	L				M2 S3 P8
1147+13	D	0.64	C2	<0.50	C7	L	4.0	156	2	M1,24 S3 P1,8 SC1,2,3,4
1148-00		<0.25	C4	<1.3	C4	H	2.1	159	2	A1 S4 P1 VLB1,3,4 VAR1
1150+49		<3.1	N2	<5.4	N2					S9 P2
1152+55	T	3.5	C4	<5.3	N2	L				
1153+31		<0.25	C4	<1.0	C4	H				A1,9,12 M9 S2,9 P7
1201-04		0.37	C1	0.38	C1	L				P1
1203+64		<0.25	C1	<0.30	C1	H				A2,3,11 S2
1206+43		<0.25	C4	<1.0	C4	H				A2 M4 S3
1213+53	D	2.6	C4	<4.6	N2	L				
1215+03	C?	2.5	C3	3.2	C3	L				M13,29 S7 P1 PEAK = 2.21
1216+06	D	5.0	C3	1.2	C3	L	8.2	121	5	M29 P1 PEAK = 14.66

1039+02. P8 position is 10″ south of C1.
1055+20. 0.25-f.u. source, SEP=19′, PA=300°.
1056+43. Halo reported in C2 is spurious. Mackay (1969) finds two confusing sources 11′ to the west. The 3.′2 extent found in the 300-ft. data may also be spurious.
1106+37. Position angle of major axis determined from 300′ data is 150°
1128+45. See Fig. 2 in text. Brightness classification is unknown.
1137+66. 0.47-f.u. source, SEP=14′, PA=145°.
1148−00. 0.26-f.u. source, SEP=18′, PA=210°.
1150+49. 0.33-f.u. source, SEP=18′, PA=330°.
1152+55. 1.16-f.u. source, SEP=16′, PA=75°. See Fig. 5.
1215+03. 0.28-f.u. source, SEP=15′, PA=295°.

TABLE II (*continued*)

Source		Coordinates (1950.0) Right Ascension	Ref.	Declination	Ref.	Galactic Latitude	Flux Density	Ref.
1	2	3	4	5	6	7	8	9
1218+33	3C270.1	$12^h18^m04.^s0 \pm 0.^s4$	C1	33° 59' 49" ±2"	C1	80	2.50 ± 0.07	N2
1222+13	3C272.1	12 22 32.0 0.4	C3	13 09 40 6	C3	74	6.24 0.23	N2
1225+36	ON343	12 25 30.8 0.2	C4	36 51 43 4	C4	79	2.06 0.06	N2
1226+02	3C273.0	12 26 32.9 0.1	C1	02 19 39 2	C1	64	38.84 0.70	N1
1228+12	VIRGO A	12 28 17.8 0.6	C3	12 39 50 10	C3	74	214	KPW
1229-02	PK1229-02	12 29 25.6 0.8	N2	-02 07 28 15	N2	60	1.76 0.05	N2
1232+21	3C274.1	12 32 57.0 0.5	C2	21 37 06 4	C7	83	2.97 0.08	N2
1239-04	3C275.0	12 39 44.8 0.3	C1	-04 29 53 2	C1	58	3.34 0.08	N2
1241+16	3C275.1	12 41 27.5 0.3	C1	16 39 17 2	C1	79	2.81 0.07	N2
1249+09	PK1249+09	12 49 11.2 0.4	C3	09 12 30 4	C3	71	1.70 0.05	N2
1250+56	3C277.1	12 50 15.0 0.3	C1	56 50 37 3	C1	60	2.42 0.12	N1
1251+15	3C277.2	12 51 03.1 0.4	C4	15 58 28 4	C4	78	1.84 0.06	N2
1251+27†	3C277.3	12 51 46.0 0.2	C1	27 53 48 3	C1	89	2.89 0.08	N2
1254+47	3C280.0	12 54 41.2 0.2	C1	47 36 32 2	C1	69	5.08 0.11	N2
1306+66†	3C282	13 06 31.3 0.5	C1	66 00 10 2	C1	51	2.24 0.08	N2
1308+27	3C284.0	13 08 40.6 0.7	C4	27 44 24 15	N1	85	1.93 0.07	N1
1313+07	PK1313+07	13 13 46.1 0.4	C3	07 18 18 6	C3	69	1.91 0.06	N2
1317-00*	PK1317-00	13 17 00.3 1.2	N2	-00 35 11 20	N2	61	1.92* 0.07	N2
1317+17	PK1317+17	13 17 54.1 0.9	N2	17 58 56 15	N2	78	1.79 0.06	N2
1318+11	PK1318+11	13 18 49.7 0.3	C1	11 22 29 2	C1	72	2.18 0.06	N2
1319+42	3C285.0	13 19 05.5 0.6	C2	42 50 46 3	C7	73	2.01 0.06	N2
1323+32†	4C32.44LS	13 23 58.7 0.5	C4	32 09 53 4	C4	81	4.56 0.10	N2
1328+25†	3C287.0	13 28 16.0 0.2	C1	25 24 37 2	C1	80	6.72 0.14	N2
1328+30	3C286.0	13 28 49.7 0.2	C1	30 46 02 2	C1	80	14.78 0.30	N2
1330+02	3C287.1	13 30 21.0 0.4	C3	02 16 12 4	C3	62	3.02 0.12	N1
1336+39	3C288.0	13 36 38.4 0.3	C1	39 06 22 2	C1	74	3.32 0.09	N2
1343+50	3C289.0	13 43 28.0 0.5	C1	50 01 31 2	C1	65	2.28 0.07	N2
1345+12	PK1345+12	13 45 06.3 0.2	C1	12 32 23 2	C1	70	5.01 0.11	N2
1349+64	3C292	13 49 16.6 2.8	N2	64 44 07 20	N2	51	2.31* 0.09	N2
1350+31	3C293.0	13 50 02.8 0.4	C3	31 41 43 4	C3	76	4.42 0.11	N1
1354+01	PK1354+01	13 54 28.3 0.3	C1	01 20 16 30	N2	59	2.47 0.15	N2
1354+19	PK1354+19	13 54 42.0 0.3	C1	19 33 44 3	C1	73	2.08 0.06	N2
1355+01	PK1355+01	13 55 20.5 0.2	C4	01 01 21 30	N2	59	1.98 0.07	N2
1358+62	4C62.22LS	13 58 57.8 0.3	C4	62 25 03 4	C4	53	4.32 0.13	N2
1409+52	3C295.0	14 09 33.6 0.3	C1	52 26 14 2	C1	60	22.18 0.39	N1
1413+34†	DA 362	14 13 56.0 1.0	N2	34 59 01 30	N2	70	2.09 0.07	N2
1414+11	PK1414+11*	14 14 27.3 0.5	C3	11 02 16 8	C3	64	4.32 0.18	N1
1416+06	3C298.0	14 16 38.8 0.1	C1	06 42 23 2	C1	60	5.66 0.15	N1
1419+41	3C299.0	14 19 06.5 0.3	C1	41 58 30 2	C1	66	2.95 0.10	N2
1420+19	3C300.0	14 20 40.8 0.2	C2	19 49 28 30	N2	67	3.44 0.08	N2
1422+20	PK1422+20	14 22 37.3 0.2	C4	20 14 01 8	C6	67	1.72 0.05	N2
1425-01	3C300.1	14 25 56.6 0.2	C1	-01 10 41 2	C1	53	3.30 0.17	N1
1427+07†	PK1427+07	14 27 32.7 0.6	C3	07 29 45 20	C3	59	1.99 0.12	N2
1434+03	PK1434+03	14 34 25.8 0.3	C1	03 37 12 2	C1	55	2.86 0.07	N2
1441+52	3C303.0	14 41 23.6 0.3	C1	52 14 19 2	C1	57	2.46 0.07	N2
1442+10	OQ172	14 42 50.2 0.8	N2	10 11 37 15	N2	58	2.43 0.06	N2
1448+63	3C305.0	14 48 17.1 0.3	C1	63 28 37 2	C1	49	2.94 0.09	N2
1452+16†	PK1452+16	14 52 02.7 1.3	N2	16 34 30 20	N2	59	1.88 0.10	N2
1452-04	3C306.1	14 52 24.7 0.4	C5	-04 09 20 15	N1	46	1.86 0.11	N1
1502+26	3C310.0	15 02 48.0 0.5	C2	26 12 36 8	C7	60	7.67 0.27	N1
1508+08	3C313.0	15 08 33.0 0.4	C2	08 03 07 4	C7	51	3.65 0.09	N2
1509+01†	PK1509+01	15 09 53.0 0.2	C1	01 32 23 2	C1	47	2.12 0.06	N2
1511+26	3C315.0	15 11 31.0 0.2	C2	26 18 37 8	C7	58	3.87 0.10	N2
1514+00	PK1514+00	15 14 06.7 0.4	C3	00 26 10 6	C3	45	2.44 0.07	N2
1514+07	3C317.0	15 14 17.0 0.1	C1	07 12 17 3	C1	50	5.35 0.14	N1

1222+13. There exists a 45° difference in position angle between structures determined at CIT and Cambridge. 300-ft data find the source extended 4'.3 EW.
1250+56. A2 gives <7" EW by <8".5 NS.
1251+27. 0.23-f.u. source, SEP=15', PA=290°.
1306+66. 0.20-f.u. source, SEP=15', PA=255°. 4'.8 EW extent of source found in 300-ft data may be spurious.
1317−00. 1.39-f.u.+0.53-f.u. double. See Fig. 5.
1323+32. 1.45-f.u. source, SEP=16', PA=100°.
1328+25. 1.02-f.u. source=4C25.44, SEP=19', PA=147°.
1349+64. C2 finds 1.8 f.u. in an 0'.7 diameter component and two sources within 4' EW contributing about 0.5 f.u.

TABLE II (*continued*)

Source	Class	Structure EW	Ref.	Structure NS	Ref.	T_B	Polarization %	PA(°)	Ref.	References
10	11	12	13	14	15	16	17	18	19	20
1218+33		<0.25	C1	<0.30	C1	H				A2 M3 S3
1222+13	D	<0.58*	C3	1.1*	C3	L	2.5	126	6	M1,29* S3 P1 PEAK = 5.76
1225+36		<0.25	C4	<1.0	C4	H				P4
1226+02		<0.25	C1	<0.35	C1	H	2.0	159	5	M3,11,13 S3,4,5 P1,8 SC1,2,3,4 VLB1,3,4 VAR1,2
1228+12	H	6.7	C3	7.7	C3	L	0.6	147	2	A10,13 M1,8,29 S4,8 SC3 VLB3
1229-02		<2.7	N2	<2.9	N2		1.6	24	2	S9 P1
1232+21	D	1.8	C2	0.90	C7	L	13.4	153	2	M1 S3
1239-04		<0.25	C1	<0.35	C1	H	<1.2		2	A12 S3 P1 SC1
1241+16		<0.25	C1	<0.35	C1	H	2.3	95	2	A2,12 M4,5 S3 P1 SC2,3
1249+09	D	0.96	C3	0.47	C3					M29 P1 SC(3)
1250+56		<0.25	C1	0.48*	C1	H				A2 S2,9
1251+15		2.1	C4	<1.1	C4					M2 P1 SC3
1251+27		0.38	C1	0.57	C1	L				A12 M2 S3
1254+47		<0.25	C1	<0.25	C1	H	2.4	11	1	A12 M2 S3,4 SC1
1306+66		<0.25	C1	<0.42	C1	H				P2 PEAK = 2.03*
1308+27	D	2.4	C4	<1.0	C4		3.3	3	1	M1
1313+07	D	1.6	C3	0.49	C3					M29 P1
1317-00	D	4.0	N2	6.2	N2					SC4
1317+17		<2.3	N2	<4.5	N2					P1
1318+11		<0.25	C1	<0.30	C1	H	4.6	69	2	P1,5 SC2,3
1319+42	D	1.6	C2	0.90	C7	L	5.8	40	1	M1 S3
1323+32		<0.25	C4	<1.3	C4	H				
1328+25		<0.25	C1	<0.25	C1	H	<1.3		5	A1,2,3,12 S2,4,5 SC1,2,3 VLB1,4
1328+30		<0.25	C1	<0.25	C1	H	9.0	34	1	A1,2,3,12 S4,5 SC1,2,3 VLB1,4
1330+02	C	1.0	C3	0.50	C3	L	4.2	148	2	M29 S3 P1
1336+39		<0.25	C1	<0.25	C1	H	<1.7		1	A2 S3
1343+50		<0.25	C1	<0.25	C1	H				A2 M4 S3 P3
1345+12		<0.25	C1	<0.30	C1	H	<0.9		2	P1,8 SC2,3,4 VLB5
1349+64		3.9	N2	4.7	N2	L				S3 P2 PEAK = 1.99
1350+31	H*	2.2	C3	2.2	C3	H	1.7	74	1	A3,12 M2,29 S3
1354+01		0.30	C1	<6.2	N2	L				P1,5
1354+19		<0.25	C1	0.48	C1	H	8.0	81	2	S9 P8 SC3 VAR2
1355+01		<0.25	C4	<4.7	N2					SC3
1358+62		<0.25	C4	<1.1	C4	H				
1409+52		<0.25	C1	<0.30	C1	H	<0.4		1	A2 M3,5 S2,4,5 SC1(1)
1413+34		<0.35	C4	<2.0	C4	(H)				
1414+11	D	2.1	C3	2.8	C3	L	10.2	30	2	M29 S3 P1 PEAK = 3.96
1416+06		<0.25	C1	<0.30	C1	H	<0.7		2	A1,3,12 S3,4,5 P1 SC1,2,3,4
1419+41		<0.25	C1	<0.25	C1	H				A2,11 S3 P8 SC1
1420+19		0.52*	C2	<3.7	N2	L	2.0	88	5	A12 M1 S3
1422+20		<0.25	C4	<1.0	C4					S9 P7
1425-01		<0.25	C1	<0.50	C1	H	<1.0		2	P1 SC2,4 PEAK = 2.81*
1427+07	C	1.8	C3	4.3	C3					M29 P1,5 PEAK = 1.76
1434+03		<0.25	C1	<0.30	C1	H	0.9	125	2	P1
1441+52		0.42*	C1	<0.30	C1	L	4.7	81	1	M2 S3
1442+10		<3.7	N2	<3.2	N2	(H)				
1448+63		<0.25	C1	<0.30	C1	H	1.7	167	1	A2 S3
1452+16		5.7	N2	4.5	N2					PEAK = 1.52
1452-04										P1
1502+26		1.7	C2	3.5	C7	L	<1.8		5	M2 S3 PEAK = 7.00
1508+08	D	1.6	C2	1.0	C7	L	2.1	37	2	S3
1509+01		<0.25	C1	<0.42	C1	H				P1
1511+26		0.90	C2	1.4	C7	L	4.9	113	5	M2 S3
1514+00	T	2.8	C3	2.6	C3	L	8.0	133	2	M29 P1 SC(3)
1514+07		<0.25	C1	0.50	C1	H	1.0	69	5	S3 P1 SC(1)

1350+31. M2 resolves into discrete components, A12 treats as not resolved.
1413+34. 0.26-f.u. source, SEP=20′, PA=75°.
1414+11. This source is frequently denoted as 3C296 but lies 2′.5 north of the position given by Bennett (1962).
1420+19. C2 does not separate the fainter component given by M1.
1425−01. 4′.2 extent of source found in 300-ft data may be spurious.
1427+07. 0.46-f.u. source, SEP=9′, PA=65°.
1441+52. M2 gives 12′ extent in PA=125°.
1452+16. 1.51-f.u. source=PK1453+16, SEP=25′, PA=80°.
1509+01. 0.25-f.u. source, SEP=15′, PA=305°.

TABLE II (*continued*)

Source		Coordinates (1950.0) Right Ascension	Ref.	Declination	Ref.	Galactic Latitude	Flux Density	Ref.
1	2	3	4	5	6	7	8	9
1517+20	3C318.0	$15^h17^m50^s.7 \pm 0^s.3$	C1	20° 26' 54" ± 2"	C1	55°	2.50 ± 0.07	N2
1518+04†	PK1518+047	15 18 44.6 0.2	C4	04 41 31 20	N2	47	4.01 0.09	N2
1522+54	3C319.0	15 22 44.4 0.3	C2	54 38 58 30	N2	51	2.38 0.06	N2
1523+03	PK1523+03	15 23 18.2 0.2	C1	03 18 59 2	C1	46	1.86 0.06	N2
1529+35	3C320.0	15 29 29.4 0.4	C4	35 44 07 15	N2	55	1.80 0.06	N2
1529+24†	3C321.0	15 29 39.0 0.4	C3	24 13 17 5	C3	53	3.59 0.08	N2
1533+55	3C322.0	15 33 46.4 0.3	C4	55 46 41 4	C4	49	1.94 0.13	N1
1538+14	4C14.60	15 38 28.4 0.9	N2	14 57 56 15	N2	48	1.77 0.06	N2
1543+00†	DW1543+00	15 43 36.1 0.3	C4	00 35 50 5	C4	40	1.71 0.05	N2
1545+21	3C323.1	15 45 31.3 0.2	C1	21 01 38 3	C1	49	2.49 0.07	N2
1547+21	3C324.0	15 47 37.3 0.3	C1	21 34 44 2	C1	49	2.28 0.06	N2
1548+05	DW1548+05	15 48 06.9 0.2	C4	05 36 05 4	C4	42	2.52 0.07	N2
1549+62	3C325.0	15 49 14.1 0.6	C1	62 50 22 2	C1	44	3.62 0.12	N2
1549+20*	3C326	15 49 52.4 4.0	N2	20 14 42 20	N2	48	3.54* 0.15	N2
1553+20†	3C326.1	15 53 57.4 0.2	C1	20 13 00 2	C1	47	2.35 0.06	N2
1555+00	DW1555+00	15 55 17.6 0.2	C4	00 06 40 4	C4	37	1.89 0.06	N2
1559+02	3C327.0	15 59 56.1 1.0	C3	02 06 16 5	C3	37	8.95 0.19	N1
1600+33†	4C33.38LS	16 00 11.8 0.2	C4	33 35 07 4	C4	48	2.36 0.06	N2
1602+01	3C327.1	16 02 12.9 0.2	C1	01 26 02 2	C1	37	4.07 0.09	N2
1603+00	PK1603+00	16 03 39.1 0.3	C1	00 08 30 3	C1	35	2.26 0.06	N2
1607+26†	CTD 93	16 07 09.2 0.2	C1	26 49 20 2	C1	46	4.43 0.10	N2
1608+33	3C329	16 08 09.8 0.4	C3	33 06 26 5	C3	47	1.85 0.08	N1
1609+66	3C330.0	16 09 16.1 1.0	C2	66 04 34 4	C7	40	6.98 0.16	N2
1611+34	DA 406	16 11 48.0 0.2	C4	34 20 17 4	C4	46	2.92 0.07	N2
1615+21	3C333	16 15 05.1 0.3	C4	21 14 51 8	C6	42	1.97 0.11	N1
1615+35*	4C35.40	16 15 39.2 0.5	C4	35 10 11 20	N2	45	2.38 0.09	N2
1615+32	3C332.0	16 15 47.2 0.2	C2	32 29 54 15	N2	45	2.40 0.06	N2
1616+13	3C335	16 16 57.2 2.0	N1	13 46 05 75	N1	39	1.81 0.12	N1
1618+17	3C334.0	16 18 06.8 0.3	C1	17 43 38 3	C1	41	2.12 0.13	N1
1622+23	3C336.0	16 22 32.5 0.2	C1	23 52 06 3	C1	42	2.71 0.07	N2
1624+41	4C41.32	16 24 18.4 0.7	C4	41 41 23 4	C4	44	2.08 0.06	N2
1626+27	3C341.0	16 26 02.0 0.3	C1	27 48 14 5	C1	42	2.44 0.09	N2
1626+39	3C338.0	16 26 55.4 0.3	C2	39 39 32 3	C7	43	3.53 0.09	N2
1627+44	3C337.0	16 27 19.7 0.4	C1	44 25 37 2	C1	43	2.97 0.07	N2
1627+23	3C340.0	16 27 29.8 0.4	C1	23 26 44 2	C1	40	2.38 0.06	N2
1629+12	4C12.59	16 29 25.0 1.3	N2	12 02 23 15	N2	36	1.76 0.08	N2
1634+62*	3C343.0	16 34 01.4 0.6	C1	62 51 43 2	C1	39	5.17 0.14	N2
1637+62*	3C343.1	16 37 55.1 0.5	C1	62 40 34 2	C1	39	4.66 0.10	N2
1638-02†	4C-02.69	16 38 03.5 0.2	C4	-02 34 01 4	C4	27	1.76 0.05	N2
1638+12	OS164	16 38 27.0 0.8	N2	12 25 46 15	N2	34	2.08 0.06	N2
1641+39	3C345.0	16 41 17.7 0.3	C1	39 54 10 1	C1	40	6.30 0.16	N1
1641+17	3C346.0	16 41 34.5 0.2	C1	17 21 21 2	C1	35	3.64 0.14	N1
1643+02	4C02.42	16 43 10.7 0.8	N2	02 17 39 20	N2	28	1.94 0.10	N2
1645+17	PK1645+17	16 45 27.8 0.2	C1	17 25 28 2	C1	34	2.08 0.08	N2
1648+05	3C348.0	16 48 40.1 0.6	C3	05 04 28 5	C3	28	44.43 0.74	N1
1658+47	3C349.0	16 58 04.8 0.2	C2	47 07 08 5	C7	38	3.18 0.08	N1
1658+14†	4C14.68	16 58 22.0 0.9	N2	14 53 16 15	N2	31	1.83 0.06	N2
1704+60	3C351.0	17 04 04.5 0.3	C1	60 48 50 3	C1	36	3.52 0.10	N2
1709+46	3C352.0	17 09 17.8 0.4	C1	46 05 06 2	C1	36	1.86 0.07	N1
1716+00	DW1716+00	17 16 49.9 0.2	C4	00 40 14 4	C4	20	2.18 0.06	N2
1717-00	3C353.0	17 17 54.6 0.6	C3	-00 55 55 4	C3	19	56.22 1.02	N1
1722-02	PK1722-02	17 22 00.0 0.4	C4	-02 39 29 12	C7	17	2.32 0.06	N2
1726+31	3C357.0	17 26 27.0 0.3	C2	31 48 25 5	C7	30	2.72 0.17	N1
1739+17†	PK1739+17	17 39 26.9 1.3	N2	17 21 58 20	N2	22	2.00 0.06	N2
1756+13†	4C13.65	17 56 13.2 0.2	C4	13 28 42 4	C4	17	2.29 0.06	N2

1518+04. 0.35-f.u. source = PK1518+045, SEP = 9′, PA = 175°.
1529+24. Wide, unequal double; M2 refers to the brighter south following source only. Also an 0.54-f.u. source lies 18′ in PA = 35° from the 4′ double.
1543+00. 0.35-f.u. source, SEP = 12′, PA = 260°.
1545+21. M1 gives 65″ separation in PA = 22°. P8 position is that of northern M1 component.
1549+20. 3C326+NRAO 485; centroid position and total flux density given. See Fig. 5.
1553+20. Confused region; 4′.2 EW extent of source found in 300-ft data may be spurious. 1.06-f.u. source, SEP = 27′, PA = 230°.
1600+33. 0.37-f.u. source, SEP = 20′, PA = 245°.
1607+26. 0.18-f.u. source, SEP = 18′, PA = 355°.
1615+35. See Fig. 6.

TABLE II (*continued*)

Source	Class	Structure EW	Ref.	Structure NS	Ref.	T_B	Polarization %	PA(°)	Ref.	References
10	11	12	13	14	15	16	17	18	19	20
1517+20		<0.'25	C1	<0.'30	C1	H	2.0	142	1	A2,3 S2 P8 SC1,2,3
1518+04		<0.30	C4	<2.7	N2	H	<1.0		2	P1
1522+54	D	0.73	C2	<4.3	N2	L	2.9	108	1	M1 S2
1523+03		<0.25	C1	<0.35	C1					P1
1529+35		<0.25	C4	<3.6	N2					A12 M2 S3
1529+24	D?	3.0	C3	2.8	C3	L	7.6	28	5	M2*,29 S3
1533+55		<0.25	C4	<1.1	C4					M1 S3
1538+14		<4.8	N2	<4.8	N2					P1,6 SC3
1543+00		<0.25	C4	<1.3	C4					
1545+21		0.47*	C1	0.83*	C1	L	3.0	3	5	M1,4 S3 P8*
1547+21		<0.25	C1	<0.30	C1	H	7.7	86	1	A2,12 S3
1548+05		<0.25	C4	<1.2	C4	H				A10 P1 VLB3,4
1549+62		<0.25	C1	<0.30	C1	H				M2 S2
1549+20		*								M2
1553+20		<0.25	C1	0.37	C1	H	1.2	129	2	A2 S3 PEAK = 2.18*
1555+00		<0.25	C4	<1.3	C4					A10 VLB3,4 VAR2
1559+02	D	3.4	C3	0.60	C3	L	4.7	9	5	M29 S2 P1 PEAK = 8.50
1600+33		<0.25	C4	<1.0	C4	H				
1602+01		<0.25	C1	<0.35	C1	H	<1.7		5	S3 P1
1603+00		<0.25	C1	<0.42	C1	H	4.2	129	2	P1
1607+26		<0.25	C1	<0.25	C1	H	<1.0		2	A10,11 VLB3,4
1608+33	D	0.91	C3	<0.70	C3					M29 P2
1609+66	D	0.83	C2	0.35	C7	L	4.4	167	1	M1 S3
1611+34		<0.25	C4	<1.0	C4	H				A10 VLB3,4
1615+21		0.35	C4	1.0	C6		3.8	111	2	P2 PEAK = 1.56
1615+35	T	5.7	C4	6.4	N2	L				PEAK = 1.91
1615+32		0.47*	C2	<3.9*	N2	L				M1 S2,3
1616+13		*								PEAK = 0.74
1618+17		0.73	C1	0.45	C1	L	<2.6		1	M1 S3 P1
1622+23		<0.25	C1	0.37	C1	H	3.1	28	5	A12 M2,4,5 S3
1624+41		<0.50	C4	<1.3	C4	(H)				
1626+27		0.80	C1	0.82	C1	L				M1 S3 PEAK = 2.30*
1626+39	D	0.77	C2	<0.30	C7	L	3.5	57	1	M1,25 S3
1627+44		0.63	C1	<0.35	C1	L				M1 S3
1627+23		0.63	C1	<0.30	C1	L				M1 S3 P8
1629+12		4.7	N2	<4.6	N2					P1,6 PEAK = 1.59
1634+62		<0.25	C1	<0.30	C1	H	1.2	100	1	A2 S2,4
1637+62		<0.25	C1	<0.30	C1	H				A2 S2,4
1638-02		<0.30	C4	<1.3	C4					P1
1638+12		<3.3	N2	<3.5	N2	(H)				P1,6
1641+39		<0.25	C1	<0.35	C1	H	5.5	92	1	A1,2,3 S4 VLB1,3,4 VAR1,2
1641+17		<0.25	C1	<0.35	C1	H	0.8	69	2	A2 P1,8
1643+02		<3.7	N2	<5.9	N2					P1,9
1645+17		<0.25	C1	<0.30	C1	H				S2 P1 SC3
1648+05	D	1.9	C3	<0.40	C3	L	1.5	46	5	M29 S3
1658+47	D	0.63	C2	0.83	C7	L	4.6	83	1	M1 S3
1658+14		<1.8	N2	<4.3	N2					P1
1704+60		0.38	C1	0.45	C1	L	<1.6		1	M2*S3 PEAK = 3.12*
1709+46		<0.25	C1	<0.42	C1		4.4	82	1	A2 S3
1716+00		<0.25	C4	<1.3	C4	H				
1717-00	D	3.7	C3	0.85	C3	L	2.8	168	5	M29 S3 PEAK = 53.62
1722-02	D	2.3	C4	3.5	C7		2.6	52	2	P1,5
1726+31	D	0.99	C2	0.45	C7	L	<1.8		1	M1 PEAK = 2.30
1739+17		4.2	N2	4.9	N2	L				P1 PEAK = 1.69
1756+13		<0.25	C4	<1.1	C4					M2 P1

1615+32. M1 gives 54″ separation in PA=17°.
1616+13. N1 quotes 12′ extent for equivalent circular Gaussian.
1626+27. 3.'6 EW extent found from full-beam data may be related to 0.2-f.u. confusing source found in interferometer data to lie 7′ west of source.
1634+62 & 1637+62. SEP=29′, PA=113°.
1638−02. 0.19-f.u. source, SEP=18′, PA=125°; extended background.
1658+14. 0.16-f.u. source, SEP=15′, PA=90°; extended background.
1704+60. C1 does not separate the fainter component given by M2. 3.'9 by 3.'7 extent of source found in N2 data is not supported by N1 or C1 data.
1739+17. 0.38-f.u. source, SEP=17′, PA=95°.
1756+13. 0.22-f.u. source, SEP=15′, PA=70°.

TABLE II (*continued*)

Source		Coordinates (1950.0) Right Ascension	Ref.	Declination	Ref.	Galactic Latitude	Flux Density	Ref.
1	2	3	4	5	6	7	8	9
1759+13	PK1759+13	$17^h59^m21^s.5 \pm 0^s.3$	C1	$13^\circ 51' 22'' \pm 2''$	C1	17°	1.82 ± 0.07	N2
1800-02	PK1800-02	18 00 13.2 0.6	C4	-02 07 24 15	N2	9	1.81 0.06	N2
1807+69	3C371.0	18 07 17.7 0.6	C1	69 48 57 2	C1	29	2.59 0.13	N1
1812+00	DA448	18 12 37.5 3.4	N2	00 01 16 50	N2	8	2.19 0.31	N2
1819+39†	4C39.56	18 19 42.4 0.2	C4	39 41 07 4	C4	22	3.39 0.08	N2
1820+17†	PK1820+17	18 20 09.0 0.2	C4	17 58 34 4	C4	14	1.76 0.05	N2
1821+01	4C01.55	18 21 32.4 2.2	N2	01 46 44 15	N2	6	2.53 0.09	N2
1828+48	3C380.0	18 28 13.4 0.2	C1	48 42 40 2	C1	23	14.11 0.29	N1
1829+29	4C29.56	18 29 17.9 0.4	C1	29 04 57 2	C1	16	2.84 0.07	N2
1830+28†	4C28.45	18 30 52.1 0.9	N2	28 31 16 15	N2	16	1.74 0.05	N2
1832+47	3C381.0	18 32 24.5 0.5	C2	47 25 13 15	N1	22	3.79 0.18	N1
1832+31	4C31.51	18 32 25.2 0.2	C4	31 34 00 4	C4	17	2.06 0.06	N2
1833+32	3C382.0	18 33 12.5 0.4	C2	32 39 11 8	C7	17	5.65 0.45	N1
1833+65	3C383	18 33 32.7 0.6	C1	65 19 13 2	C1	26	2.38 0.23	N1
1834+19	PK1834+19	18 34 29.1 0.9	C4	19 38 35 20	N2	11	1.78 0.09	N2
1835+13	4C13.67	18 35 12.7 0.8	N2	13 28 04 15	N2	9	2.00 0.06	N2
1836+17	3C386.0	18 36 12.4 0.4	C2	17 09 10 10	C7	10	6.82 0.25	N1
1842+45	3C388.0	18 42 35.5 0.3	C1	45 30 22 2	C1	20	5.57 0.23	N1
1843+09	3C390.0	18 43 15.4 0.3	C1	09 50 29 2	C1	5	4.65 0.16	N1
1901+31†	3C395	19 01 02.2 0.4	C1	31 55 13 2	C1	11	3.64 0.12	N2
1914+30	3C399.1	19 14 00.0 0.3	C2	30 14 23 15	N2	8	2.70 0.07	N2
1922+33	4C33.48	19 22 25.1 0.2	C4	33 23 35 15	N2	8	3.76 0.09	N2
1922+35	3C400.1	19 22 43.5 0.6	C4	35 16 35 15	N1	9	2.27 0.12	N1
1925-01*	DA 482	19 25 51.8* 2.0	N2	-01 13 02* 30	N2	-8	3.25* 0.30	N2
1934+36*#	4C36.35	19 34 24.9 1.5	N2	36 41 02 20	N2	7	2.04* 0.07	N2
1939+60	3C401.0	19 39 38.4 0.3	C1	60 34 30 2	C1	17	4.75 0.14	N1
1940+50	3C402.0	19 40 22.7 0.4	C2	50 29 40 15	N1	13	2.94 0.12	N1
1949+02	3C403.0	19 49 43.9 0.4	C3	02 22 43 4	C3	-12	5.85 0.14	N1
1949-01	3C403.1	19 49 54.7 3.0	N1	-01 25 07 20	N1	-14	1.75 0.13	N1
1957+40	CYG A	19 57 44.5 0.5	C2	40 35 02 20	N1	5	1590	KPW
2003-02	4C-02.79	20 03 32.1 0.2	C4	-02 32 17 4	C4	-17	2.01 0.06	N2
2012+23	3C409.0	20 12 18.2 0.3	C1	23 25 42 3	C1	-6	13.04 0.27	N2
2018+23	PK2018+23	20 18 54.7 0.9	N2	23 09 10 15	N2	-7	1.75 0.05	N2
2019+09	3C411.0	20 19 44.4 0.2	C1	09 51 33 2	C1	-14	3.18 0.08	N2
2030+25	3C414	20 30 42.9 0.9	N2	25 42 06 15	N2	-8	1.81 0.06	N2
2031+21†	PK2031+21	20 31 20.9 0.4	C4	21 35 49 15	N2	-10	1.95 0.06	N2
2037+51†	3C418.0	20 37 07.3 0.3	C1	51 08 36 2	C1	6	5.23 0.31	N1
2044-02	3C422	20 44 34.1 0.3	C1	-02 47 27 2	C1	-26	2.24 0.06	N2
2045+06	3C424.0	20 45 44.4 0.2	C1	06 50 10 2	C1	-22	2.04 0.12	N1
2050+36	DA 529	20 50 54.3 1.0	N2	36 23 58 15	N2	-5	4.84 0.11	N2
2050+55*	DA 530	20 50 59.8 4.2	N2	55 08 52 60	N2	6	7.17* 0.34	N2
2059+28	3C426	20 59 48.6 0.2	C4	28 23 32 4	C4	-11	1.72 0.08	N1
2111+62	3C429	21 11 39.8 0.6	C1	62 02 35 2	C1	9	2.53 0.08	N1
2117+60	3C430.0	21 17 01.9 0.4	C1	60 35 34 4	C1	7	7.32 0.29	N1
2121+29*†	DA 545	21 21 29.1 0.8	C3	29 59 41 3	C3	-14	2.75 0.09	N2
2121+24	3C433.0	21 21 30.6 0.2	C1	24 51 18 3	C1	-17	11.68 0.27	N1
2126+07	3C435.0	21 26 37.6 0.3	C1	07 19 51 3	C1	-30	2.01 0.06	N2
2128+04	PK2127+04	21 28 02.6 0.2	C1	04 49 03 3	C1	-31	3.98 0.09	N2
2131-02	4C-02.81	21 31 35.3 0.8	N2	-02 06 44 15	N2	-36	1.80 0.06	N2
2134+00	PK2134+004	21 34 05.3 0.2	C4	00 28 28 4	C4	-35	3.13 0.08	N2
2141+27	3C436.0	21 41 58.0 0.2	C2	27 56 33 4	C7	-18	3.26 0.09	N1
2145+15†	3C437.0	21 45 01.3 0.2	C1	15 06 46 2	C1	-28	2.84 0.07	N2
2145+06	PK2145+06	21 45 36.0 0.2	C1	06 43 43 2	C1	-34	2.97 0.07	N2
2147+14*	PK2147+14	21 47 59.4 0.2	C1	14 35 43 2	C1	-29	2.42 0.11	N1
2148+14*	PK2148+14	21 48 21.0 0.2	C1	14 19 34 2	C1	-29	2.13 0.08	N1

1807+69. A2 gives <7″ EW by <7″.5 NS.
1819+39. 0.63-f.u. source, SEP=9′, PA=60°.
1820+17. 0.45-f.u. extended source, SEP=15′, PA=265°.
1830+28. 0.15-f.u. source, SEP=19′, PA=300°.
1901+31. 0.69-f.u. source, SEP=14′, PA=95°.
1925−01. Position is that of an unresolved 1.03-f.u. source. The centroid of the 2.22-f.u. (peak 0.30 f.u.) extended region surrounding it is 10′.1 east. See Fig. 5.
1934+36. 1.06-f.u.+0.97-f.u. double. See Fig. 5.
1949−01. N1 quotes 4′.1 extent for equivalent circular Gaussian.

TABLE II (*continued*)

Source	Structure					T_B	Polarization			References
	Class	EW	Ref.	NS	Ref.		%	PA(°)	Ref.	
10	11	12	13	14	15	16	17	18	19	20
1759+13		<0.25	C1	0.35	C1					SC2,3
1800-02		1.3	C4	<2.7	N2					P1
1807+69		0.48*	C1	0.38*	C1	L				A2,4 S3 VLB5,6 VAR1
1812+00		16.8	N2	16.5	N2					PEAK = 0.63
1819+39		<0.25	C4	<1.0	C4	H				P2,7
1820+17		<0.25	C4	<1.1	C4					P1
1821+01		<5.0	N2	<8.7	N2					P1
1828+48		<0.25	C1	<0.25	C1	H	1.2	57	1	A1,2,3 S3,4 VLB1,4 VAR1,2
1829+29		<0.25	C1	<0.25	C1					
1830+28		<2.7	N2	<4.6	N2					
1832+47		<0.25	C2			H				M1
1832+31		<0.25	C4	<1.0	C4					P7
1833+32	D	1.4	C2	1.4	C7		3.8	41	1	M1 SC3
1833+65		<0.25	C1	<0.30	C1	H				P2
1834+19	T	4.7	C4	5.4	N2					P5 PEAK = 1.42
1835+13		<4.5	N2	<4.4	N2					
1836+17		1.4	C2	2.7	C7	L	3.0	61	5	M2,26
1842+45		0.52	C1	<0.35	C1	L	<1.0		1	M2
1843+09		<0.25	C1	<0.30	C1		0.6	46	1	S3 SC3
1901+31		<0.25	C1	<0.25	C1					S3
1914+30		<0.25	C2	<4.1	N2		10.1	55	1	
1922+33		<0.25	C4	(1.7)	C4					P9
1922+35	D	1.6	C4							
1925-01	H	19.5	N2	35.7	N2					
1934+36	D	7.3	N2	10.4	N2					
1939+60		<0.25	C1	0.33	C1		1.3	26	1	M2
1940+50	D	1.3	C2	4.5	C7		2.3	111	1	M1
1949+02	D	1.2	C3	0.67	C3		2.5	120	5	M29 S3 SC(3)
1949-01		*								PEAK = 1.50
1957+40	D	1.5	C2	0.8	C8	H	<0.2		4	M1,6,30 S4,8
2003-02		<0.25	C4	<1.3	C4					
2012+23		<0.25	C1	0.37	C1	H	<1.4		5	M2 SC2,3
2018+23		<3.3	N2	<2.8	N2					
2019+09		0.32	C1	<0.35	C1		2.0	61	5	S3
2030+25		<3.2	N2	<3.0	N2					
2031+21	D	1.8	C4	<3.3	N2					
2037+51		<0.25	C1	<0.25	C1		1.3	176	1	A1,3 S4 VLB4 VAR2
2044-02		<0.25	C1	<0.35	C1	H	1.4	100	2	A3 S2
2045+06		<0.25	C1	<0.30	C1	H	3.8	105	5	S3
2050+36		<3.8	N2	<3.2	N2					
2050+55	D	19.2	N2	24.7	N2					
2059+28		<0.25	C4	<1.0	C4					
2111+62		<0.25	C1	<0.30	C1					
2117+60		0.68	C1	0.93	C1	L	2.1	73	1	M1
2121+29	D?	6.6	C3	<0.45	C3					M29 VAR3 PEAK = 2.46
2121+24		0.28	C1	0.50	C1	H	5.0	145	5	M2 S3 SC(3)
2126+07		0.57	C1	<0.50	C1	L				M2 S1,3 SC3
2128+04		<0.25	C1	<0.33	C1	H				A1 S4 SC2,3 VLB1,2,3,4
2131-02		<4.0	N2	<3.2	N2					A10 VLB3
2134+00		<0.25	C4	<1.2	C4	H				A10 VLB3,4 VAR2
2141+27	D	<0.25	C2	0.80	C7		3.8	34	1	M1
2145+15		<0.25	C1	0.62	C1	H	7.0	14	2	M2 S3
2145+06		<0.25	C1	<0.30	C1	H				A1 S4,9 SC2,3 VLB2,3,4 VAR2
2147+14		<0.42	C1	<0.30	C1	H	<1.2		2	M1 S2 VLB1
2148+14		<0.42	C1	<0.30	C1	H	4.5	90	2	M1 S3

2031+21. 0.98-f.u. extended source, SEP=13′, PA=345°.
2037+51. Small diameter source at the edge of HB21.
2050+55. 4.99-f.u.+2.18-f.u. double; both components are extended. See Fig. 5.
2121+29. 0.47-f.u. source, SEP=14′, PA=250°. See Fig. 5.
2145+15. 0.30-f.u. source, SEP=14′, PA=105°.
2147+14 & 2148+14. SEP=17′, PA=162°.

TABLE II (*continued*)

Source		Coordinates (1950.0) Right Ascension	Ref.	Declination	Ref.	Galactic Latitude	Flux Density	Ref.
1	2	3	4	5	6	7	8	9
2151+47†	DA 567	$21^h51^m36^s.0 \pm 1^s.8$	N2	47° 01' 56" ±20"	N2	-5°	2.18 ± 0.06	N2
2153+37	3C438.0	21 53 45.6 0.3	C1	37 46 13 2	C1	-12	6.70 0.14	N1
2200+42	VR042.22.1	22 00 39.3 0.1	C4	42 02 10 4	C4	-10	4.60*	N2
2201+31	4C31.63	22 01 01.4 0.2	C4	31 31 08 4	C4	-18	1.80 0.06	N2
2201+62	3C440	22 01 50.4 0.8	C1	62 25 57 2	C1	5	2.96 0.09	N1
2203+29	3C441.0	22 03 49.2 0.4	C1	29 14 46 3	C1	-20	2.51 0.08	N1
2207+37†	4C37.65	22 07 12.5 0.3	C4	37 27 50 15	N2	-14	1.72 0.05	N2
2209+08	PK2209+08	22 09 32.1 0.3	C1	08 04 26 2	C1	-37	1.80 0.06	N2
2210+01	PK2210+01	22 10 05.2 0.2	C1	01 38 00 2	C1	-42	2.60 0.07	N2
2212+13	3C442.0	22 12 19.6 1.1	C2	13 36 01 15	N1	-34	3.29 0.18	N1
2221-02	3C445.0	22 21 15.5 0.3	C2	-02 21 41 20	N2	-46	5.59 0.12	N2
2223+21	PK2223+21	22 23 14.6 0.2	C4	21 02 51 4	C4	-30	2.59 0.07	N2
2229+39	3C449.0	22 29 05.8 0.2	C2	39 06 14 15	N1	-15	3.62 0.12	N1
2230+11	CTA 102	22 30 07.7 0.2	C1	11 28 23 2	C1	-38	6.01 0.13	N2
2243+39	3C452.0	22 43 33.0 0.9	C2	39 25 28 4	C7	-17	10.53 0.26	N1
2244+36	4C36.47	22 44 13.0 0.2	C4	36 40 44 4	C4	-19	2.03 0.06	N2
2247+11*†	PK2247+11	22 47 21.2 0.7	C3	11 19 20 15	C3	-41	2.38* 0.10	N2
2247+14	PK2247+14	22 47 56.8 0.4	C1	14 03 56 2	C1	-39	2.10 0.06	N2
2249+18	3C454.0	22 49 07.8 0.5	C1	18 32 44 2	C1	-35	2.06 0.07	N1
2251+15	3C454.3	22 51 29.4 0.1	C1	15 52 56 2	C1	-38	11.84 0.23	N1
2251+24	PK2251+24	22 51 44.6 0.2	C4	24 29 28 4	C4	-30	1.88 0.06	N2
2252+12	3C455.0	22 52 34.6 0.2	C1	12 57 36 2	C1	-40	2.93 0.12	N1
2255+41	4C41.45	22 55 05.8 1.1	N2	41 38 19 15	N2	-16	2.21 0.06	N2
2309+18	3C457	23 09 38.4 0.4	C3	18 29 14 10	C3	-38	1.83 0.09	N1
2309+09	3C456.0	23 09 56.6 0.4	C1	09 03 09 2	C1	-46	2.51 0.08	N1
2310+05	3C458.0	23 10 19.8 0.5	C3	05 00 42 6	C3	-49	2.70 0.08	N1
2311+46	4C46.47	23 11 28.5 0.4	C4	46 55 47 15	N2	-12	1.88 0.06	N2
2314+03	3C459.0	23 14 02.2 0.2	C1	03 48 55 2	C1	-51	4.17 0.10	N1
2324-02	PK2324-02	23 24 20.1 0.2	C4	-02 18 44 4	C4	-57	2.36 0.06	N2
2324+40	3C462	23 24 30.7 0.3	C1	40 31 38 2	C1	-19	2.38 0.12	N1
2335+26*	3C465.0	23 35 57.5 0.8	C2	26 44 38 10	C7	-33	7.51 0.20	N1
2337+22	3C466	23 37 51.9 0.5	C1	22 04 14 4	C1	-37	2.13 0.07	N1
2341+53†	4C53.53	23 41 22.4 0.5	C4	53 32 16 15	N2	-7	2.47 0.07	N2
2344+09	PK2344+09	23 44 03.5 0.3	C1	09 14 07 2	C1	-50	2.04 0.06	N2
2347-02	PK2347-02	23 47 52.7 0.8	N2	-02 41 17 15	N2	-61	1.75 0.05	N2
2351+45	4C45.51	23 51 50.7 1.7	N2	45 36 06 15	N2	-15	2.12 0.06	N2
2352+49†	DA 611	23 52 37.8 1.9	N2	49 33 42 20	N2	-12	2.93 0.12	N2
2354+47†	4C47.63	23 54 57.5 0.7	C4	47 10 13 15	N2	-14	1.83 0.06	N2
2356+43†	3C470.0	23 56 02.4 0.5	C1	43 48 01 2	C1	-17	1.88 0.06	N2

2151+47. 0.21-f.u. source, SEP=9′, PA=10°.
2200+42. BL Lac. Flux density varied from 4.57 f.u. to 6.06 f.u. during the course of the observations.
2207+37. 0.22-f.u. source, SEP=16′, PA=120°.
2212+13. South following source shown by M2 is not included.
2243+39. M1 resolves earliest component of C2 into more complex structure.
2247+11. Flux density, measured during another observing program, is somewhat less reliable. There is an 0.70-f.u. source, SEP=7′, PA=225°, and an 0.43 source, SEP=20′, PA=25°. See Fig. 5.

Contour maps for 18 sources are given in Fig. 5. These include most of the sources which were well resolved by the 300-ft observations. The coordinates are for epoch 1950.0 and the half-power beamwidth is shown to the right of each block of plots. The contour interval is normally 0.2 f.u. per beam area with the addition of a dashed contour at the 0.1-f.u. level. For some intense sources, contours have been omitted; those given are labeled to avoid ambiguity.

Table III contains detailed information on confusing, weak sources in the neighborhoods of catalogue sources denoted with daggers (†) in column 1 of Table II. The designations of the confusing sources have been carried to the tenths of degrees in declination to distinguish them from catalogue sources or other previously known sources. The peak flux densities from the 300-ft observations are listed if they differ significantly from the integrated flux density. Typical errors in these flux densities are ±0.04 f.u. The position angle (PA) is measured from the catalogue source towards the nearby source.

TABLE II (*continued*)

Source	Structure Class	EW	Ref.	NS	Ref.	T_B	Polarization %	PA(°)	Ref.	References
10	11	12	13	14	15	16	17	18	19	20
2151+47		6.'2	N2	4.'8	N2					PEAK = 1.71
2153+37		<0.25	C1	<0.25	C1	H	0.6	120	1	M2 S3
2200+42		<0.25	C4	<1.0	C4					A10,11 VLB3,4 VAR2
2201+31		0.41	C4	<1.0	C4					P7 VAR2
2201+62		<0.25	C1	<0.30	C1					
2203+29		<0.25	C1	0.45	C1	H				M2 S3
2207+37		<0.40	C4	<3.5	N2					
2209+08		<0.25	C1	<0.30	C1		5.1	40	2	S9 P5 SC3
2210+01		<0.25	C1	<0.30	C1	H	1.1	130	2	SC3
2212+13	C	4.0	C2	3.4	C7	L	4.1	63	2	M2*PEAK = 2.72
2221-02	D	1.0	C2	7.6	N2	L	4.5	132	2	PEAK = 4.62
2223+21		<0.25	C4	<1.0	C4	H				A11
2229+39	D	0.74	C2	7.0	C7		2.6	66	1	M2 PEAK = 2.45
2230+11		<0.25	C1	<0.30	C1	H	4.6	111	5	A1,3 S4 SC2,3,4 VLB1,2,3,4 VAR2
2243+39	T*	3.2	C2	1.0	C7	L	4.0	24	1	M1,21 PEAK = 10.04
2244+36		<0.25	C4	<1.3	C4					P7
2247+11	C	4.2	C3	3.3	C3	L	4.6	2	2	M29
2247+14		<0.25	C1	<0.30	C1	H	5.4	177	2	P6
2249+18		<0.25	C1	<0.58	C1	H	2.0	62	2	A1,2,4 S2 SC1,2,3,4
2251+15		<0.25	C1	<0.35	C1	H	7.1	61	5	A1,2,3 S3,4 SC1,2,3,4 VLB1,2,3,4 VAR1,2
2251+24		<0.25	C4	<1.0	C4					P7 SC3
2252+12		<0.25	C1	<0.30	C1	H	1.6	167	2	A2 S3 SC1,2,3,4
2255+41		<0.25	C4	<1.5	C4					
2309+18	D	1.5	C3	2.3	C3					M29
2309+09		<0.25	C1	<0.30	C1	H	<2.5		5	A2 S3 SC1,2,3
2310+05	T	2.6	C3	0.83	C3	L	3.0	33	5	M29 S3 SC3
2311+46		<0.40	C4	<3.5	N2					
2314+03		<0.25	C1	<0.30	C1	H	2.9	4	5	S3 SC1,2,3,4
2324-02	D	0.83	C4	<1.3	C4	L	5.2	149	2	
2324+40		<0.25	C1	<0.30	C1					
2335+26	C	3.7	C2	5.0	C8	L	*			M1,27 PEAK = 6.29
2337+22		<0.25	C1	<0.35	C1	H				A11 S3 P2
2341+53		<0.30	C4	<1.1	C4					PEAK = 2.32*
2344+09		<0.25	C1	<0.30	C1	H				S9 SC3 PEAK = 1.87*
2347-02		<2.9	N2	<3.9	N2					
2351+45		4.4	N2	<4.0	N2					PEAK = 1.94
2352+49		4.5	N2	4.4	N2					VAR3 PEAK = 2.49
2354+47	D	1.6	C4	<4.6	N2					
2356+43		<0.25	C1	<0.35	C1		7.8	73	1	M2

2335+26. See Fig. 5. Two discrepant polarization measures: 1.8%±0.8% in PA=112° (Ref. 1) and <0.3% (Ref. 2).

2341+53. 3.'8 EW extent of source found in 300-ft data may be spurious. 0.20-f.u. source, SEP=16′, PA=275°.

2344+09. 4.'8 NS extent of source found in 300-ft data may be spurious.

2352+49. 0.29-f.u. source, SEP=17′, PA=255°.

2354+47. 1.03-f.u. source, SEP=25′, PA=5°.

2356+43. 0.31-f.u. source, SEP=17′, PA=25°.

The east–west structure of the resolved sources obtained with the new CIT interferometer observations are listed in Table IV, for the resolved sources. The table is similar in form to that of Fomalont (1968). The source designation is given in column 1, and each structural component is given a letter designation. The flux density and standard error for the source and each component at 1400 MHz are listed in column 3. Column 4 lists the east–west diameter in arc minutes and its standard error. The position of each component in arc minutes with respect to the source centroid is given in column 5; the accuracy is implied by the number of significant figures. The right ascension of the centroid, its standard error, and the right asension for each component are given next in column 6. Notes are given in column 7. An asterisk or number refers to a comment given at the end of the table. In those cases in which widely separated components have been catalogued separately in Tables II and III, the designations assigned in those tables are given in column 7.

For the source 1615+35 a Fourier inversion was made on the interferometric data. The resultant east–west strip scan distribution is shown in Fig. 6.

III. COMPLETENESS OF THE PRESENT CATALOGUE AND ASSESSMENT OF THE 1400-MHZ SURVEYS

A. Completeness of the Catalogue for $|b|>20°$

Our aim has been to compile a catalogue of sources that is essentially complete at $|b|>20°$ in the area of sky considered, for sources with $S_{1400}\geq 2.00$ f.u. and equivalent Gaussian diameters <10 arc min. Of the 4.30 sr of sky studied at these galactic latitudes, 2.68 sr were surveyed independently by two or more of the published 1400-MHz surveys, principally by the DA and OSU surveys. We expect the joint completeness of the 1400-MHz surveys in this area of sky to be close to 100%; this expectation is justified by the following considerations.

Firstly, the signal-to-noise ratio in the OSU survey

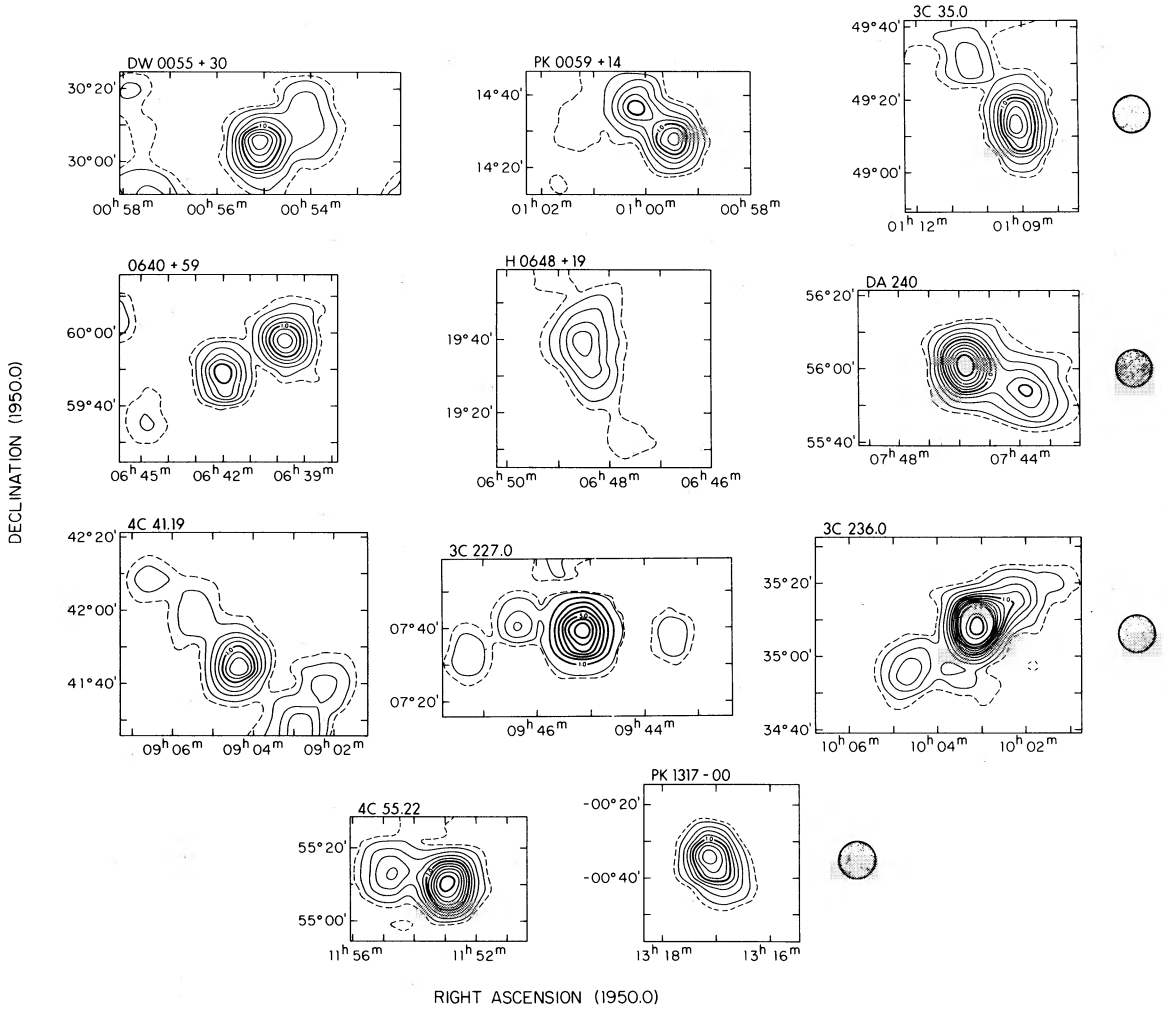

FIG. 5. Contour maps from the full-beam data of 18 large-diameter sources and confused regions.

DW0055+30. Both components are extended in the full-beam data.
PK0059+14. Tabulated as a single source in Table II, but the wide separation between components casts doubt on the physical association.
3C35.0. Mackay (1969) mapped only the south-preceding component; the north-following source may be related.
0640+59. See note to PK0059+14.
H0648+19. This object is classified as a single complex source in Table II, but may consist of several unrelated components.
DA 240. Both components are extended. The field contains several galaxies from a nearby cluster.
4C41.19. Some of the sources shown may be physically related, but no detailed structural data are available on the individual components.
3C227.0. The central component is an aligned triple in position angle 86° (Fomalont 1971a); the components at 09^h43^m and 09^h46^m may be physically related.
3C236.0. The main component, <3 arc sec in extent (Clark and Hogg 1966), is identified with a 15th magnitude galaxy having a redshift $z=0.0988$ (Elsmore and Mackay 1969). If it is related to some or all of the surrounding components, the over-all extent is of the order 1–4 Mpc (H=100 km/sec/Mpc). The confused nature of the object was noted by Fomalont (1968).
4C55.22. The main component is triple (cf. Table IV), but interferometric data for the NS structure are lacking.
PK1317−00. This source was resolved as a 1.4+0.5-f.u. double in the full-beam fitting procedure. The separation is small enough that the components are probably physically associated.

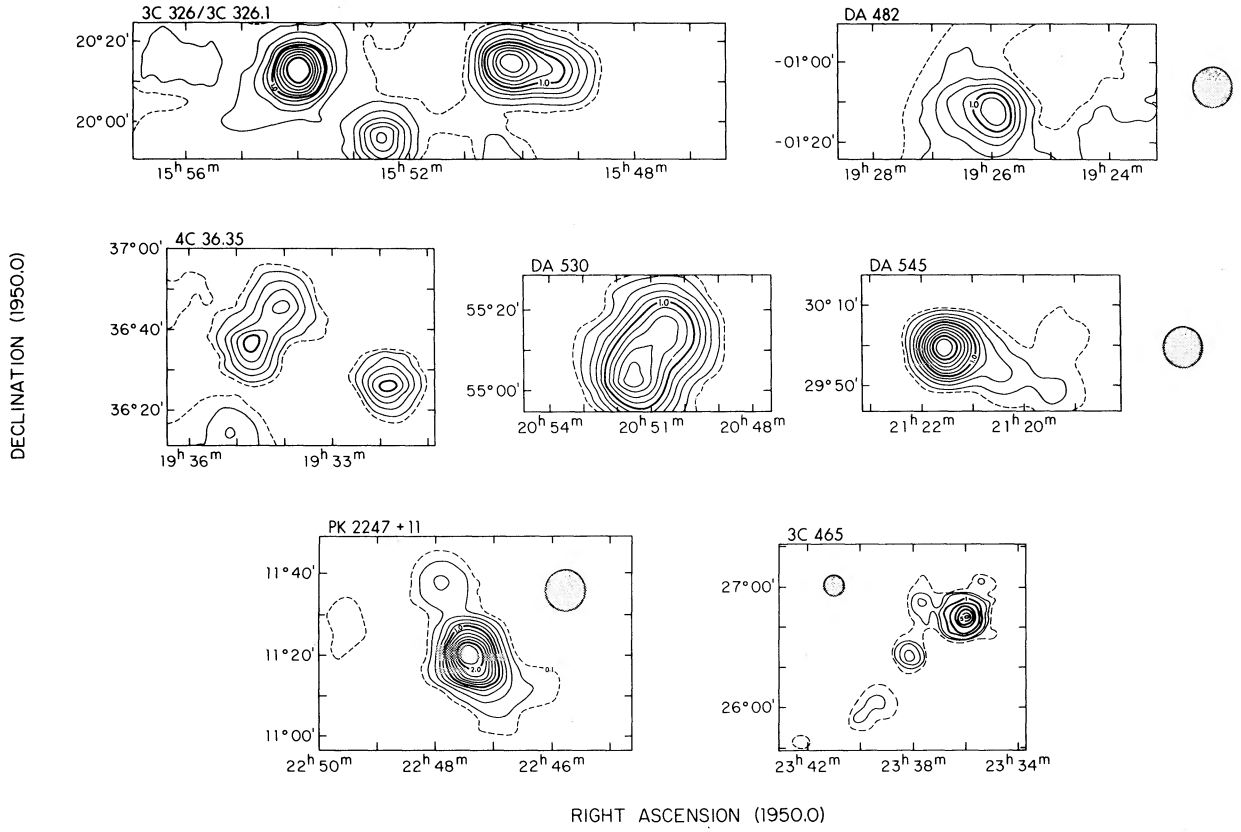

FIG. 5. (*continued*)

3C326 (1549+20). This source is centered on a ridge of the North Galactic Spur and runs parallel to it (Mackay 1969). As the separation into components is ambiguous, only the total flux and centroid position are given in Table II. The preceding component is denoted as NRAO 485 by Pauliny-Toth *et al.* (1966).

3C326.1 (1553+20). The main component lies on an extended region of emissivity, not included in the flux density tabulated in Table II.

DA 482. This low-latitude source was fitted as an unresolved 1.03-f.u. source plus a 2.22-f.u. extended region.

4C36.35. See note to PK0059+14.

DA 530. 2.18+4.99-f.u. double. The north-preceding component is 8′ EW by 10′ NS; the south-following component is 10′ EW by 18′ NS.

DA 545. Fomalont (1971a) resolves the central component as a 2.2+0.6-f.u. double separated 6′.6 in position angle 90°.

PK2247+11. The detailed structure found by Fomalont (1971a) aligns with the over-all structure shown here.

3C465. This map is reproduced at half the scale of those preceding. The field shown covers part of the Pegasus cluster of galaxies. The main radio component, which is centered on NGC 7720, is itself complex, showing seven separate components (Macdonald *et al.* 1966).

at 2.00 f.u. is $>20:1$, so we expect this survey alone to be essentially 100% complete at this flux-density level away from very intense confusing emission, provided that it is not subject to short-term gain fluctuations. Secondly, the joint completeness of two surveys covering the same area of sky should be higher than the individual completeness of either. If a given source has a probability of 5% of being missed by either survey, its probability of being missed by both is 0.25%, unless the reason for its absence is common to both surveys. Absences caused by intense confusion will be correlated between surveys with similar resolving powers, but the east–west resolving powers of the DA and OSU surveys are sufficiently dissimilar that many such absences will not be correlated.

Both of these considerations are supported by data obtained in compiling our catalogue. No sources with $S_{1400} \geqslant 2.00$ f.u. in our list are missing from the OSU survey in the 1.89-sr area common to both, and although the OSU flux densities do show considerable scatter relative to those measured by us (Sec. III.D), only one such source (OM370, $S_{\mathrm{OSU}}=1.47$ f.u.) fell below the 1.50-f.u. cutoff used in compiling the finding list. Our selection from the OSU survey thus suffered one absence from 109 sources with $S_{1400} \geqslant 2.00$ f.u. in the area of sky it covered. This is consistent with our presumption that the OSU survey is essentially complete at 2.00 f.u.

Furthermore, all seven sources at $|b|>20°$ with $S_{1400} \geqslant 2.00$ f.u. found from our reobservation of sources included in spectral studies of lower-frequency catalogues lay in the area of sky covered only by the DA survey. It is therefore reasonable to presume our 'finding list' to be essentially complete in the 2.68 sr covered by more than one 1400-MHz survey.

TABLE III. Confusing sources.

Catalogue source	Nearby source	Coordinates (1950.0) Right ascension	Declination	b	Integrated flux density	Peak flux density	Separation	Position angle
4C40.01	0010+40.2	$00^h10^m20^s.2$	40°16′47″	−21°	0.43	0.32	19′.8	199°
3C22.0	0049+51.0	00 49 51.0	51 02 00	−11	0.28		17.8	70
DW0055+30	0054+30.2	00 54 01.9	30 13 52	−32	0.72	0.65	15.7	305
3C31.0	0105+32.3	01 05 51.2	32 19 53	−30	0.17		18.4	53
4C56.02	0109+56.1	01 09 49.7	56 10 35	− 6	0.15		16.9	109
3C35.0	0110+49.5	01 10 26.3	49 30 54	−13	0.48		21.0	38
PK0128+03	0129+04.0	01 29 53.9	04 02 14	−57	0.20		19.2	79
4C34.07	0221+34.2	02 21 49.6	34 15 40	−24	0.49	0.41	18.2	295
OA132	0325+39.3	03 25 43.8	39 23 01	−13	0.33		13.9	193
4C40.11	0328+40.6	03 28 24.4	40 40 39	−12	0.15		17.9	126
CTA 26	0336−01.7	03 36 30.5	−01 42 32	−41	0.58		15.3	332
	0337−02.0	03 37 45.9	−02 04 07	−42	0.30		14.2	124
PK0411+05	0411+05.4	04 11 15.7*	05 29 02	−31	0.58		11.3	279
PK0428+20	0429+20.5	04 29 22.8	20 31 47	−18	0.26	0.14	17.9	88
3C130.0	0449+52.3	04 49 00.8	52 18 45	5	0.34	0.26	18.8	3
PK0458−02	0458−01.8	04 58 11.6	−01 51 07	−25	0.22	0.16	14.4	211
3C135.0	0511+00.9	05 11 05.4*	00 57 05*	−21	0.60*		8.2	300
4C27.15	0517+27.8	05 17 37.5	27 49 03	− 5	0.30		17.6	62
	0517+27.5	05 17 48.2	27 34 51	− 5	0.32	0.21	19.0	109
OG050	0530+07.2	05 30 45.0	07 17 03	−13	0.36		17.7	138
PK0530+04	0530+04.3	05 30 37.5	04 20 52	−15	0.22		17.3	10
3C159	0621+40.3	06 21 52.2	40 22 28	12	1.13	1.05	17.3	11
4C69.10	0655+69.6	06 55 56.3	69 41 04	26	0.43		15.5	180
3C172.0	0659+25.5	06 59 40.8	25 33 08	13	0.17	0.13	17.2	29
4C44.15	0700+44.5	07 00 58.9	44 30 10	20	0.16		19.0	106
4C42.23	0703+42.7	07 03 44.3	42 47 42	20	0.34	0.15	12.9	27
4C37.21LS	0756+37.7	07 56 28.7	37 46 32	29	1.60		17.5	118
PK0812+02	0813+02.0	08 13 30.6	02 04 44	19	0.40		10.9	87
4C37.24	0828+38.1	08 28 33.1	38 06 54	35	0.15		16.4	27
4C32.25LS	0829+32.6	08 29 12.7	32 37 35	34	0.17	0.12	14.0	55
3C202.0	0831+17.4	08 31 27.8	17 28 45	30	0.59		19.1	337
3C210.0	0854+28.2	08 54 42.8	28 17 07	38	0.25		15.9	336
4C41.19	0905+42.0	09 05 33.6	42 00 24	42	0.41	0.31	19.7	43
3C227.0	0946+07.7	09 46 17.2	07 42 38	42	0.48		17.6	78
PK0949+00	0950+00.2	09 50 13.7	00 14 39	39	0.77		11.9	79
3C236.0	1002+35.2	10 02 17.6	35 16 05	53	1.33	0.87	12.2	307
	1004+34.9	10 04 34.5	34 57 04	54	0.88	0.75	21.7	123
PK1055+20	1054+20.3	10 54 26.9	20 18 01	62	0.25		19.3	301
3C263.0	1138+65.8	11 38 32.0	65 53 34	49	0.47		13.7	143
PK1148−00	1147−00.3	11 47 31.7	−00 22 53	58	0.26		18.4	211
4C49.22	1149+50.0	11 49 49.2	50 03 45	64	0.33	0.22	18.2	328
4C55.22	1154+55.2	11 54 34.7	55 14 43	60	1.16	0.73	15.9	75
PK1215+03	1214+04.0	12 14 07.8	04 01 04	65	0.28	0.17	14.7	295
3C277.3	1250+27.9	12 50 42.4	27 59 14	89	0.23		15.1	291
3C282	1304+65.9	13 04 09.3	65 56 00	51	0.20		15.0	254
4C32.44LS	1325+32.1	13 25 13.3*	32 07 21	80	1.45		16.0	99
3C287.0	1329+25.1	13 29 03.1	25 08 30	80	1.02	0.80	19.3	147
DA 362	1415+35.0	14 15 28.9	35 04 44	70	0.26	0.11	19.9	73
PK1427+07	1428+07.5	14 28 05.7	07 33 18	59	0.46	0.31	8.9	67
PK1452+16	1453+16.6	14 53 44.0	16 39 34	59	1.51	1.36	24.8	78
PK1509+01	1509+01.6	15 09 02.8	01 41 02	47	0.25		15.2	305
PK1518+047	1518+04.5	15 18 48.1*	04 33 01	47	0.35		8.5	176
3C321.0	1530+24.4	15 30 25.2	24 27 19	53	0.54	0.46	17.5	37
DW1543+00	1542+00.5	15 42 47.5	00 33 39	40	0.35		12.3	260
3C326.1	1552+19.9	15 52 26.5	19 56 20	47	1.06		27.1	232
4C33.38LS	1558+33.4	15 58 45.4	33 27 24	48	0.37	0.24	19.6	247
CTD 93	1607+27.1	16 07 00.9	27 07 10	46	0.18		17.9	354
4C−02.69	1638−02.7	16 38 59.3	−02 44 11	27	0.19		17.7	125
4C14.68	1659+14.8	16 59 23.3	14 53 01	30	0.16		14.8	91
PK1739+17	1740+17.3	17 40 39.4	17 19 47	22	0.38	0.20	17.4	97
4C13.65	1757+13.5	17 57 12.8	13 34 13	17	0.22		15.5	69

TABLE III (*continued*)

Catalogue source	Nearby source	Coordinates (1950.0) Right ascension	Declination	b	Integrated flux density	Peak flux density	Separation	Position angle
4C39.56	1820+39.7	$18^h20^m20^s0$*	39°45′26″	22	0.63		8′.8	61°
PK1820+17	1819+17.9	18 19 04.8	17 57 01	14	0.45	0.22	15.3	264
4C28.45	1829+28.6	18 29 36.1	28 40 25	16°	0.15	0.12	19.0	299
3C395	1902+31.9	19 02 06.2	31 54 15	11	0.69	0.63	13.6	94
PK2031+21	2031+21.8	20 31 05.2	21 48 28	−10	0.98	0.26	13.2	344
DA 545	2120+29.9	21 20 29.1	29 55 26	−14	0.47		13.7	252
3C437.0	2145+15.0	21 45 57.3	15 03 26	−28	0.30		13.9	104
DA 567	2151+47.1	21 51 47.7	47 10 57	− 5	0.21		9.2	12
4C37.65	2208+37.3	22 08 23.1	37 19 07	−15	0.22		16.5	122
PK2247+11	2247+11.2	22 47 00.8	11 14 03	−41	0.70		7.3	227
	2247+11.6	22 47 52.3	11 37 33	−41	0.43		19.7	23
4C53.53	2339+53.5	23 39 31.1	53 34 16	− 7	0.20		16.4	277
DA 611	2350+49.4	23 50 57.2	49 29 01	−12	0.29		17.0	254
4C47.63	2355+47.5	23 55 06.0	47 35 33	−14	1.03	0.83	25.3	3
3C470	2356+44.0	23 56 40.3	44 03 26	−17	0.31		16.9	24

* Data from CIT observations.

Within this area, 17 sources found by us to have $S_{1400} \geqslant 2.00$ f.u. were missing from the DA survey, including the supplementary unpublished list. The supplemented DA survey can be inferred to have a completeness of 88±3% at 2.00 f.u. at these galactic latitudes. In the remaining 1.62 sr at $|b| > 20°$, the completeness of our finding list rests mainly on that of the DA survey alone. If the DA survey achieved 88±3% completeness in this area of sky also, 11±3 sources with $S_{1400} \geqslant 2.00$ f.u. would be missing. As noted above, our catalogue contains seven sources at $|b| > 20°$ with $S_{1400} \geqslant 2.00$ f.u. obtained from our reobservation of sources not detected in 1400-MHz surveys, all seven of which lie in this 1.62-sr area. We can infer that our catalogue may be missing 4±3 sources at $|b| > 20°$, as we have detected seven of the eleven 'expected' to be missing from the DA list. We thus infer a completeness of 98±2% for our catalogue at $|b| > 20°$ and $S_{1400} \geqslant 2.00$ f.u., for sources with equivalent Gaussian diameters <10 arc min.

B. Completeness of the Catalogue for $5° < |b| < 20°$

A similar analysis for the lower galactic latitudes, where 0.54 sr of the 2.15 sr observed by us have been covered by two or more 1400-MHz surveys, indicates a completeness of 83±9% for the DA survey at $S_{1400} > 2.00$ f.u. This implies that 16±3 sources would be missing in the area covered by the DA survey alone, while we have detected nine sources at this flux-density level by reobserving sources not detected in 1400-MHz surveys. We infer that our catalogue is missing 7±3 sources with $S_{1400} \geqslant 2.00$ f.u. in this area of sky, the corresponding completeness being 92±4%. This may slightly overestimate our completeness in this area, because the assumption that absences from the various 1400-MHz surveys are generally uncorrelated will not hold in areas of the sky confused by intense galactic radiation.

The over-all completeness of the catalogue at $|b| > 5°$ for sources with $S_{1400} \geqslant 2.00$ f.u. and with equivalent Gaussian diameters less than 10 arc min is estimated as 97±2%. The main areas of incompleteness are expected to be those within a few degrees of very intense discrete sources or close to intense fluctuations in the background radiation. The completeness for sources with equivalent Gaussian diameters between 10 and 40 arc min is essentially that of the DA survey.

C. Assessment of the DA Survey

Figure 7 shows the flux densities obtained by us and by the DA survey (Galt and Kennedy 1968 and private communication) at $|b| > 20°$ for sources whose equivalent diameters were not shown by the DA observations to be >40 arc min. There is a strong tendency for the DA flux densities to be overestimated for $S_{1400} < 5$

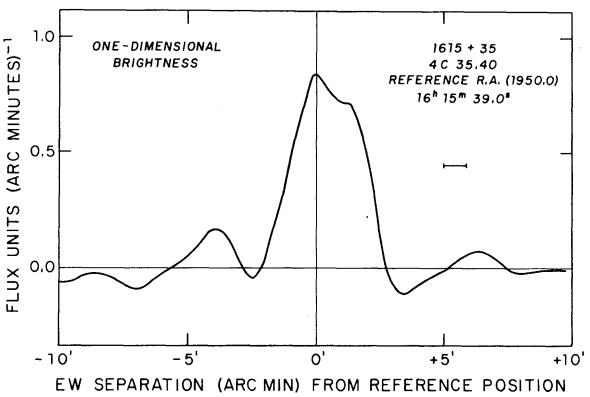

FIG. 6. Strip scan distribution in position angle 90° for 1615+35=4C35.40.

TABLE IV. New east–west interferometric observations of resolved sources.

Source	Comp.	Flux density (f.u.)	East–west diameter (arc min)	Position (arc min)	Right ascension (1950.0)	Notes
0109+49		2.2±0.2			$01^h09^m05^s.9\pm0^s.7$	*
	A	0.3 0.2	0.4±0.4	−1.5	01 08 56.8	
	B	1.9 0.2	2.1 0.3	0.21	01 09 07.2	
0246+42		1.9 0.2			02 46 15.8 0.5	1
	A	0.8 0.2	0.6 0.4	−0.71	02 46 11.9	
	B	1.1 0.2	0.7 0.3	0.64	02 46 16.3	
0512+24		3.8 0.2			05 12 57.5 0.4	1
	A	0.6 0.1	0.3 0.3	−2.08	05 12 48.3	
	B	3.2 0.1	4.7 0.3	0.4	05 12 59.1	
0703+42		2.8 0.3			07 03 12.5 0.7	
	A	0.7 0.5	2.0 1.6	−1.0	07 03 04.7	
	B	1.6 0.5	0.9 0.2	−0.32	07 03 14.2	
	C	0.5 0.1	<1.0	3.17	07 03 29.7	
0745+56		2.5 0.2			07 45 45.2 1.5	*
	A	1.0 0.2	7.1 0.5	0	07 45 45.2	
	B	1.5 0.1	0.4 0.1	0.09	07 45 45.9	
0821+39		2.7 0.2			08 21 48.7 1.8	
	A	1.5 0.1	0.7 0.1	−2.25	08 21 37.1	
	B	1.2 0.1	1.5 0.3	2.89	08 22 03.7	
0945+40		2.0 0.2			09 45 50.1 0.5	
	A	1.7 0.1	0.3 0.1	−0.37	09 45 48.2	
	B	0.3 0.1	<1.0	2.13	09 46 01.4	
1106+37		3.3 0.3			11 06 58.6 1.2	1
	A	0.8 0.1	1.5 0.3	−3.56	11 06 40.5	
	B	1.3 0.1	<0.5	0.72	11 07 02.3	
	C	1.2 0.1	<0.5	1.69	11 07 07.2	
1141+37		2.0 0.2			11 41 49.6 0.8	
	A	1.3 0.1	<0.5	−1.13	11 42 44.0	
	B	0.7 0.1	<0.5	2.0	11 42 59.6	
1152+55		2.2 0.3			11 52 46.9 1.3	*
	A	0.5 0.1	<1.0	−2.42	11 52 29.9	
	B	0.3 0.1	<1.5	−1.08	11 52 39.3	
	C	1.4 0.1	1.6 0.2	1.06	11 52 54.4	
1213+53		2.7 0.2			12 13 00.9 0.7	1
	A	2.2 0.2	<0.5	−0.4	12 12 58.1	
	B	0.5 0.2	<1.0	2.2	12 13 14.4	
1251+15		2.0 0.2			12 51 03.1 0.4	*
	A	0.6 0.2	2.1 0.7	−0.2	12 51 02.4	
	B	1.4 0.2	0.4 0.2	0.07	12 51 03.4	
1308+27		2.1 0.2			13 08 40.6 0.7	
	A	0.9 0.1	0.9 0.1	−1.39	13 08 34.3	
	B	1.2 0.1	0.8 0.1	1.03	13 08 45.3	
1518+04						*
	A	3.5 0.2	<0.3		15 18 44.60 0.14	1518+047
	B	0.8 0.2	0.8 0.4		15 18 48.10 0.65	1518+045
1615+35		2.6 0.3			16 15 39.2 0.5	
	A	0.2 0.2	<2.0	−4.1	16 15 09.4	
	B	1.8 0.2	2.1 0.6	0.0	16 15 39.0	
	C	0.6 0.2	1.4 1.0	1.6	16 15 46.6	
1638−02						*
	A	0.3 0.1	0.7 0.1	−2.06	16 37 52.8±0.3	1638−02.7?
	B	1.8 0.1	<0.3	0.36	16 38 03.50 0.14	1638−02
1722−02		2.5 0.2			17 22 00.0 0.4	
	A	0.3 0.1	1.1 0.3	−2.06	17 21 51.8	
	B	2.2 0.1	1.2 0.1	0.26	17 22 01.0	
1834+19		1.8 0.2			18 34 29.1 0.9	1
	A	0.4 0.1	1.4 0.3	−3.4	18 34 14.7	
	B	0.3 0.2	1.2 0.3	−0.1	18 34 28.5	
	C	1.1 0.3	4.3 0.6	1.3	18 34 34.5	
1922+35		2.4 0.2			19 22 43.5 0.6	
	A	1.2 0.1	0.9 0.1	−0.84	19 22 39.7	
	B	1.2 0.1	<0.3	0.81	19 22 47.5	

TABLE IV (*continued*)

Source	Comp.	Flux density (f.u.)	East–west diameter (arc min)	Position (arc min)	Right ascension (1950.0)	Notes
2031+21		2.2±0.3			$20^h31^m20^s.9$ 0.4	*
	A	1.6 0.5	2.0±1.0	−0.5	20 31 19.0	
	B	0.6 0.1	<1.0	1.32	20 31 26.6	
2324−02		2.4 0.2			23 24 20.1 0.2	
	A	1.7 0.2	1.0 0.2	−0.25	23 24 19.1	
	B	0.7 0.2	<0.5	0.58	23 24 22.4	
2341+53						*
	A	0.3 0.1	<1.0	−1.75	23 41 09.0 0.7	2339+53.5?
	B	2.4 0.1	<0.3	0.23	23 41 22.4 0.5	2341+53
2354+47		1.6 0.2			23 54 57.5 0.7	
	A	0.8 0.1	0.8 0.1	−0.85	23 54 52.6	
	B	0.8 0.1	1.1 0.1	0.80	23 55 02.3	

Notes to Table IV

1. The model fit of the interferometer data is fair. Structure may be more complex.
0109+49. A complex source (Mackay 1969). Two components can be separated by present measurements, but the model fit by Gaussian components is rather inadequate.
0745+56. These inteferometric observations refer only to the north-following component of 0744+55 listed in Table II.
1152+55. May be confused by 1154+55.2 listed in Table III.
1251+15. Model fit uncertain; the solution given disagrees with the 3C Map (Mackay 1969) but data are not inconsistent with this map within the uncertainties imposed by noise.
1518+04. Double north–south, separation 10 arc min (Parkes catalogue). Probably a nonphysical double. Flux density of 1518+045 in disagreement with the 300′ measurement given in Table III.
1638−02. Component A may be related to the confusing source 1638−02.7 listed in Table III. A lobe shift of 11′.9 is possible.
2031+21. Confusing source 2031+21.8 listed in Table III is probably resolved out in the interferometric data.
2341+53. Component A may be related to the confusing source 2339+53.5 listed in Table III. A lobe shift of 11′.9 is possible.
2355+47. Confused by 2355+47.5 listed in Table III.

f.u., due in most cases to confusion of the type shown in Fig. 2. This accounts for the discrepancy between the DA flux densities and those of the CTD survey (Kellermann and Read 1965) discussed by Galt and Kennedy (1968) and attributed by them to partial resolution of some sources by the CTD interferometer.

The overestimation of the DA flux densities led us to reject from our catalogue 99 sources at $|b|>5°$ with flux densities $\geqslant 1.7$ f.u. in the published DA list. Our catalogue contains 14 sources whose flux densities were given by DA as between 1.0 and 1.7 f.u., and 33 sources which were missing from the DA survey. The original DA data were inspected at the positions of strong missing sources; the majority of absences above 3.00 f.u

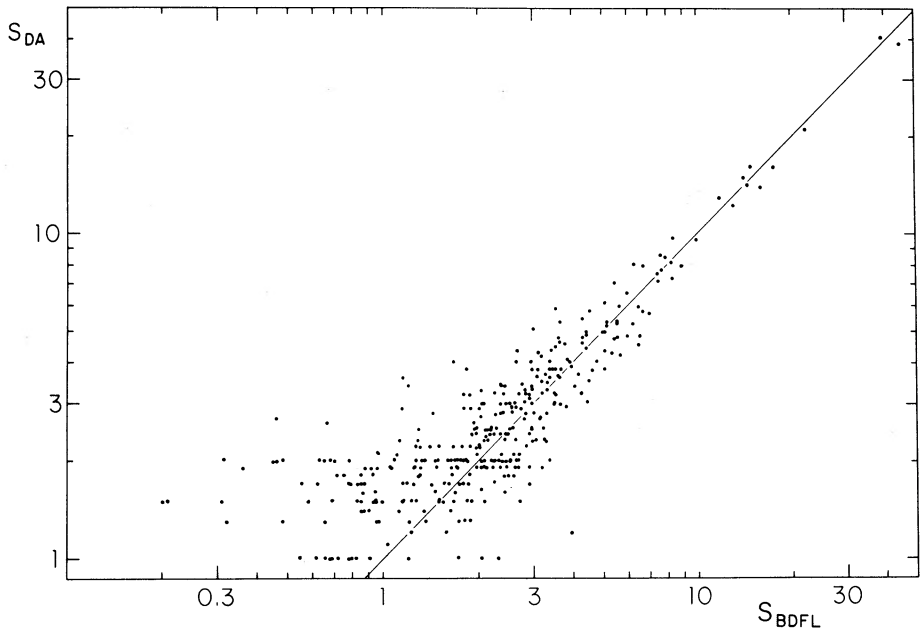

FIG. 7. Comparison of the full-beam flux density S_{BDFL} and the DA flux density S_{DA}. A line through the origin of slope unity is shown.

appears to have been caused by a small number of unusually poor sets of data with high values of the rms noise.

Our data on the 99 rejected DA sources are included in Table V. For the more intense sources tabulated, the NRAO positional errors are comparable to those given for the full-beam data in Sec. I.D. For sources with flux densities $S_{1400}<0.5$ f.u. or with angular sizes >10 arc min, the positional errors are larger, and the quoted positions are rounded accordingly.

The unreliability of the DA flux-density measurements implies that the number-flux density relationships (Galt and Kennedy 1968) and spectral-index distributions (Galt and Kennedy 1968; van der Laan 1969) derived from the DA survey are also unreliable.

D. Assessment of the OSU Survey

Figure 8 shows the flux densities obtained by us and by the OSU surveys (Kraus 1964; Kraus and Dixon 1965; Kraus *et al.* 1966; Scheer and Kraus 1967; Dixon and Kraus 1968; Fitch *et al.* 1969; Ehman *et al.* 1970) for all sources at $|b|>20°$ reobserved by us. This figure includes data obtained by us for OSU sources with flux densities <1.50 f.u. in the OSU lists. Such sources were observed at NRAO when they appeared as confusing sources in the fields of more intense objects, or between the observations of sources in the catalogue as observing time permitted. The reobservation is complete for sources with flux densities $\geqslant 1.50$ f.u. in the OSU lists, except for the sources OF 176 ($S_{OSU}=1.62$ f.u.) and OP 335 ($S_{OSU}=1.69$ .fu.).

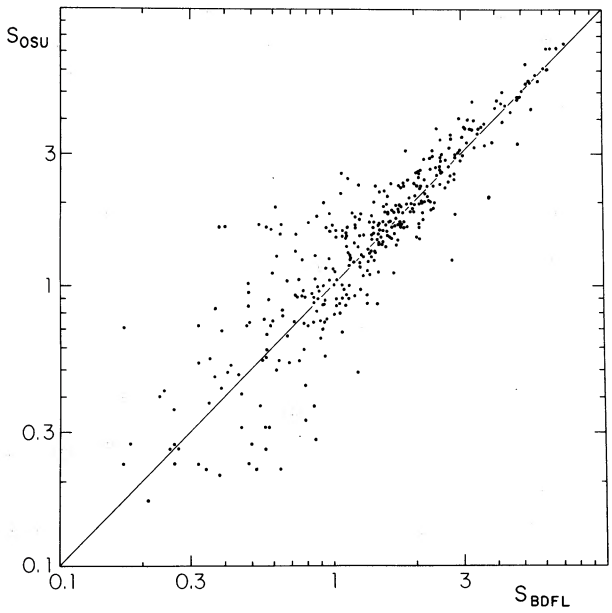

FIG. 8. Comparison of the full-beam flux density S_{BDFL} and the OSU flux density S_{OSU}. Sources with $S_{OSU}<1.5$ f.u. were not part of the main program but were selected at random and observed as time permitted. A line through the origin of slope unity is shown.

There is a tendency for the OSU flux densities to be overestimated in the approximate flux-density range 1–3 f.u. (Fig. 8). The effect is most severe for sources noted in the OSU lists as 'extended', 'confused', or 'unresolved' (Bridle and Davis 1970). This overestimation led us to reject 37 sources from the published OSU lists whose flux densities were given there as $\geqslant 1.7$ f.u. Data on these 37 rejected sources are included in Table V. Many of the OSU overestimations are due to confusion in the fan beam, particularly for the '*e*', '*c*', and '*u*' observations at OSU.

Systematic underestimates in the OSU flux densities below 1 f.u. have been reported by Jauncey and Niell (1971). It therefore appears that the OSU flux densities are somewhat unreliable below ~ 3 f.u., so that results of number-flux density and spectral analyses using OSU data on such sources will be questionable.

E. Assessment of Other Surveys near 1400 MHz

Figure 9(a) shows the flux densities obtained by us and by the DW survey (Davis 1967) for sources at $|b|>20°$. The flux densities are generally in good agreement; the effects of confusion and partial resolution are, of course, similar for the two sets of flux densities as both were obtained with the same instrument. A least-squares fit to the relation between the two sets of flux-density measurements gives $S_{DW}=(0.998\pm0.034)S_{BDFL}+(0.106\pm0.060)$ f.u., where S_{BDFL} is the flux density obtained in the present observations.

Four sources assigned flux densities $S_{1400}\geqslant 1.7$ f.u. in the DW list have been rejected from our catalogue. Our data on these are included in Table V.

Figure 9(b) shows the flux densities obtained by us and by the CTD interferometric survey (Kellermann and Read 1965) for 34 unresolved sources at $|b|>20°$. There are a small number of sources with $S_{1400}\sim 1$ f.u. whose flux densities appear substantially overestimated in CTD. A least-squares fit to the relation between the two sets of flux-density measurements gives $S_{CTD}=(1.009\pm0.006)S_{BDFL}+(0.078\pm0.047)$ f.u. Five sources assigned flux densities $\geqslant 1.7$ f.u. in the CTD list have been rejected from our catalogue. Data on these are also given in Table V.

Figure 9(c) shows the flux densities obtained by us and by Höglund (1967) for 34 sources in his survey at $|b|>20°$. Höglund's flux-density calibration was originally based on a value of 6.23 f.u. for the source 3C 264; we have converted his calibration to the value of 5.78 f.u. given for this source in Table II, thereby reducing all flux densities given in his survey by a factor of 0.928. Figure 9(c) shows that, after making this recalibration, there is a residual tendency for Höglund's flux densities to be overestimated above 1 f.u., but not at lower flux densities. Jauncey and Niell (1971) find a slight tendency for Höglund's flux densities to be underestimated below 1 f.u.; this is not inconsistent with the data shown in Fig. 9(c). A least-squares fit to the rela-

TABLE V. Sources with $S_{1400} \geq 1.7$ f.u. in other surveys rejected from the present catalogue.

Survey name	Survey flux density	NRAO measurements: Flux density	Right ascension (1950.0)	Declination (1950.0)	Notes	Comments
DA 10	1.8 P	0.41±0.05 0.22 0.04	00h20m50s.2 00 20 03	43°46′45″ 44 03 04		
DA 12	3.0 P	<0.4	(00 24 10)	(66 25)	1	
H 0030+19	1.9	1.69 0.07	00 30 01.1	19 37 21	2	
DA 19 OB 063.9	2.2 P 2.29 c	1.44 0.06	00 38 18.1	08 36 34	3 III	
DA 20	2.0 P	1.69 0.07	00 38 45.1	−02 00 20	3	8′.6 EW×4′NS. Peak=1.22 f.u.
DA 24	4.8 P		(00 49 30)	(65 32)		Extended background feature.
DA 31	2.0 P	1.68 0.07 0.27 0.04	00 55 42.5 00 54 08.5	26 35 47 26 51 24	3,4	
DA 34	1.9 P	1.01 0.06	01 00 06.8	25 36 08	5	
OC 312	2.20 u	1.56 0.07 0.48 0.04	01 07 32.5 01 06 42.7	31 31 13 31 34 12	II	
OC−038	2.10 c	1.60 0.07 0.49 0.04	01 22 54.3 01 22 51.0	−00 20 59 −00 36 57	IV	
DA 44	2.2 P	1.60 0.07	01 24 45.6	08 59 09		
DA 48	1.8 P	1.57 0.07	01 27 38.8	25 52 49		
DA 50	1.8 P	1.25 0.06	01 28 45.9	06 08 12		
DA 57	3.8 P	<0.2	(01 40 00)	(55 20)	1	
DA 58	1.7 P	1.11 0.06	01 41 20.3	33 57 01		
DA 60	2.1 P	0.68 0.10 0.57 0.05 0.28 0.04	01 45 40 01 46 08.9 01 47 16.7	06 01 06 07 57 06 16 22		Broad feature extended ∼23′ EW. Peak=0.28 f.u.
DA 65 DW 0157+40	1.8 P 1.8	0.82 0.05 0.72 0.05	01 57 05.4 01 57 47.3	40 35 24 40 32 53	5	Possibly a physical double source.
OD 007	1.71 p	1.55 0.07	02 04 30.0	06 44 51	III	
DW 0224+67	1.7	1.06 0.06	02 24 40.2	67 08 00		Variable (MacDonell and Bridle 1971).
CTD 20	2.0	1.27 0.06	02 34 56.9	28 35 24		
OD 065	1.83 p	1.28 0.06 0.59 0.06	02 38 25.7 02 38 25	08 32 12 08 21	III	12′ EW. Peak=0.38 f.u.
DA 88	1.8 P	0.79 0.05 0.35 0.05 0.31 0.04	02 58 45.3 02 59 24 02 57 32.3	35 38 32 35 22 30 35 35 03	4	16′ EW. Peak=0.19 f.u.
OE 342	1.75 e		(03 25 42)	(33 39)	II	Extended background feature.
DA 111 OE 361	3.3 P 3.03 u	1.36 0.06	03 37 02.1	31 59 57	4,5 II	
DA 112	2.6 E?	0.64 0.04	03 40 04.2	20 51 39		
OA 134	1.7	0.91 0.05	03 44 37	40 34	V,5	
DA 116	1.9 P	1.21 0.06 0.26 0.04	03 49 02.2 03 47 11	26 15 32 26 11 50		
OE 188	1.82 u	0.99 0.16 0.98 0.05 0.24 0.05 0.21 0.04	03 53 01.8 03 53 26.9 03 51 20 03 54 37	12 25 12 56 39 12 34 13 07	III	7′ EW×9′.8 NS. Peak=0.61 f.u. 6′.2 EW×6′.4 NS. Peak=0.72 f.u. ∼13′ NS. Peak=0.15 f.u.
OE 390	2.28 e,n	0.66 0.05 0.46 0.07 0.21 0.15	03 56 35 0 03 57 13 03 56 27	32 12 15 32 36 31 54	II 5 5	 ∼15′ NS. Peak=0.27 f.u. Possibly extended NS.
DA 121 OE 097	2.0 P 1.85 p	1.66 0.07	03 58 34.4	00 27 56	3,5 III	
DA 128	2.0 P	1.27 0.06	04 09 45.2	22 57 32		
OF−016	2.18 p,c	1.55 0.07	04 09 49.0	−01 07 10	IV	
DA 135	2.0 P	1.04 0.06	04 19 39.1	14 00 56	5	

TABLE V. (*continued*)

Survey name	Survey flux density	NRAO measurements (1950.0) Flux density	Right ascension	Declination	Notes	Comments
OF−035	1.94 p	1.55±0.07	04^{h}20^{m}43^s.6	−01°27′24″	IV	
DA 136	2.4 E?	0.67 0.05	04 23 18.5	30 43 21	5	
OF 041	2.31 c	1.25 0.06	04 23 40.5	04 43 50	III	
		0.73 0.05	04 25 09.4	04 50 31		
		0.7 0.1	04 23 58	05 12		At edge of observed field.
DA 143	2.0 R	<0.4	(04 36 00)	(27 00)	1	
DA 151	1.7 P	0.84 0.05	04 48 33.0	−04 36 59		
		0.41 0.04	04 46 39.1	−04 34 26		
DA 155	2.3 P	1.05 0.06	04 56 50.6	27 01 01	4,5	4′ EW. Peak=0.97 f.u.
OF 097	1.97 p	1.59 0.07	04 57 15.9	02 24 43	III	
DA 160	2.4 P	1.01 0.06	05 06 17.5	29 53 58	5	
DA 162	2.3 R		(05 08 30)	(27 09)	1	Extended background feature.
DA 164	2.3 P	0.89 0.05	05 10 54.8	31 08 10	5	Galactic latitude=4°.5.
DA 182	1.8 P	0.93 0.06	05 34 21.7	−03 10 39	4,5	
H 0535+20	2.0	<0.4	(05 35 22)	(20 40 30)		Data from D. G. MacDonell (private communication).
DA 194	1.7 P	1.39 0.06	05 52 47.3	12 32 13	5	
		0.68 0.05	05 54 15.0	12 37 49		Extended 10′ in PA 130°. Peak=0.52 f.u.
DA 195	2.0 P		(05 55 22)	(10 10)	1	Extended background source.
DA 207	4.8 P	1.68 0.07	06 20 25.1	31 38 48		
		1.42 0.06	06 21 44.4	32 06 27		
		0.44 0.04	06 19 25.5	31 56 16		
		0.42 0.04	06 19 20	31 31		Extended ∼13′ NS. Peak=0.27 f.u.
DA 208	2.0 P?	1.13 0.06	06 21 52.2	40 22 28	4	Confused by 3C 159 (Table II).
OH 239	1.84 p	1.44 0.06	06 23 45	26 25 11	II,2	
H 0632+19	2.5	1.33 0.09	06 31 54.3	19 11 52		10′.5 EW×8′.2 NS. Peak 0.75 f.u.
		0.79 0.05	06 32 22.2	18 57 11		9′.8 EW. Peak 0.57 f.u.
		0.66 0.06	06 32 28	19 19 57		∼10′ EW. Peak 0.46 f.u.
DA 220	1.7 P	1.49 0.06	06 39 36.6	59 58 28		4C60.10.
		1.15 0.06	06 41 55.3	59 48 48		4C59.07 LS.
DA 223	1.8 P	1.19 0.05	06 47 55	69 23	2	Possibly confused in DA by NRAO 251.
DA 224	1.8 P	0.65 0.05	06 49 23.6	42 35 46		∼6′ NS. Peak=0.57 f.u.
		0.22 0.04	06 51 10	42 51		
		1.1	06 52 45	42 41		Position and flux density uncertain. Source at edge of observed field.
DA 238	2.0 P	1.30 0.07	07 40 59.5	38 010 9	3	
		0.58 0.05	07 42 19.3	37 39 33		
OI−088	2.15 p	0.89 0.06	07 52 17.6	−02 39 13	IV	6′ EW. Peak=0.77 f.u.
		0.85 0.13	07 52 24.6	−02 13		9′ EW. Peak=0.63 f.u. Confusing emission to north.
OJ−005	1.97 p,c	1.26 0.06	08 03 01.6	−00 49 35	IV	
		0.54 0.05	08 02 39.1	−01 01 54		7′.2 EW. Peak=0.45 f.u.
DA 253	2.0 P	0.60 0.05	08 32 05.9	26 22 31		5′.6 EW. Peak=0.53 f.u.
		0.48 0.05	08 32 10.6	26 44 22		
		0.21 0.04	08 34 22	26 24		
DA 256	2.0 P	<0.4	(08 42 48)	(58 00)	1	
H 0852+20	1.8	1.03 0.06	08 51 55.9	20 18 01		
DA 263	2.0 P	1.22 0.06	09 06 37.2	01 33 40	3	4′ EW. Peak=1.14 f.u.
		0.65 0.05	09 06 32.3	01 06 31		4′.7 EW. Peak=0.59 f.u.
		0.34 0.04	09 07 07.4	00 58 15		
DA 265	2.2 P	1.36 0.06	09 11 17.0	17 28 42		
		0.21 0.04	09 12 49	17 20		
OK 393	2.01 n	1.43 0.06	09 55 24	32 38 10	II,2	

TABLE V. (*continued*)

Survey name	Survey flux density	NRAO measurements (1950.0) Flux density	Right ascension	Declination	Notes	Comments
OL 302	1.70	1.44±0.06	$10^h01^m38^s.6$	32°06′29″	I	4′ EW. Peak = 1.34 f.u.
DA 283	2.0 P	1.62 0.08	10 07 25.9	41 47 30		
DA 285	2.0 P	0.75 0.05	10 17 47.1	31 53 38		
DA 286 / OL 231	1.9 P / 1.71 p	1.63 0.07	10 19 08	22 14 39	2 / II	
DA 291	2.0 P	1.61 0.07	10 49 46.4	20 46 15		
DA 295	2.2 P	1.22 0.06	11 06 10	25 17 30	2	
OM−029	1.85 p	1.62 0.07	11 16 52	−02 46 40	IV,2	
H 1123+20	1.9	0.88 0.05 0.60 0.05	11 23 23 3 11 23 10.7	20 22 44 20 08 47		
DA 302	2.0 P	1.04 0.06	11 25 41.3	58 50 22		
DA 303	2.0 P	0.74 0.06 0.46 0.04	11 30 15.7 11 31 24.4	45 15 04 45 21 36		9′.2 EW×6′ NS. Peak = 0.49 f.u. Confused by 1128+45. See Fig. 2.
DA 309	1.8 P	0.69 0.05 0.19 0.04	11 42 47.8 11 44 00	05 11 58 05 16		
DA 313	2.0 P	1.65 0.09 0.68 0.05	11 51 17.2 11 48 53.2	38 27 00 38 42 17		∼3′ EW×9′.5 NS. Peak = 1.21 f.u. 4′.6 EW. Peak = 0.62 f.u.
OM 295	1.70 n	1.39 0.06	11 56 57.0	29 31 31	II	
ON 121	2.16 u	1.07 0.06	12 12 43.8	17 46 36	III	5′.5 EW×4′ NS. Peak = 0.89 f.u.
DA 327	2.4 P	1.5 0.2 0.6 0.2 0.3 0.1	12 33 58.0 12 33 37.2 12 32 17.9	16 48 49 16 54 58 17 04 17		Data from Fomalont (1971a). Full beam data from present observations.
DA 329	2.0 P	1.59 0.07 0.26 0.06	12 42 24.4 12 41 43	41 04 50 41 04		Large right-ascension discrepancy with DA.
DA 336	1.7 P	0.79 0.05 0.62 0.07	12 55 01.8 12 56 45.0	37 00 39 36 48	3	∼10′ EW. Peak = 0.44 f.u.
DA 337	2.1 P	1.11 0.06 0.68 0.05 0.33 0.04	13 05 22.2 13 04 32.8 13 05 49.0	06 58 27 06 44 15 06 37 11		∼3′.6 EW. Peak = 1.05 f.u.
DA 340	2.8 P	1.43 0.07	13 12 24.0	69 53 38	5	5′.5 EW×3′.1 NS. Peak = 1.21 f.u.
DA 348	2.3 P	1.13 0.06	13 33 03.9	41 14 51		∼6′.2 EW. Peak = 0.97 f.u.
DA 351	1.7 P	1.25 0.06	13 47 17	21 21 40	2	
DA 356	2.7 P	0.46 0.05 0.37 0.04	13 57 03.2 13 55 18.9	13 39 02 13 37 55	3	∼11′ EW. Peak = 0.31 f.u.
DA 358	1.9 P	0.96 0.05	14 03 33.8	−02 29 27		
OQ 209	2.44 n	1.13 0.06 0.78 0.05	14 06 02.4 14 05 40.6	24 01 31 23 46 08	II	
OQ 112	1.84 p	1.68 0.07	14 07 42.8	17 47 35	III	6′.0 EW. Peak = 1.45 f.u.
CTD 87	1.8	1.47 0.06 0.32 0.04	14 23 33.7 14 23 33.1	24 18 12 24 30 14	5	
DA 359	1.7 P	0.85 0.05 0.47 0.06 0.34 0.04 0.25 0.05	14 07 47.2 14 06 39.4 14 05 44.7 14 06 33	31 39 26 31 51 30 31 34 38 31 39		∼8′.5 EW. Peak = 0.36 f.u.
OQ 292	1.99 e	0.92 0.09	14 55 26	24 47 53	II	8′ EW. Peak = 0.72 f.u. Confusing emission to north.
OR 103	1.82 p	1.59 0.09 0.29 0.04 0.17 0.05	15 01 57.5 15 01 13 15 01 06	10 41 07 10 27 10 45	III	
DA 373	1.7 P	0.83 0.05	15 03 47.4	69 08 19	3	
OR 219 / CTD 90	2.35 p / 1.8	1.64 0.07 0.23 0.04	15 11 28.2 15 11 52	23 49 53 23 37	II	

TABLE V. (*continued*)

Survey name	Survey flux density	NRAO measurements: Flux density	(1950.0) Right ascension	Declination	Notes	Comments
DA 380	1.9 P	0.36±0.07	15h14m30s	21°33′00″	3,5	20′ EW. Peak=0.17 f.u.
DW 1520−04	1.9	1.28 0.06	15 20 06.3	−04 43 25		
DW 1535+13	1.8	1.68 0.07	15 35 11.6	13 54 24		
DA 387	1.8 P	1.29 0.06	15 40 49	60 25 42	2	
DA 394	3.6 P	1.15 0.06	15 55 19.9	07 17 35		
DA 405	2.2 P	1.31 0.06	16 10 10.2	22 30 27		
		0.36 0.04	16 09 52.0	22 45 32		
DA 417	1.9 P	1.25 0.06	16 34 33	26 54 18	2	
DA 418	1.9 P	0.88 0.05	16 36 19.4	−03 07 35		
		0.34 0.04	16 33 50	−03 15		
DA 421	2.3 P	1.29 0.06	16 41 23.5	37 35 39	2	
DA 424	2.0 P	0.46 0.04	16 46 10.0	37 48 32		
		0.39 0.07	16 45 50	37 53		6′.7 EW.
		0.38 0.06	16 45 43	38 03		10′ EW×9′ NS. Peak=0.20 f.u.
OS 077	2.55 c		(16 46 17)	(08 37)	III	Extended background feature.
DA 429	1.9 P	0.92 0.05	17 04 05.1	17 03 14		
		0.20 0.04	17 01 48	16 49		13′ EW. Peak=0.12 f.u.
DA 433	2.0 P	0.73 0.06	17 14 47.0	−02 02 19		6′.3 EW. Peak=0.62 f.u.
		0.64 0.05	17 14 07.4	−01 56 39		
DA 436	2.0 P	1.40 0.06	17 32 28.4	16 02 29	5	
DA 437 / CTD 101	1.9 P / 1.8	1.65 0.07	17 35 34.6	24 02 35		
DA 440	1.7 P	1.42 0.06	17 47 29.3	59 44 09	3	
		0.35 0.04	17 48 31	59 54		
OT 081	1.96 c	1.05 0.06	17 49 09.8	09 39 25	III	7′ NS. Peak=0.89 f.u.
		0.57 0.04	17 50 08.7	09 58 30		
DA 443	2.5 P	1.29 0.06	17 53 58.1	53 06 32		
		0.20 0.04	17 52 22	53 01		
DA 445	2.0 P	0.45 0.04	17 56 55.5	39 38 46	3,4	11′ NS. Peak=0.32 f.u.
		0.27 0.04	17 54 16	38 49 01		8′ EW. Peak=0.21 f.u.
DA 446	3.2 P	<0.15	(18 03 15)	(04 23)	5	
DA 450	4.8 E		(18 26 15)	(00 29)	5	Extended background feature.
DA 465	2.0 E?		(18 46 25)	(27 57)	1	Extended background feature.
DA 469	1.7	1.04 0.07	18 57 16.5	32 48 06	4	15′ EW×5′ NS. Peak=0.53 f.u.
DA 474	5.0 P		(19 11 45)	(00 08)	1,5	
DA 478	2.3 P	1.20 0.06	19 15 45.4	55 38 48		
DA 493	2.8 P	0.58 0.05	19 49 51.9	11 30 07		Faint extended emission near DA position.
DA 499	2.0 P		(19 54 30)	(44 43)		Extended background feature. DA notes irregular background.
OW 101	2.35 c	1.02 0.06	20 01 00.7	13 57 27	III,5	
DA 513	1.7 P	1.17 0.16	20 21 19.4	16 52 21		
DA 519	2.7 E?	0.54 0.09	20 37 57.9	27 50 02		6′.9 EW×10′.7 NS. Peak=0.32 f.u.
		0.42 0.04	20 39 33	27 52 40		8′.4 EW×8′.5 NS. Peak=0.26 f.u.
DA 531	4.0 R?		(20 54 20)	(37 34)	1	Extended background feature.
OW 093	1.83 c	1.17 0.06	20 56 00.1	05 31 05	III,5	
DA 534	2.3 P	0.60 0.05	21 09 58.5	39 06 17		6′.3 EW×4′ NS. Peak=0.49 f.u.
		0.32 0.04	21 10 35	38 42 44		
		0.46 0.04	21 09 25	38 25 50		Embedded in background feature.
DA 543	2.0 P	0.38 0.04	21 18 47.3	41 44 02		Confused by extended background feature.
DA 544	1.7 P	1.41 0.06	21 20 56.3	15 35 37		5′.4 EW. Peak=1.25 f.u.

TABLE V (*continued*)

Survey name	Survey flux density	NRAO measurements: Flux density	Right ascension (1950.0)	Declination (1950.0)	Notes	Comments
DA 552	3.0 P	1.44±0.06	$21^h31^m49^s.7$	37°59′18″		DA notes 'irregular background'.
		0.90 0.05	21 30 33.6	38 22 40		9′.1 EW×8′.6 NS. Peak=0.53. f.u.
		0.48 0.04	21 29 48.7	38 09 02		13′ EW. Peak=0.30 f.u.
DA 556	1.7 P	0.62 0.05	21 37 38	17 10 57		9′.2 EW. Peak=0.46 f.u.
		0.33 0.04	21 37 00	17 02 25		23′ EW. Peak=0.13 f.u.
DA 557	1.8 P	0.60 0.05	21 40 22.9	40 05 52		6′ NS. Peak=0.53 f.u. DA notes
		0.27 0.04	21 37 51	39 56 23		'irregular background'.
DA 564 / OX 182	3.4 P / 1.77 c	1.20 0.14	21 48 34	13 34 16	2 III	
DA 569	2.0 P	0.56 0.05	21 51 58.2	42 27 22		
OY 080	1.85 c	1.62 0.07	22 48 16.7	06 46 27	III	
OY 187	1.71 c	1.63 0.07	22 51 52.3	13 25 38	III	3′.8 EW. Peak=1.53 f.u.
OZ 108	1.79 u	0.87 0.05	23 05 17.5	18 45 00	III	
		0.50 0.05	23 04 59.6	19 04		6′ EW. Peak=0.43 f.u.
DA 593	2.9 E?	1.15 0.06	23 08 54.3	25 31 12		
		0.27 0.15	23 11 08	25 28		Extended background feature: ∼20′ NS.
OZ 023	1.74 c	1.24 0.07	23 13 44.5	01 12 04	III	5′ NS. Peak=1.13 f.u.
		0.41 0.06	23 13 16	01 26		12′ EW×10′ NS. Peak=0.20 f.u.
DA 599	1.9 P	1.08 0.07	23 18 09.1	07 56 02		8′ EW. Peak=0.85 f.u.
		1.06 0.06	23 20 04.3	07 55 55		
		0.78 0.10	23 18 44	08 07		12′.7 EW. Peak=0.49 f.u.
		0.23 0.04	23 22 10	07 49		
CTD 139	2.0	1.33 0.06	23 19 31.7	27 16 34		
		0.54 0.10	23 21 24	27 20		18′ EW. Peak=0.26 f.u.
DA 600	3.0 P	1.44 0.09	23 20 07.0	50 41 12	5	
DA 609	3.3 P	0.36 0.04	23 43 48.3	08 36 33		
H 2345+18	1.8	1.61 0.07	23 45 57.6	18 28 18	2	

Notes to Table V

1. No identifiable discrete source in field mapped at NRAO.
2. Data from Pauliny-Toth *et al.* (1966).
3. Companion <0.2 f.u. within 15′ of source.
4. Noted in DA as confused with another source.
5. Probably confused in original observations by extended background feature.

I. Scheer and Kraus 1969.
II. Dixon and Kraus 1968.
III. Fitch *et al.* 1969.
IV. Ehman *et al.* 1970.
V. Dixon 1970.

Classification codes from DA catalogue

P=Point source.
E=Extended.
R=Ridge.

Classification codes from OSU catalogue

c=confused source.
e=extended source.
p=point source.
n=noisy data.
u=several components.

tion between the two sets of data shown in Fig. 9(c) gives $S_{BH}^* = (1.011\pm0.038)S_{BDFL} + (0.074\pm0.067)$ f.u., where S_{BH}^* is Höglund's flux density corrected as above. Six sources with $S_{BH}^* \gtrsim 1.7$ f.u. have been rejected from our catalogue. Our data on these are also given in Table V.

F. Assessment of the Parkes 1410-MHz Flux Densities

Figure 10 shows the flux densities obtained by us and by the Parkes catalogue (Shimmins and Day 1968; Ekers 1969) for all sources common to both lists at $|b|>20°$, $\delta>-5°$. There is no evidence in this declination range for any systematic discrepancy. The revised version of the Parkes catalogue (Ekers 1969) gives improved 1410-MHz flux densities on a calibration scale uniform between the various declination zones of the survey. We have compared this scale with that of Kellermann *et al.* (1969), on which our measurements are based, by comparing the revised Parkes 1410-MHz flux densities with our own for 71 sources with equiv-

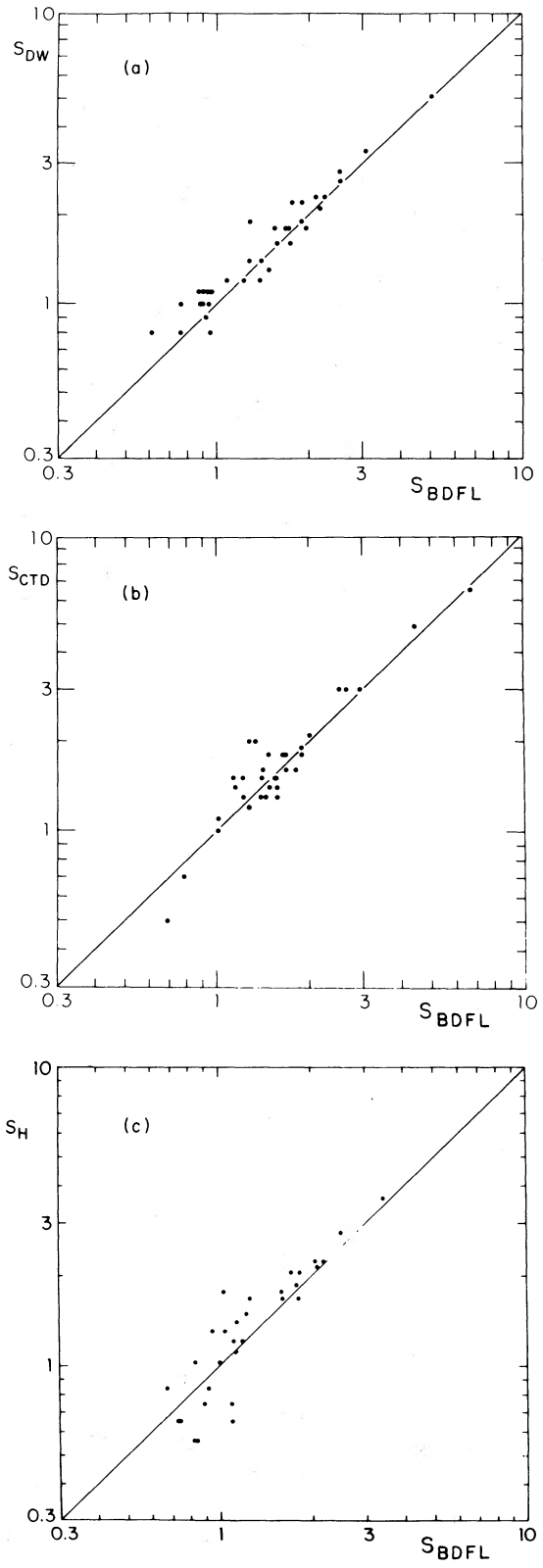

FIG. 9. Comparison of the full-beam flux density S_{BDFL} with (a) Dwingeloo flux density S_{DW}, (b) CTD flux density S_{CTD}, and (c) Höglund flux density S_H. A line through the origin of slope unity is shown in each case.

alent Gaussian diameters <30 arc sec. A least-squares linear fit to the relation between the two sets of measurements gives

$$S_{PKS} = (0.989 \pm 0.007) S_{BDFL} - (0.049 \pm 0.038) \text{ f.u.}$$

We conclude that the Parkes calibration scale for $\delta > -5°$ is identical to that of our catalogue, and hence to that of Kellermann *et al.*, to within experimental uncertainties.

However, the flux densities in the Revised Parkes Catalogue for southern declinations appear to be systematically low by as much as 12%. This effect was determined by a comparison with the CIT flux densities (Fomalont 1968) and the GMW flux densities (Gardner, Morris, and Whiteoak 1969). The results are shown in Table VI. The CIT flux densities have been divided by 1.04 to conform to the KPW flux-density scale. Only small-diameter sources (<2 arc min) were used in the comparison.

The agreement between the CIT and GMW flux densities is good. South of declination −40° the drop in the CIT flux-density scale is certainly due to attenuation effects which were present for these low elevation observations but which were not corrected for. Thus, assuming the GMW scale is within a few per cent of the KPW flux-density scale even south of −40° declination, we conclude that the Revised Parkes Catalogue flux densities are ∼12% low south of declination −20°, 4% low between 0° and −20°, and, as described above, in good agreement with KPW north of the equator.

G. The 1400-MHz Flux Densities Derived by Witzel, Véron, and Véron

Witzel *et al.* (1971) have derived flux densities for intense sources at 1400 MHz by averaging the observations of other workers, weighted according to standard errors assigned to each observer by comparison with the flux densities given by Kellermann *et al.* (1969). The over-all inhomogeneity of the data used by Witzel *et al.* to estimate their flux densities leads to a corresponding inhomogeneity in their uncertainties due to calibration, partial resolution, and confusion. Table II gives 1400-MHz flux densities for all sources in their list, with uniform, and smaller, uncertainties due to these effects. However, their publication provides accurate flux densities at 2695 and 5009 MHz for many sources in our list.

IV. SPECTRAL CONTENT OF THE STATISTICALLY COMPLETE SAMPLE

The radio continuum spectra of the 98±2% complete sample of sources with $S_{1400} \geq 2.00$ f.u. at $|b| > 20°$ have been studied by Guindon (1971) and by Bridle, Kesteven, and Guindon (1972 and in preparation) in the frequency range 100 MHz to 10.6 GHz. Their spectral data, combined with that of Witzel *et al.* (1971), permit

TABLE VI. Systematic error of Parkes flux densities at 1410 MHz.

Declination range	S_{PKS}/S_{CIT}	No.	S_{GMW}/S_{CIT}	No.	S_{PKS}/S_{GMW}	No.
0° to 20°	0.98±0.01	66	1.01±0.03	50	0.98±0.02	50
−20° to 0°	0.96±0.02	56	1.01±0.02	37	0.95±0.02	37
−40° to −20°	0.88±0.01	81	1.03±0.01	47	0.86±0.02	47
−50° to −40°	0.95±0.03	41	1.07±0.03	28	0.89±0.02	28
−90° to −50°	...		...		0.88±0.01	41

the spectral index α between 400 and 5000 MHz to be determined for these sources with a typical uncertainty of ~0.05. [We adopt the definition $S(\nu)=S_0\nu^{-\alpha}$, so that sources with 'transparent' spectra are assigned positive spectral indices.] The distribution of α_{400}^{5000} among the 234 sources is shown in Fig. 11.

The asymmetry of the spectral-index distribution towards low values of α defines clearly the low-index population noted in the smaller CTD sample (Kellermann and Read 1965) by Williams and Bridle (1967) and Kellermann *et al.* (1968). Sources with $\alpha_{400}^{5000}<0.5$ comprise 19^{+2}_{-3}% of the present sample. The 45 such sources are the major class of source in this catalogue which is proportionally less represented in comparable catalogues compiled at lower frequencies, but which dominates catalogues compiled at higher frequencies (e.g., Pauliny-Toth *et al.* 1972).

Of these 45 sources, 41 have been observed at CIT, of which only two were resolved. 1514+00 consists of three individually resolved components; the central component, identified with a 17^{m}E galaxy, has a flux density approximately twice that of each of the symmetrically placed outer components. 1807+69 is known to be variable, and comparison of the CIT and Cambridge data indicates that about 80% of the flux density originates in an unresolved component; the source is identified with an optically variable N galaxy. 1514+00 is thus the only clearcut instance of a source in this spectral population that is resolved by our observations. Twenty-eight of the sources have very fine structure shown by interplanetary scintillation or by the detection of fringes in long-baseline interferometer experiments, and 15 are known radio variables. Twenty-four are confirmed or suspected QSOs, 7 are noncompact galaxies, 2 are N or Seyfert galaxies, and 5 are empty fields. There are no published identifications for the remaining 7 sources.

The 45 sources with $\alpha_{400}^{5000}<0.5$, $S_{1400}\geq 2.00$ f.u. and $|b|>20°$ have an integral number count exponent $\gamma=1.88\pm0.27$, essentially the same as that for the complete sample as a whole (Bridle *et al.* 1972).

V. SUMMARY

We have obtained accurate flux densities for 424 discrete radio sources with 1400-MHz integrated flux densities ≥ 1.70 f.u. in the declination range $-5°<\delta<+70°$ at galactic latitudes $|b|>5°$. Our data contain

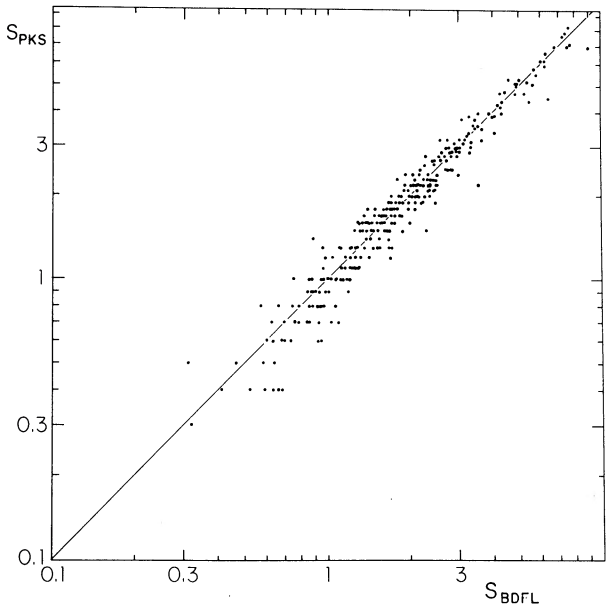

FIG. 10. Comparison of the full-beam flux density S_{BDFL} with the Revised Parkes flux density S_{PKS} for $\delta>-05°$. A line through the origin of slope unity is shown.

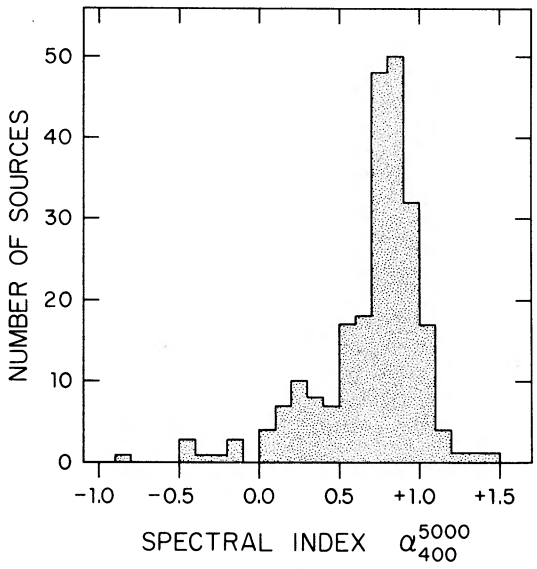

FIG. 11. The spectral-index distribution between 400 and 5000 MHz for the 234 sources with $S_{1400}\geq 2.00$ f.u., $|b|\geq 20°$, and angular extent <10 arc min.

a $98\pm2\%$ complete sample of 234 sources with $S_{1400} \geqslant 2.00$ f.u. at $|b| > 20°$ and with equivalent Gaussian angular diameters <10 arc min. This group of sources (defined in column 16 of Table II) provides an unbiased sample selected at 1400 MHz suitable for all statistical studies of the properties of extragalactic radio sources. For the convenience of users of this sample, the catalogue contains references to more accurate positions, to studies of both extended and fine structure in the sources, and to observations of radio variability, in addition to our flux densities, positions, and angular structures. Data on the integrated 1400-MHz polarizations of the sources have also been assembled.

The number of sources in this complete sample is comparable to the 210 sources at $|b| > 20°$ in the *Revised Third Cambridge Catalogue* (Bennett 1962), and is sufficiently large to permit meaningful statistical analysis of major subgroups of the sample. Our use of both full-beam and interferometric observations of sources in this work ensures that the completeness of samples drawn from Table II is not a function of angular size below $\sim$10 arc min, while still providing well-determined positions for most sources.

It is hoped that these data will also prove valuable to radio astronomers seeking to calibrate the performance of instruments operating at 1400 MHz. Tables II and III and Fig. 5 give detailed information on possible problems of confusion which would affect such use of the data. The source list may also be useful for studies of neutral-hydrogen absorption in directions away from the galactic plane in the northern sky.

VI. ACKNOWLEDGMENTS

We are indebted to numerous colleagues who have made available unpublished information at various stages of this work. Prof. J. D. Kraus and Dr. R. S. Dixon supplied the OSU catalogue in a preliminary punched-card form, and Dr. J. R. Ehman made the southernmost section of this catalogue available in advance of publication. Dr. J. A. Galt and Mr. J. E. D. Kennedy gave access to unpublished data from the DA survey. Dr. I. I. K. Pauliny-Toth, Dr. A. E. Niell, and D. G. MacDonell provided us with unpublished 1400-MHz data obtained with the 300-ft telescope. Dr. K. I. Kellermann supplied unpublished information on sources studied with long-baseline interferometers, and on variable sources. Dr. W. J. Medd made available updated information on variability obtained by the Astrophysics Branch of the National Research Council of Canada. Dr. D. E. Hogg supplied information concerning new variable sources obtained from observations with the NRAO three-element interferometer.

We thank the Directors of the National Radio Astronomy Observatory and the Owens Valley Radio Observatory for allocating observing time for this work. A. H. B. and J. L. held visiting appointments at the NRAO and CIT, respectively, during parts of the period in which it was performed. A. H. B. also acknowledges financial support from the National Research Council of Canada.

REFERENCES

Anderson, B., and Donaldson, W. 1967, *Monthly Notices Roy. Astron. Soc.* **137**, 81.
Backer, D. C., Hazard, C., Jauncey, D. L., and Sutton, J. 1970, *Astron. J.* **75**, 529.
Bailey, J. A., and Pooley, G. G. 1968, *Monthly Notices Roy. Astron. Soc.* **138**, 51.
Bash, F. N. 1968, *Astrophys. J. Suppl.* **16**, 373.
Bennett, A. S. 1962, *Mem. Roy. Astron. Soc.* **68**, 163.
Biraud, F., Lequeux, J., and Le Roux, E. 1960, *Observatory* **80**, 116.
Bologna, J. M., McClain, E. F., and Sloanaker, R. M. 1969, *Astrophys. J.* **156**, 815.
Branson, N. J. B. A. 1965, *Observatory* **85**, 250.
Bridle, A. H., and Davis, M. M. 1970, paper presented at IAU Symposium No. 44 (Uppsala), reported in *External Galaxies and Quasi-stellar Objects*, edited by D. S. Evans (D. Reidel Publ. Co., Dordrecht), 1972, p. 437.
Bridle, A. H., Davis, M. M., Fomalont, E. B., and Lequeux, J. 1972, *Nature Phys. Sci.* **235**, 123.
Bridle, A. H., Kesteven, M. J. L., and Guindon, B. 1972, *Astrophys. Lett.*, in press.
Broderick, J. J., Kellermann, K. I., Shaffer, D. B., and Jauncey, D. L. 1972, *Astrophys. J.* **172**, 299.
Broten, N. W., Clarke, R. W., Legg, T. H., Locke, J. L., Galt, J. A., Yen, J. L., and Chisholm, R. M. 1969, *Monthly Notices Roy. Astron. Soc.* **146**, 313.
Clark, B. G., and Hogg, D. E. 1966, *Astrophys. J.* **145**, 21.
Clark, B. G., and Miley, G. K. 1969, *Astrophys. Lett.* **4**, 207.
Clarke, R. W., and Batchelor, R. A. 1965, *Nature* **207**, 511.
Clarke, R. W., Broten, N. W., Legg, T. H., Locke, J. L., and Yen, J. L. 1969, *Monthly Notices Roy. Astron. Soc.* **146**, 381.
Clarke, T. W., Frater, R. H., Large, M. I., Munro, R. B., and Murdoch, H. S. 1969, *Aust. J. Phys. Astrophys. Suppl.* No. 10.
Cohen, M. H. 1969, *Ann. Rev. Astron. Astrophys.* **7**, 619.
Cohen, M. H., Cannon, W., Purcell, G. H., Shaffer, D. B., Broderick, J. J., Kellermann, K. I., and Jauncey, D. 1972, *Astrophys. J.*, in press.
Cohen, M. H., Gundermann, E. J., and Harris, D. E. 1967, *ibid.* **150**, 767.
Cohen, M. H., and Shaffer, D. B. 1971, *Astron. J.* **76**, 91.
Conway, R. G., Kellermann, K. I., and Long, R. J. 1963, *Monthly Notices Roy. Astron. Soc.* **125**, 261.
Davis, M. M. 1967, *Bull. Astron. Inst. Neth.* **19**, 201.
De Jong, M. L. 1967, *Astrophys. J.* **148**, 651.
Dixon, R. S. 1970, *Astrophys. J. Suppl.* **20**, 1.
Dixon, R. S., and Kraus, J. D. 1968, *Astron. J.* **73**, 381.
Ehman, J. R., Dixon, R. S., and Kraus, J. D. 1970, *ibid.* **75**, 351.
Ekers, J. A. (Ed.) 1969, *Aust. J. Phys. Suppl.* No. 7.
Elsmore, B., and Mackay, C. D. 1969, *Monthly Notices Roy. Astron. Soc.* **146**, 361.
Fitch, L. T., Dixon, R. S., and Kraus, J. D. 1969, *Astron. J.* **74**, 612.
Fomalont, E. B. 1967, *Publ. Owens Valley Radio Obs.* **1**, No. 3.
——. 1968, *Astrophys. J. Suppl.* **15**, 203.
——. 1971a, *Astron. J.* **76**, 513.
——. 1971b, *Publ. Owens Valley Radio Obs.* **1**, No. 5.
Fomalont, E. B., and Moffet, A. T. 1971, *Astron. J.* **76**, 5.
Fomalont, E. B., Wyndham, J. D., and Bartlett, J. F. 1967, *ibid.* **72**, 445.
Galt, J. A., and Kennedy, J. E. D. 1968, *ibid.* **73**, 135.
Gardner, F. F., Morris, D., and Whiteoak, J. B. 1969, *Aust. J. Phys.* **22**, 79.
Graham, I. 1970, *Monthly Notices Roy. Astron. Soc.* **149**, 319.
Guindon, B. 1971, M.Sc. thesis, Queen's University at Kingston, Ontario.
Gulkis, S., Sutton, J., and Hazard, C. 1969, *Astrophys. J.* **157**, 1047.
Harris, D. E., and Gundermann-Hardebeck, E. 1969, *Astrophys. J. Suppl.* **19**, 115.
Hazard, C. 1962, *Monthly Notices Roy. Astron. Soc.* **124**, 343.

Hazard, C., Mackey, M. B., and Nicholson, W. 1964, *Nature* **202**, 227.
Hazard, C., Gulkis, S., and Sutton, J. 1968, *Astrophys. J.* **154**, 413.
Hogg, D. E. 1969, *ibid.* **155**, 1099.
Höglund, B. 1967, *Astrophys. J. Suppl.* **15**, 61.
Jauncey, D. L., and Niell, A. E. 1971, *Nature Phys. Sci.* **229**, 223.
Jauncey, D. L., Bare, C. C., Clark, B. G., Kellermann, K. I., and Cohen, M. H. 1970, *Astrophys. J.* **160**, 337.
Kellermann, K. I., and Read, R. B. 1965, *Publ. Owens Valley Radio Obs.* **1**, No. 2.
Kellermann, K. I., and Pauliny-Toth, I. I. K. 1968, *Ann. Rev. Astron. Astrophys.* **6**, 417.
Kellermann, K. I., Pauliny-Toth, I. I. K., and Davis, M. M. 1968, *Astrophys. Lett.* **2**, 105.
Kellermann, K. I., Pauliny-Toth, I. I. K., and Williams, P. J. S. 1969, *Astrophys. J.* **157**, 1.
Kellermann, K. I., Clark, B. G., Jauncey, D. L., Cohen, M. H., Shaffer, D. B., Moffet, A. T,, and Gulkis, S. 1970, *ibid.* **161**, 803.
Kellermann, K. I., Jauncey, D. L., Cohen, M. H., Shaffer, D. B., Clark, B. G., Broderick, J. J., Rönnäng, B., Rydbeck, O. E. H., Matveyenko, L., Moiseyev, I., Vitkevich, V. V., Cooper, B. F. C., and Batchelor, R. A. 1971, *ibid.* **169**, 1.
Kraus, J. D. 1964, *Nature* **202**, 269.
Kraus, J. D., and Dixon, R. S. 1965, *ibid.* **207**, 587.
Kraus, J. D., Dixon, R. S., and Fisher, R. O. 1966, *Astrophys. J.* **144**, 559.
Little, L. T., and Hewish, A. 1968, *Monthly Notices Roy. Astron. Soc.* **138**, 393.
Long, R. J., Smith, M. A., Stewart, P., and Williams, P. J. S. 1966, *ibid.* **134**, 371.
Macdonald, G. H., and Kenderdine, S. 1967, *Nature* **215**, 603.
Macdonald, G. H., and Miley, G. K. 1971, *Astrophys. J.* **164**, 237.
Macdonald, G. H., Neville, A. C., and Ryle, M. 1966, *Nature* **211**, 1241.
Macdonald, G. H., Kenderdine, S., and Neville, A. C. 1968, *Monthly Notices Roy. Astron. Soc.* **138**, 259.
MacDonell, D. G., and Bridle, A. H. 1971, *Nature Phys. Sci.* **234**, 88.
Mackay, C. D. 1969, *Monthly Notices Roy. Astron. Soc.* **145**, 31.
——. 1970, *Astrophys. Lett.* **5**, 173.
Maltby, P., and Moffet, A. T. 1962, *Astrophys. J. Suppl.* **7**, 141.
Merkelijn, J. K. 1969, *Aust. J. Phys.* **22**, 237.
Miley, G. K., Rickett, B. J., and Gent, H. 1967, *Nature* **216**, 974.
Miley, G. K., Hogg, D. E., and Basart, J. 1970, *Astrophys. J.* **159**, L19.
Miley, G. K., and Wade, C. M. 1971, *Astrophys. Lett.* **8**, 11.
Mitton, S. 1970a, *Monthly Notices Roy. Astron. Soc.* **149**, 101.
——. 1970b, *Astrophys. Lett.* **5**, 207.
——. 1970c, *ibid.* **6**, 161.
Mitton, S., and Ryle, M. 1969, *Monthly Notices Roy. Astron. Soc.* **146**, 221.
Moffet, A. T., Schmidt, M., Slater, C. H., and Thompson, A. R. 1967, *Astrophys. J.* **148**, 283.
Morris, D., and Berge, G. L. 1964, *Astron. J.* **69**, 641.
Morris, D., and Radhakrishnan, V. 1963, *Astrophys. J.* **137**, 147.
Moseley, G. F., Brooks, C. C., and Douglas, J. N. 1970, *Astron. J.* **75**, 1015.
Olsen, E. T. 1967, *ibid.* **72**, 738.
Palmer, H. P., Rowson, B., Anderson, B., Donaldson, W., Miley, G. K., Gent, H., Adgie, R. L., Slee, O. B., and Crowther, J. H. 1967, *Nature* **213**, 789.
Parker, E. A., Elsmore, B., and Shakeshaft, J. R. 1966, *ibid.* **210**, 22.
Parker, E. A., and Kenderdine, S. 1967, *Observatory* **87**, 124.
Pauliny-Toth, I. I. K., Wade, C. M., and Heeschen, D. S. 1966, *Astrophys. J. Suppl.* **13**, 65.
Pauliny-Toth, I. I. K., Kellermann, K. I., Davis, M. M., Fomalont, E. B., and Shaffer, D. B. 1972, in preparation.
Ryle, M., Elsmore, B., and Neville, A. C. 1965, *Nature* **207**, 1024.
Ryle, M., and Windram, M. D. 1968, *Monthly Notices Roy. Astron. Soc.* **138**, 1.
Scheer, D. J., and Kraus, J. D. 1967, *Astron. J.* **72**, 536.
Shimmins, A. J., and Day, G. A. 1968, *Aust. J. Phys.* **21**, 377.
Sutton, J., Hazard, C., and Gulkis, S. 1967, *Astron. J.* **72**, 831.
Talen, J. L. 1965, *ibid.* **70**, 694.
Taylor, J. H. 1966, *Astrophys. J.* **146**, 646.
——. 1967, *ibid.* **150**, 421.
Taylor, J. H., and De Jong, M. L. 1968, *ibid.* **151**, 33.
Thomson, J. R., Kraus, J. D., and Andrew, B. H. 1968, *ibid.* **154**, L1.
van der Laan, H. 1969, *Bull. Astron. Inst. Neth.* **20**, 171.
von Hoerner, S. 1965, *Astrophys. J.* **142**, 1265.
Wade, C. M. 1970, *ibid.* **162**, 381.
Wade, C. M., Gent, H., Adgie, R. L., and Crowther, J. H. 1970, *Nature* **228**, 146.
Wade, C. M., and Miley, G. K. 1971, *Astron. J.* **76**, 101.
Williams, P. J. S., and Bridle, A. H. 1967, *Observatory* **87**, 280.
Williams, P. J. S., and Stewart, P. 1967, *Monthly Notices Roy. Astron. Soc.* **135**, 319.
Wills, D. 1967, *ibid.* **135**, 339.
Wills, D., and Bolton, J. G. 1969, *Aust. J. Phys.* **22**, 775.
Witzel, A., Véron, P., and Véron, M. P. 1971, *Astron. Astrophys.* **11**, 171.
Wright, M. 1970, *Monthly Notices Roy. Astron. Soc.* **150**, 271.